EXPERIMENTAL AND NUMERICAL EVALUATION OF COMETABOLISM IN SEQUENCING BATCH REACTORS

By

Chien-chun Shih

A DISSERTATION

Submitted to

Michigan State University

in partial fulfillment of the requirements

for the degree of

DOCTOR OF PHILOSOPHY

Department of Civil and Environmental Engineering

1995

ABSTRACT

EXPERIMENTAL AND NUMERICAL EVALUATION OF COMETABOLISM IN SEQUENCING BATCH REACTORS

By

Chien-chun Shih

The potential use of sequencing batch reactors (SBRs) for cometabolism was evaluated both experimentally and numerically. Mass balance considerations were used to develop a numerical computer-based methodology for SBR design capable of accommodating cometabolic transformation terms. The experimental system was a phenol-fed enrichment capable of trichloroethylene (TCE) cometabolism. This system was used to evaluate the effects of growth substrate feeding pattern on community structure and cometabolism; the stability of cometabolism; the toxicity of transformation products; and strategies for recharge of cometabolic activity. Modeling efforts were made to predict TCE transformation in bench-scale SBRs.

Phenol feeding patterns altered the structure and function of phenol-fed enrichments. Cells from a pulse fed reactor exhibited high phenol utilization rates, high diversity, high levels of cometabolic activity, and good settleability. Cells from a continuously fed reactor were predominately filamentous, exhibiting slow rates of TCE transformation and poor settleability. In this culture, isolates capable of degrading TCE were rare, and TCE transformation capacities varied greatly.

Stable and consistent TCE removal was obtained in a bench-scale SBR modified to include a recharge stage to rejuvenate cometabolic activity. Over the TCE concentration range from 0.5 to 5 mg/l, an average of 85-95% of the input TCE was biotransformed and

about 5-10% of TCE was air stripped. Toxic effects, including a decrease in total biomass and reduced TCE transformation activity, were observed for a short period at the beginning of TCE addition. Subsequently, biomass levels recovered, and TCE transformation activity resumed. The adapted system exhibited consistent TCE transformation capacity, suffering no additional toxic effects for the remaining test period (about 150 days). A numerical model capable of predicting TCE removal in the SBR was developed and verified.

I would like to give my greatest appreciation to my advisor Dr. Craig Criddle of the Department of Civil and Environmental Engineering for his encouragement, understanding, and assistance in my research.

A special thank you is given to Dr. James Tiedje, Dr. Mark Worden and Dr. Robert Hickey for their reviews of the manuscrips and suggestions. They enlarged my views of biological processes with different viewpoints.

Over past five years, many fellow students and friends gave me considerable assistance and made my Spartan life more enjoyable. I would like to thank all of them from my heart. I appreciate Dr. Jizhong Zhou and Ms. Mary Ellen Davey for their help in culture isolation and characterization, Mr. Yanliyang Fan for his assistance in instrument operation, Dr. Xianda Zhao and Myung-Keun Chung for their valuable comments and assistance in computer programming and environmental engineering.

I would also like to thank my lab workers, Dr. Mike Dybas, Sadhana Chauhan, Greg Tartara and Blake Key for their help in microbiological assays and sharing of laboratory resources. Mr. Wen-Hsiao Chang and Hwan Bae for their knowledge of mass transfer and modeling issues. Your visits to our lab are always enjoyable and has enriched my knowledge in different fields.

Special thanks go to my parents and my sisters, whose patient, unfaltering support and encouragement have made the task an enjoyable one. As a poor rural grower, I would like to express my greatest appreciation to Taiwan government for scholarship assistance.

ACKNOWLEDGMENTS

I would like to give my greatest appreciation to my advisor Dr. Craig Criddle of the Department of Civil and Environmental Engineering for his encouragement, understanding, and assistance in my research.

A special thank you is given to Dr. James Tiedje, Dr. Mark Worden and Dr. Robert Hickey for their reviews of the manuscript and suggestions. They enlarged my views of biological processes with different viewpoints.

Over past five years, many fellow students and friends gave me considerable assistance and made my Spartan life more enjoyable. I would like to thank all of them from my heart. I appreciate Dr. Jizhong Zhou and Ms. Mary Ellen Davey for their help in culture isolation and characterization, Mr. Yanlyang Pan for his assistance in instrument operation, Dr. Xianda Zhao and Myung-Keun Chang for their valuable comments and assistance in computer programming and environmental engineering.

I would also like to thank my lab coworkers, Dr. Mike Dybas, Sadhana Chauhan, Greg Tartara and Blake Key for their help in microbiological assays and sharing of laboratory resources, Mr. Wang-kuan Chang and I-yuan Hsu for their knowledge of mass transfer and modeling issues. Discussion with them is always enjoyable and has enriched my knowledge in different fields.

Special thanks go to my parents and my sisters, whose patient, unfaltering support and encouragement have made the task an enjoyable one. As a poor rural grower, I would like to express my greatest appreciation to Taiwan government for scholarship assistance.

Without this support, I would not have had the opportunity to purse my Ph.D. degree in the United States.

TABLE OF CONTENTS

TABLE OF CONTENTS

LIST OF TABLES

LIST OF FIGURES

NOMENCLATURE

English Symbols

A	dynamic cell age, time^{-1}
b	endogenous decay coefficient, time^{-1}
C	concentration of nongrowth substrate, mass per volume
E_S	efficiency of substrate removal, as a percentage
E_{SN}	efficiency of TKN oxidation, as a percentage
E	efficiency of solid stabilization, as a percentage
f_d	biodegradable fraction of active biomass
f_N	organic nitrogen fraction of biodegradable suspended solid
k	maximum rate of substrate utilization per unit weight of microorganism, time^{-1}
k_c	maximum rate of nongrowth substrate utilization per unit weight of microorganism, time^{-1}
K_La	overall mass transfer coefficient, time^{-1}
k_h	first order rate coefficient for hydrolytic conversion of degradable substrate to soluble substrate, time^{-1}
K_s	half velocity coefficient, equal to substrate concentration when $r_S=(1/2)k$
M	Mass
Ma	mass of active cells
N_r	number of reactors
N_w	number of cycles between wasting events
Q	influent flowrate, volume per time

r	ratio of volume of reactor at the beginning of fill to the volume of reactor at the end of fill.
r_s	rate of substrate utilization, mass per volume per time
r_{Xa}	rate of active biomass production, mass per volume per time
S	substrate concentration, mass per volume
S_N	TKN concentration, mass per volume
SRT	mean solid residence time, time
SVI	sludge volume index
t	time
t_o	time to fill reactor to the volume V_o, time
t_c	time to complete full SBR cycle
t_d	time for decanting
t_f	fill time
t_i	idle time
t_r	time for the react period
t_s	time for the settling period
U	specific utilization rate, time-1
V	reactor volume
V_o	the volume in an SBR at the beginning of the fill period
V_{SBR}	the volume in an SBR at the end of the fill period
V_w	volume of wasted suspended solids
X	total suspended solids, mass per volume
X_a	active biomass concentration, mass per volume
X_d	degradable suspended solid concentration, mass per volume
X_h	aerobic heterotrophic biomass concentration
X_i	inert biomass concentration, mass per volume
X_{in}	inorganic suspended solid concentration, mass per volume

X_N	nitrifying biomass concentration, mass per volume
X_r	refractory suspended solid concentration, mass per volume
X_v	Volatile suspended solids, mass per volume
Y	growth yield coefficient, mass per mass
Y_N	growth yield coefficient for nitrifiers, mass per mass
w	ratio of wasted sludge to total suspended solids ($=100V_w/V_o$)

Superscripts and subscripts

o	superscript denoting reactor influent stream
o	subscript denoting initial condition
e	subscript denoting reactor effluent stream
L	liquid phase
g	gas phase

Greek Symbols

θ	hydraulic residence time, time
θ_c	solid residence time, time
γ_{Xd}	COD to weight ratio for X_d, mass of substrate per mass of biodegradable solid
γ_{Xa}	COD to weight ratio for X_a, mass of substrate per mass of active biomass
μ	specific cell growth rate, time^{-1}
μ_m	maximum specific cell growth rate, time^{-1}

CHAPTER 1

INTRODUCTION AND RESEARCH OBJECTIVES

1.1 Introduction

Over the past two decades, contamination of groundwater by volatile organic compounds (VOCs) has been reported with increasing frequency. More than 40% of the US population uses groundwater as the drinking water supply, often without any treatment other than disinfection. Groundwater contamination is thus a serious public health concern. Methods for remediation of contaminated groundwater include carbon adsorption, air stripping, chemical oxidation, and biological processes. The advantage of chemical and biological processes is that these methods result in partial or complete destruction of the contaminant. The advantage of biological process over chemical processes is typically economic.

Within the wide range of biological processes now available, sequencing batch reactors (SBRs) have proven to be cost-effective and flexible, and are established technology for the removal of nutrients, BOD, and hazardous substances. In an SBR system, reactors pass through a repeating sequence of operations, including fill, react, settle, and decant. Conditions during the fill and react periods can be manipulated to enable selection of microbial communities with desirable properties. In principle, VOC removal can be accomplished in an SBR, but the conventional cycle must be modified to enable degradation of highly halogenated compounds, such as trichloroethylene (TCE). Such compounds are "nongrowth substrates" and are degraded by cometabolism. Nongrowth substrates cannot support microbial growth and can only be broken down if a growth

substrate capable of inducing and sustaining the desired cometabolic activity is added at some point during the SBR cycle. The time oriented operation of an SBR is well suited for addition of growth substrate in a manner that can induce and sustain cometabolic activity.

1.2 Research Objectives

This project was designed to investigate and exploit the operational flexibility of SBRs for cometabolic transformations. Lack of design criteria and standardized design methodology have prevented wide spread use of SBR technology (Arora et al., 1985). This deficiency became especially apparent in attempting to apply SBR technology for cometabolism. Accordingly, one of the first goals of this work was development of an SBR design theory that could accommodate kinetic expressions for cometabolism. This was accomplished using a classification scheme for suspended solids and substrates, developing mass balance equations for each substrate and solid type, and iteratively solving the resulting system of differential equations. Control strategies and design procedures were also explored. A second objective of this work was to explore operating strategies that might enrich for organisms capable of cometabolism. The effects of different growth substrate (phenol) feeding patterns and selective effects of repeated exposure to a nongrowth substrate (trichloroethylene) were evaluated. A final objective was to experimentally evaluate use of SBR technology for cometabolism. Concepts and experience acquired in accomplishing the earlier objectives were applied in the design, operation, and simulation of a bench scale SBR.

1.3 Overview of the chapters

This project was design in four phases. Each phase constitutes one chapter in the dissertation. SBR simulation and design were the major focus of the first phase. In the second phase, selection of a cometabolizing population by varying the pattern of growth substrate addition was investigated. Community structure and isolate studies were

conducted in this phase. The third phase consisted of a brief investigation of TCE toxicity. Cell viability after TCE transformation was the major concern. The effects of TCE transformation toxicity on cell selection and recharge of cometabolic activity were evaluated. In the fourth phase, a bench-scale SBR conducting TCE transformation was monitored and simulated numerically. The major concern in this phase was the stability of TCE transformation activity. Removal mechanisms and degradation kinetics were also evaluated. The dissertation concludes with a summary of the most important results and recommendations for design and operation of SBRs for cometabolism. Suggested future studies are also indicated.

Literature cited

Arora, M. L., E. F. Barth, and M. B. Umphres. "Technology evaluation of SBRs." J. WPCF 57 (8 1985): 867-875.

CHAPTER 2

BACKGROUND

2.1 Selection of a model system for cometabolism

The overall objective of this work is to evaluate the potential use and design of sequencing batch reactors for cometabolic transformation of hazardous substances. Many experimental systems can be envisioned for this purpose. The first important design decision is selection of a matching pair of growth and nongrowth substrates. The growth substrate must induce nonspecific enzymes that can attack the target nongrowth substrate(s), it must support a cometabolizing microbial population or community, and it must supply reducing power for sustained transformation of the nongrowth substrate(s). From the standpoint of ease of laboratory operation and establishment of mass balances, substrates that are nonvolatile and are highly soluble in water are advantageous. However, most growth and nongrowth substrates are volatile and dissolve poorly in water, so some compromise is necessary. In selection of a model system, aerobic conditions are also useful because of the relative ease of culture manipulation. Phenol is a growth substrate that satisfies many of the desired experimental needs - it is essentially nonvolatile and induces oxygenase activity toward halogenated alkenes under aerobic conditions. Accordingly, phenol was selected as the growth substrate. Several halogenated alkenes can be transformed by phenol-induced oxygenase activity. Of these, the most common groundwater contaminant is trichloroethylene (TCE). Thus, TCE was selected as the model nongrowth substrate. In the following sections, the properties of

TCE and phenol are described further, as are the microbial communities that degrade these compounds.

2.2 Properties of trichloroethylene

Trichloroethylene is a synthetic chlorinated organic chemical that fulfills all of the requirements for the ideal degreasing solvent (Table 2-1). It is only slightly soluble in water and forms an azeotrope with water, resulting in a mixture with a lower boiling point and vapor density. It is also highly volatile. When released to the atmosphere, it is destroyed by photooxidation with a half-life of about one day (Schaumburg, 1990).

TCE is generally inhibitory to microbial growth. Exposure of a growing batch culture of *Escherichia coli* to 0.009 mg/L of TCE increased doubling time by 131% and induced 22 stress proteins (Blom et al., 1992). It is mutagenic to *Salmonella typhimurium* and *Escherichia coli* K-12 when activated by liver microsomes, and it is a suspected carcinogen in some tested animals (Miller and Guengerich 1982).

The World Health Organization (WHO) recommends a drinking water guidance level of 30 µg/l based on a carcinogenic end point. In the United States, the current maximum concentration in drinking water under the Safe Water Drinking Act is 5 ppb (US EPA, 1987). For effects other than cancer, the US EPA recommends a water quality criterion of 6.77 mg/L.

2.3 Causes and status of TCE contamination

TCE was widely used from the forties to the seventies as a degreasing agent, dry cleaning solvent, extractant for food processing, refrigerant, heat-exchange liquid, fumigant, reactant and solvent for organic synthesis, and general anesthetic in medicine and dentistry. In 1976, it was identified as a suspected carcinogen, and its uses were severely curtailed. Nevertheless, for the nearly 30 year period of widespread use, there

Table 2-1 Chemical/physical properties of TCE

Property	Value	Reference
Chemical formula	$Cl_2C=CHCl$	(1)
Molecular weight	131.40	(1)
Physical state	Colorless liquid	(1)
Boiling point	86.7 °C	(1)
Melting point	- 73 °C	(1)
Density	1.4 g/mL at 25 °C	(1)
Vapor pressure	77 mm Hg at 25 °C	(1)
Vapor density	4.5 (air = 1)	(2)
Lower explosive limit in air	12.5%	(2)
Upper explosive limit in air	90.0%	(2)
Autoiginition temperature	410 °C	(2)
Henry 's constant (dimensionless)	0.356 at 25 °C	(3)
Water solubility	1000 mg/L at 20 °C	(1)
log K_{ow}	2.29	(4)
K_p for algae	2.4 mL H_2O/mg VS	(5)
log EC_{50}	3.16 µmol/L	(6)

Reference: (1) Weast 1992, (2) Fan 1988, (3) Mackay and Leinonen 1975, (4) Burcell 1978, (5) Smets and Rittmann 1988, (6) Kamlet et al., 1986.

was little control on TCE release and disposal. The most common disposal method was landfilling or direct disposal to land. When applied to unsaturated soil, TCE volatilizes and simultaneously migrates downward to the water table. Because it is denser than water, organic phase TCE arriving at the water table continues to sink until further vertical migration is prevented by a confining clay or rock layer. Trapped or pooled TCE below the water table serves as a long-term slow-release source of TCE. Under anaerobic conditions, TCE that dissolved in water can be reductively dechlorinated, yielding dichloroethylene isomers, vinyl chloride, and ethylene or ethane. TCE can also be produced anaerobically, by reductive dechlorination of tetrachloroethylene. Little aerobic degradation of TCE is observed unless growth substrates are present that induce the requisite oxygenase activity. These factors help to explain why TCE is such a pervasive groundwater contaminant. Nationwide surveys of drinking water supplies revealed that TCE was present in up to 34% of water supplies tested in the U.S. (Conglio et al., 1980; Westrick et al., 1984). The highest levels of TCE were associated with leaching from landfill waste disposal sites, where it was detected at 28% of waste sites examined (Josephson, 1986).

As described above, TCE has had many applications. As a result, it has been discharged to surface waters and groundwater by industry, commerce, and individual consumers. About 90% of the TCE produced in 1974 was used in industrial degreasing. The US EPA estimated that approximately 310,200 tons of wasted solvent were produced by degreasing operations in 1974. Lesser amounts were used and discarded by dry cleaners, septic tank cleaners, and other cleaning operations. By 1980, TCE solvent waste production had decreased to 234,000 tons (Vogel et al., 1987), and, by 1985, industrial TCE usage had dropped to 90,000 ton/yr. Until recently, many common consumer products contained TCE. Some of these entered the environment by way of the septic tank, sewer, or municipal landfills. Among these were pipe and drain cleaners, shoe polish, spot removers, upholstery cleaners, paint remover, and septic tank cleaners.

2.4 Biodegradation of TCE

Until the early 1980s, TCE was considered non-biodegradable under aerobic condition and slowly transformable under anaerobic conditions (Bouwer et al., 1981). This perception changed in 1985, when Wilson and Wilson (1985) observed aerobic degradation of TCE in a soil column exposed to natural gas. It is now known that TCE will degrade either anaerobically or aerobically, if an appropriate growth substrate is present. To date, anaerobic processes have found limited acceptance for bioremediation applications, in large part because of concerns that partial dechlorination products, such as vinyl chloride, would accumulate. Vinyl chloride is a known human carcinogen. The products of aerobic TCE biotransformation are believed to be less harmful.

Early observations of aerobic TCE degradation eventually established that TCE was cometabolized by methanotrophic microorganisms. The nonspecific enzyme methane monooxygenase (MMO) was responsible for fortuitous oxidation of the TCE. Similar TCE-degrading monooxygenase systems were discovered in the ammonia-oxidizing bacteria (Arciero et al, 1989; Vanilli et al., 1990) and the propane-oxidizing bacteria (Wacket et al., 1989). However, TCE cometabolism was not found in all microbial populations possessing broad-specificity microbial oxygenase activity. Bacteria that contained nitropropane dioxygenase, cyclohexane monooxygenase, cytochrome P-450 monooxygenase, 4–methoxgbezoate monooxygenase and hexane monooxygenase did not degrade TCE (Wacket et al., 1989).

Another group of microorganism that exhibited TCE cometabolism activity were the bacteria that degraded aromatic compounds. Some *Pseudomonas* species produce aromatic oxygenases that can degrade TCE (Nelson et al., 1987; Wackett and Gibson 1988). Phenol and toluene are the typical inducing agents for this activity. Isopropylbenzene, isoprene and propylene utilizing bacteria also exhibit TCE

cometabolism activity. The active species include *Rhodococcus*, *Alcaligenes*, and *Xanthobacter* (Dabrock et al., 1992; Ensign et al., 1992; Ewers et al., 1990).

Under aerobic condition, TCE may be oxidized according to the following equation:

$$CHCl=CCl_2 + H_2O + 1.5O_2 \longrightarrow 2CO_2 + 3HCl \qquad (2\text{-}1)$$

Reaction 2-1 is highly favorable ($\Delta G^{\circ\prime}$=-1065 KJ/mole) but reducing equivalents and ATP are not made available to the organism by the oxidation (Dabrock et al., 1992). In fact, the oxygenase requires reducing power. Therefore, it is not surprising that aerobic growth on TCE has yet to be reported.

2.5 Aerobic TCE degradation pathway

The pathway for aerobic degradation of TCE has been investigated in detail for mammalian cytochrome P-450 and for soluble methane monooxygenase (sMMO). It is expected that ammonia monooxygenase (AMO) and aromatic oxygenase (AO) systems function in much the same way, with similar degradation products.

Oxidation of TCE by sMMO was investigated in detail as a model for understanding monooxygenase-dependent chloroolefin dechlorination (Fox et al., 1990). Little et al. (1988) concluded that TCE degradation is a cometabolic process that provides little or no benefit to the organisms. Methanotrophic bacterium strain 46-1 initiated the degradation of TCE, but was unable to metabolize some intermediates like dichloroacetic acid and glyoxylic acid. The use of purified enzyme components, obtained from *Methylosinus trichosporium* OB3b, allowed an unambiguous determination of the reaction products. sMMO oxidized haloalkenes largely to epoxide intermediates. This was demonstrated by the formation of diagnostic adduct upon reaction with 4-(p-nitrobenzy)pyridine. Furthermore, the predicted stable decomposition products of

epoxides were identified in the enzyme reaction mixtures. As shown in Figure 2-1, the predominant fate of the epoxide appears to be hydration followed by carbon–carbon bond scission. These spontaneous reactions led to the formation of the major products carbon monooxide and formic acid. Methanotrophs can oxidize carbon monooxide and formic acid further to carbon dioxide (Colby et al., 1977). Under moderately acidic conditions, TCE epoxide hydrolyzes to dichloroacetic acid and glyoxylic acid (Little et al., 1988). Chloral has also been observed as a minor (6%) product. Chloral is derived from TCE via an intramolecular chlorine migration reaction (Miller and Guengerich, 1982). Further oxidation of chloral produces trichloroacetate and reduction yields 2,2,2-trichloroethanol. Products analysis of reaction mixtures containing synthetic TCE-epoxide exhibited no detectable chloral formation, indicating that chloral was likely generated at the sMMO active site. Chloral hydrate has been shown to be a product for TCE cometabolism in four different methanotrophs expressing sMMO. Chloral hydrate is biologically transformed to trichloroethanol and trichloroacetic acid. Mixed cultures containing methanotrophs were capable of more extensive mineralization of TCE to carbon dioxide than a pure culture (Little et al., 1988).

In aromatic oxygenase systems, formate, carbon monoxide, glyoxylic acid were detected in pure cultures (Wacket and Householder 1989; Winter et al., 1989). For *P. cepacia* G4, TCE completely degraded to CO_2, Cl- and unidentified, nonvolatile products (Nelson et al., 1986). A summary of the reported water soluble products of aerobic TCE biotransformation is provided in Table 2-2.

A turnover- and time-dependent inactivation of the sMMO protein components occurred during oxidation of TCE in vitro (Fox et al., 1990). Inactivation was caused by a diffusible reaction product as demonstrated by covalent modification of sMMO with 1,2,^{14}C-TCE. In-vivo experiments with toluene dioxygenase-containing strain of

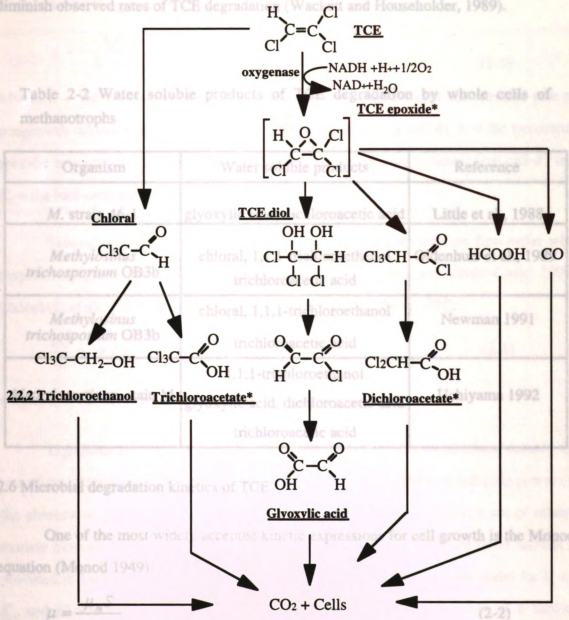

Figure 2-1 Pathways of transformation for TCE by methanotrophic mixed culture. *indicates possible or know carcinogenic metabolites

Pseudomonas putida indicated that toxic products can profoundly disrupt metabolism and diminish observed rates of TCE degradation (Wackett and Householder, 1989).

Table 2-2 Water soluble products of TCE degradation by whole cells of methanotrophs

Organism	Water soluble products	Reference
M. strain 46-1	glyoxylic acid, dichloroacetic acid	Little et al., 1988
Methylosinus trichosporium OB3b	chloral, 1,1,1-trichloroethanol trichloroacetic acid	Oldenhuis et al., 1989
Methylosinus trichosporium OB3b	chloral, 1,1,1-trichloroethanol trichloroacetic acid	Newman 1991
Methylocystis sp. stain M	1,1,1-trichloroethanol glyoxylic acid, dichloroacetic acid trichloroacetic acid	Uchiyama 1992

2.6 Microbial degradation kinetics of TCE

One of the most widely accepted kinetic expressions for cell growth is the Monod equation (Monod 1949):

$$\mu = \frac{\mu_m S}{K_s + S} \qquad (2\text{-}2)$$

where, S = the concentration of substrate (mg/L), μ = the specific growth rate (d^{-1}), μ_m = the maximum specific growth rate constant (d^{-1}), and K_s is the half-saturation constant (mg/L). Since TCE does not support growth, equation 2-2 can not be used to describe changes in microorganism concentration during TCE transformation. However, saturation

kinetics using a Michaelis-Menton or Monod-like expression have been used successfully to describe TCE degradation by resting cells:

$$q_c = -\frac{k_c C}{K_c + C} \tag{2-3}$$

where, C = the concentration of nongrowth substrate (mg/L), q_c = the specific rate of nongrowth substrate degradation (mg nongrowth substrate/mg cell-d), k_c = the maximum specific non-growth substrate degradation rate (mg nongrowth substrate/mg cell-d) and K_c = the half-saturation constant (mg/L).

Several reports also describe TCE degradation kinetics that are first order with respect to TCE concentration (Dabrock et al., 1992; Henry and Grbic'-Galic' 1990; Oldenhuis et al., 1989; Strand et al., 1991; Wackett and Gibson 1988):

$$\frac{dC}{dt} = -k_c' CX \tag{2-4}$$

where, k_c' = the second order rate coefficient (L/mg-d).

Equations 2-3 and 2-4 fail to capture certain features of cometabolism, notably the loss of transformation activity in resting cells caused by a depletion of reducing power (in the absence of growth substrate) and product toxicity. In recent years, a set of related models have emerged that can account for such effects. A summary of these models is provided in Table 2-3. Also shown are simplifications of the Monod-like model for $C << K_c$ and $C >> K_c$. In these models, an important concept is the idea of a limited transformation capacity (T_c) for the nongrowth substrate (Alvarez-Cohen and McCarty 1991a). T_c is defined as:

$$T_c = \frac{dS}{dX} = \frac{mass\ of\ contaminant\ transformed}{mass\ of\ cells\ inactivated} \tag{2-5}$$

To evaluate the loss of cell activity during the cometabolism, first order decay of biomass is commonly used. The rate of cell decay can be expressed as

Table 2-3 Summary of cometabolizing kinetic expressions

Model	Differential equations for substrate utilization rate	Integrated form	Ref.
1a	$-\frac{dC}{dt}=\frac{k_c CX}{K_c+C}$ and $\frac{dX}{dt}=-bX$ so $-\frac{dC}{dt}=\frac{k_c CX}{K_c+C}e^{-bt}$	$K_c ln\left(\frac{C}{C_o}\right)+C-C_o=\frac{-k_c X_o}{b}\left(1-e^{-bt}\right)$	(1), (2)
1b $C<<K_c$	$-\frac{dC}{dt}=k_c^{'}CX$ and $\frac{dX}{dt}=-bX$ so $-\frac{dC}{dt}=k_c^{'}CXe^{-bt}$	$C=C_o e^{\left(\frac{k_c X_o}{b}\left(e^{-bt}-1\right)\right)}$	(2), (3)
1c $C>>K_c$	$-\frac{dC}{dt}=k_c X$ and $\frac{dX}{dt}=-bX$ so $-\frac{dC}{dt}=k_c CX_o e^{-bt}$	Same as model 3 where $T_c=\frac{k_c}{b}$	(4)
2a	$-\frac{dC}{dt}=\frac{k_c CX}{K_c+C}$ and $\frac{dC}{dX}=T_c$ so $-\frac{dC}{dt}=\frac{k_c C\left(X_o-\frac{1}{T_c}(C_o-C)\right)}{K_c+C}$	$t=\frac{1}{k_c}\left(\left(\frac{K_c}{C_o/T_c-X_o}\right)ln\left\{\frac{CX_o}{FC_o}\right\}+T_c ln\left\{\frac{X_o}{F}\right\}\right)$ where $F=X_o-\frac{1}{T_c}(C_o-C)$	(5)
2b $C<<K_c$	$-\frac{dC}{dt}=k_c^{'}CX$ and $\frac{dC}{dX}=T_c$ so $-\frac{dC}{dt}=k_c^{'}C\left(X_o-\frac{1}{T_c}(C_o-C)\right)$	$C=C_o\frac{F^{'}e^{-k_c^{'}F^{'}t}}{X_o-\frac{C_o}{T_c}e^{-k_c^{'}F^{'}t}}$ where $F^{'}=X_o-C_o/T_c$	(4)
2c $C>>K_c$	$-\frac{dC}{dt}=k_c X$ and $\frac{dC}{dX}=T_c$ so $-\frac{dC}{dt}=k_c\left(X_o-\frac{1}{T_c}(C_o-C)\right)$	Same as model 3 where $T_c=\frac{k_c}{b}$	(4)
3	$\frac{dX}{dt}=-bX$ and $\frac{dC}{dX}=T_c$ so $-\frac{dC}{dt}=bT_c X_o e^{-bt}$	$C=C_o-T_c X_o\left(1-e^{-bt}\right)$	(6)
4	$-\frac{dC}{dt}=\frac{k_c CX}{K_c+C}$ and $\frac{dX}{dt}=-bX-\frac{k_c X}{T_c^*}\left(\frac{C}{K_c+C}\right)$	No integrated form	(4)

Reference: (1) Galli and McCarty, 1989, (2) Schmidt, 1985, (3) Criddle et al., 1990, (4) Criddle, 1993, (5) Alvarez-Cohen and McCarty, 1991a, (6) Saez and Rittmann, 1991.

$$\frac{dX}{dt} = -bX \qquad (2\text{-}6)$$

where X = cell concentration and b = decay coefficient.

Models found in the literature prior to 1993 are obtained from various combinations of equations 2-4, 2-5 and 2-6. Criddle (1993) proposed a fourth model that unified the earlier models. Model 4 incorporated endogenous decay and product toxicity into the cell decay term and assumed that nongrowth substrate degraded with saturation kinetics.

A summary of reported kinetic models and respected rate coefficients for microbial TCE transformation is provided in Table 2-4. Since not all TCE cometabolism studies are designed to evaluate TCE degradation kinetics, some of the data presented in Table 2-4 is provided as initial rates for a specified concentration of TCE.

Methanotrophic organisms exhibit substantial variation in TCE oxidation rate due to differences in species and the type of MMO expressed. Methanotrophs possess two types of MMO: the membrane-associated or particulate form (pMMO) oxidizes TCE slowly and is induced at high copper concentrations; the cytoplasmic or soluble MMO (sMMO) oxidizes TCE at high rates and is induced at low copper concentrations (Dalton et al., 1984; Stanley et al., 1983). The copper concentration for transition from sMMO to pMMO was around 0.25 μmol copper/g biomass (Anderson and McCarty, 1994; Tsien et al., 1989). Differences in culture media composition also cause differences in the rate of TCE oxidation (Bowman and Sayler, 1994; Henry and Grbic-Galic, 1990). A current "ranking" of TCE degraders by rate is :

M. trichosporium OB3b > Methanotrophic mixed culture > *P. cepacia* G4 > *P. putida* F1 ~ *M. vaccae* JOB5 ~ *N. europera*

Table 2-4 Reported TCE degradation kinetic coefficients

Culture	Kinetic pattern	Rate constant		reference
		k_c (d^{-1})	K_c (mg/L)	
Pseudomonas cepacia G4	Monod	0.74	0.40	Folsom 1990
Methylosinus trichosporium OB3b		42	18	Brusseau 1990
sMMO of *Methylosinus trichosporium* OB3b		64	4.83	Fox 1990
Methylosinus trichosporium OB3b		19.1 +/- 8.0	55 +/- 18	Oldenhuis 1991
Methylomonas sp MM2		0.046 - 0.29	0.51-1.35	Henry 1990
		k_c'(L/mg-d)	TCE (mg/L)	
Pseudomonas putida F1	first order	0.0162	1.05 - 10.5	Wackett 1988
Methylosinus trichosporium OB3b		3.08	0.026 - 13.0	Oldenhuis 1989
Methylomonas sp MM2		0.003 - 2.3		Henry 1990
Methanotrophic mixed culture		0.007	0 - 3	Strand 1990
Pseudomonas sp JR1		0.42	3 -26	Dabrock 1992
Rhodococcus. erythroplis BD1		0.42	3-26	Dabrock 1992
		rate (d^{-1})	TCE (mg/L)	
Methanotrophic mixed culture	Initial rates (mg TCE/ mg cell-d)	0.0032	0.75	Fogel 1986
Mycobacterium vaccae JOB5		0.113	2.62	Wackett 1989
Pseudomonas putida F 1		0.112	10.5	Wackett 1988
Nitrosomonas europea		0.027 - 0.064	1.0	Vannelli 1990
Alcaligenes eutrophus JMP 134		0.019	3.3	Harker 1990
Nitrosomonas europaea		0.208	1.31	Arciero 1989
Rhodococcus erythroplis JE7		0.0141	0.8	Ewers 1990
Alcaligenes denitrificans ssp		0.0170	0.8	Ewers 1990
Xanthobacter strain Py2		0.81	15	Ensign 1992
	T_c	k_c (d^{-1})	K_c (mg/L)	
Methanotrophic mixed culture	0.036	0.54	0.42	Alvarez-Cohen 1990
Methanotrophic mixed culture	0.042	0.84	1.5	Alvarez-Cohen 1991
Nitrosomonas europaea	0.004			Hyman 1995

Note: Biomass assumptions used to standardize rate data: 0.8 mg VSS/mg cell, 0.5 mg protein/mg cell, 3.3 mg wet weight/mg cell.

Although methanotrophic bacteria generally exhibit higher TCE degradation rates, they grow slowly and TCE transformation rates are sensitive to copper concentrations.

2.7 Biodegradation of phenol

Microorganisms with phenol-degrading capacity include bacteria, such as *Pseudomonas* (Beltrame et al., 1980; Yang and Humphrey, 1975), *Nocardia* (Rizzuti and Augueliaro, 1982), and *Bacillus* (Buswell 1975); yeasts, such as *Trichosporon* (Gaal and Neujahr, 1979), *Candida* (Krug et al. 1984); and multicellular fungi, such as *Fusarium* (Anselmo et al., 1985).

Phenol is degraded through the intermediate catechol (Bayly and Barbour, 1984), but opening of the aromatic ring can proceed by either *ortho* or *meta* ring cleavage (Figure 2-2). The *ortho* pathway uses 1,2-oxygenase to open the catechol ring, generating succinate and acetyl-CoA via ß-ketoadipate (Feist and Hegeman 1969). The 1,2 monooxygenase and the two subsequent enzymes of the pathway are induced by cis,cis-muconate in *P. putida* and *P. aeruginosa*. The *meta* pathway uses a 2,3-oxygenase and is less specific. In contrast to the *ortho* pathway, all of the enzymes of the meta-cleavage pathway are induced by phenol, including phenol hydroxylase (Bayly and Barbour, 1984; Bayly et al., 1977; Feist and Hegeman, 1969). Induction of the *meta* fission pathway is required for the degradation of TCE by *P. cepacia* G4 (Nelson et al., 1987). Other TCE degraders such as *P. putida* PpF1 and *P. putida* B5, also exhibit *meta* cleavage when using toluene as growth substrate. However, not all organism using *meta* pathway for ring cleavage are able to degrade TCE (Nelson et al., 1988)

Evidence indicates that *meta* pathway may be plasmid encoded (Bayly and Barbour, 1984). The initial conversion of phenol to catechol is catalyzed by phenol hydroxylase, a NADH-dependent monooxygenase. As such, this is an energy-requiring

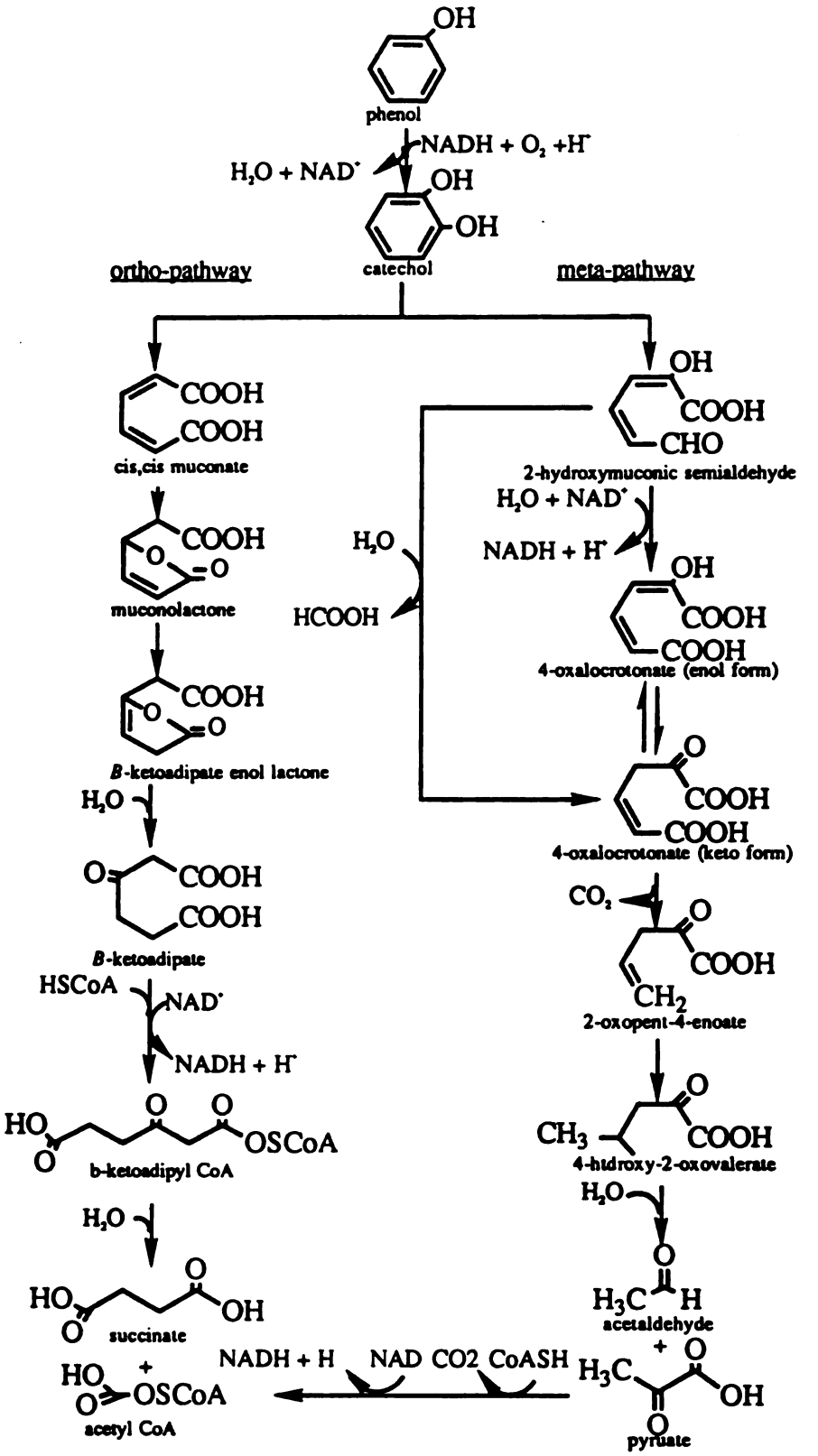

Figure 2-2 Aerobic phenol degradation pathways (modified from Allosop 1991)

step consuming the equivalent of three moles of ATP. Degradation of catechol by the *ortho* and *meta* pathways regenerates the NADH needed for the first step.

The most commonly used equation used to describe microbial growth on phenol is the Andrews or Haldane equation, representing substrate-inhibited growth (D'Adamo et al., 1984; Kotturiet al., 1991; Pawlowsky and Howell, 1973; SoKol, 1988; Szetela and Winnicki, 1981):

$$\mu = \frac{\mu_m \cdot S}{K_s + S + \frac{S^2}{K_I}} \qquad (2\text{-}6)$$

where K_I = inhibition constant (mg/L). Some researchers have concluded that phenol is not inhibitory and have modeled its degradation with Monod kinetics (Auteinrieth et al., 1991; Beltrame et al., 1980). Zero order kinetics with respect to phenol concentration have also been reported (Rizzuti and Augueliaro, 1982; Tischler and Eckenfelder, 1969). Reported kinetic expressions and kinetic parameters for aerobic phenol degradation are summarized in Table 2-5. Arguments on the inhibitory properties of phenol and its degradation kinetics might be explained by the work of Templeton and Grady (1989). They noted that cells physiologically adapt to their previous growth environment (Templeton and Grady 1989). As the dilution rate at which the cells are grown in a chemostat is increased they contain higher levels of RNA and enzymes. Consequently, when those cells are removed from chemostat and placed into batch reactors in which the substrate limitation is removed, the cells with the higher RNA and enzyme levels shift to higher specific degradation rates. A decrease in K_s with increasing dilution rate was also reported. They suggested that K_s may depend on cell geometry and physical characteristics, and that it is influenced by the rate at which the bacteria are growing. Autenrieth et al. (1991) reported zero order degradation for starved bacteria at low phenol concentration (100 mg/L), Monod kinetics for starved bacteria at high phenol concentration (650 mg/L, and Haldane kinetics for non-starving cells at high initial

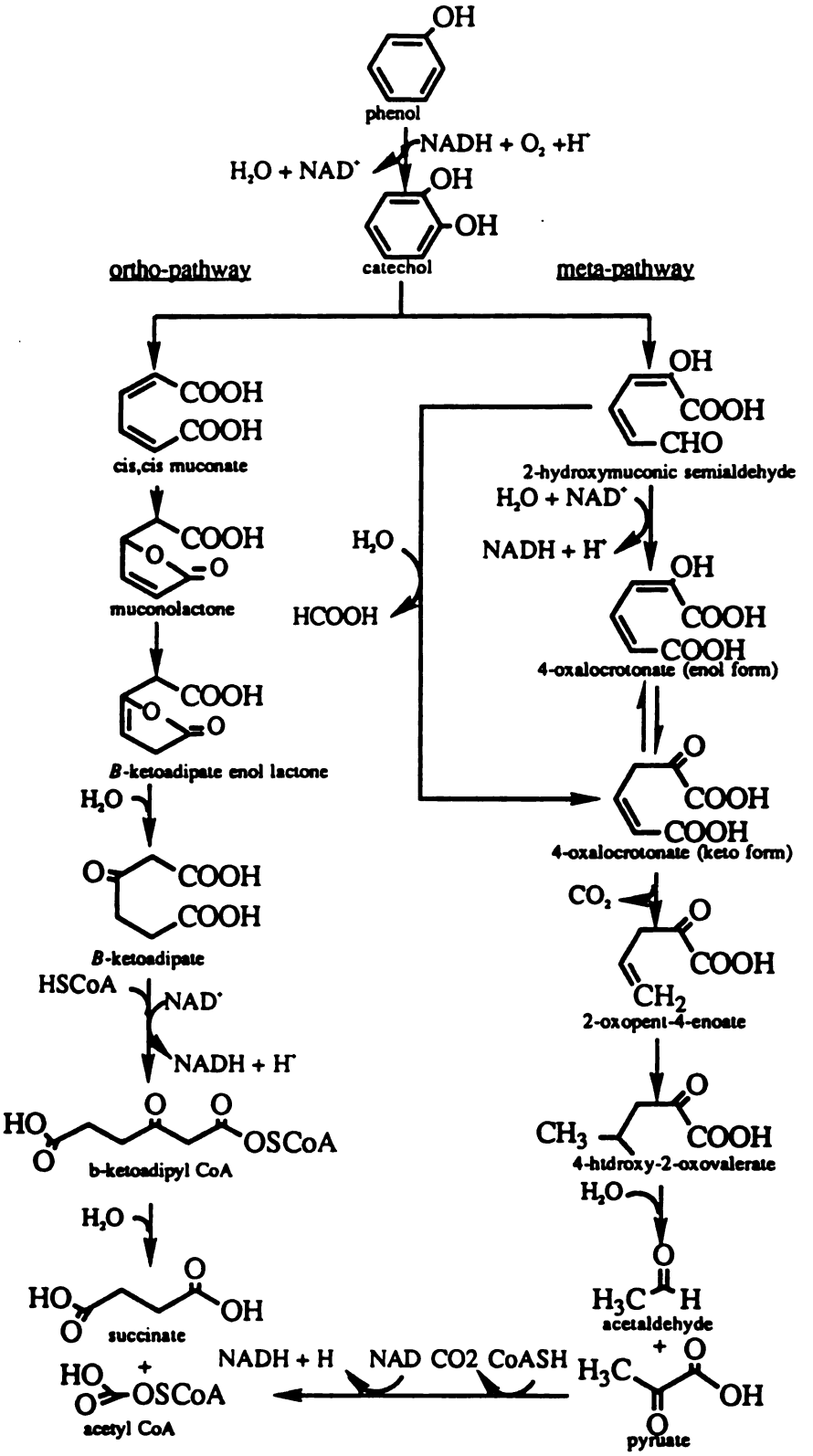

Figure 2-2 Aerobic phenol degradation pathways (modified from Allosop 1991)

step consuming the equivalent of three moles of ATP. Degradation of catechol by the *ortho* and *meta* pathways regenerates the NADH needed for the first step.

The most commonly used equation used to describe microbial growth on phenol is the Andrews or Haldane equation, representing substrate-inhibited growth (D'Adamo et al., 1984; Kotturiet al., 1991; Pawlowsky and Howell, 1973; SoKol, 1988; Szetela and Winnicki, 1981):

$$\mu = \frac{\mu_m \cdot S}{K_s + S + \frac{S^2}{K_I}} \qquad (2\text{-}6)$$

where K_I = inhibition constant (mg/L). Some researchers have concluded that phenol is not inhibitory and have modeled its degradation with Monod kinetics (Auteinrieth et al., 1991; Beltrame et al., 1980). Zero order kinetics with respect to phenol concentration have also been reported (Rizzuti and Augueliaro, 1982; Tischler and Eckenfelder, 1969). Reported kinetic expressions and kinetic parameters for aerobic phenol degradation are summarized in Table 2-5. Arguments on the inhibitory properties of phenol and its degradation kinetics might be explained by the work of Templeton and Grady (1989). They noted that cells physiologically adapt to their previous growth environment (Templeton and Grady 1989). As the dilution rate at which the cells are grown in a chemostat is increased they contain higher levels of RNA and enzymes. Consequently, when those cells are removed from chemostat and placed into batch reactors in which the substrate limitation is removed, the cells with the higher RNA and enzyme levels shift to higher specific degradation rates. A decrease in K_s with increasing dilution rate was also reported. They suggested that K_s may depend on cell geometry and physical characteristics, and that it is influenced by the rate at which the bacteria are growing. Autenrieth et al. (1991) reported zero order degradation for starved bacteria at low phenol concentration (100 mg/L), Monod kinetics for starved bacteria at high phenol concentration (650 mg/L, and Haldane kinetics for non-starving cells at high initial

Table 2-5 Phenol degradation pattern and parameters

Culture	Kinetics	μ_m (hr-1)	K_s (mg/L)	K_i (mg/L)	Y*	Reference
Mixed culture	Haldane	0.131-0.363	5-266	142-1199	NA**	D'Adamo, 1984
Mixed culture		0.66	16.5	634.4	0.7-0.9	Autenrith, 1991
P. putida sp		0.119	5.27	377	0.55	Kotturi, 1991
P. putida		0.53-1.84	0.5-1.23	8-20	NA	Sokol, 1988
Mixed culture		0.326	19.2	229	NA	Szetela, 1981
Mixed culture (Non filament)		0.260	24.5	173	0.545	Pawlowsky, 1973
Mixed culture (filaments)		0.223	5.8	934	0.616	Pawlowsky, 1973
Mixed culture	Monod	0.21	630.41	Not apply	NA	Autenrith,1991
Mixed culture		0.117	245	Not apply	0.45	Betrame, 1980
		Zero order kinetc cofficient (hr^{-1})			Y	
Mixed culture	Zero-order	0.07				Autenrith,1991
Mixed culture		0.011-0.030				Tischler, 1969
P. fluorescens		0.08				Rizzuti, 1982
Nocardia		0.37				Rizzuti, 1982

* Unit for Y = mg substrate/mg cells.

**NA = not available.

substrate concentration (600 mg/L). These different kinetic responses from the same organisms suggest that the appropriate kinetic model for phenol degradation is variable, and may depend upon the physiological state of the phenol-degrading culture. The different kinetic patterns reported in literatures may be also caused by different values for kinetic coefficients and by the phenol concentrations applied in kinetic experiments. When $S^2 << K_I$ Haldane equation can be simplified to the Monod equation. When $S^2 << K_I$ and $S >> K_s$, Haldane equation can be further simplified to the zero order (with respect to phenol concentration) form.

Phenol utilizing bacteria grow faster than methanotrophs by one or two orders of magnitude (Table 2-6). The faster growth kinetics and relative ease of addition of phenol give phenol-degrading organisms certain practical advantages in reactor systems. High growth rates enable more rapid start-up, smaller reactor volumes, and more rapid recovery from TCE product toxicity and enzyme inactivation during TCE transformation.

2.8 Cometabolism in engineered systems

As defined by Dalton and Stiring (1982), cometabolism is the "transformation of a nongrowth substrate in the obligate presence of a growth substrate or another transformable compound" (Dalton and Stirling 1982). In a more general sense, however, cometabolism can be defined as any "transformation of a nongrowth substrate that depends upon the concurrent or previous metabolism of a growth or energy substrate" (Criddle, 1993). This definition includes the case of resting cells. Nitrifiers, methanotrophs, and some pseudomonads can degrade TCE in the absence of growth substrate. Although rates of cometabolism decline in the absence of a growth substrate, the presence of growth substrate may be inhibitory as a result of competitive inhibition between the growth and nongrowth substrates.

Table 2-6 Growth kinetics for TCE degraders

Organism	Growth substrate	Y mg cell per mg growth substrate	k mg growth substrate per mg cell-day	μ_m mg cell per mg growth substrate-day	K_s mg/L	K_i mg/L	b day-1	Reference
mixed culture methanotroph	methane	0.20	0.86	0.16	0.2		0.12	Brohelm, 1990
mixed culture methanotroph	methane	0.20	0.75	0.15	0.22		0.12	Brohelm, 1990
mixed culture methanotroph	methane	0.35						Alvarez-Cohen and McCarty 1991
Methylosinus trichosporium OB3b	methane		8.37		1.47			Oldenhuis 1991
Pseudomonas cepacia G4	phenol		63		0.8	43		Folsom, 1990
Pseudomonas cepacia G4	toluene	0.16		4.56				Duetz, 1994
Pseudomonas cepacia G4	toluene			4.76	2.35			Lando, 1994
Pseudomonas mendocina KR1	toluene	0.35		10.8				Duetz, 1994
Pseudomonas putida F1	toluene	0.44		9.12				Duetz, 1994
Pseudomonas putida mt-2	toluene	0.33		9.6				Duetz, 1994
Nitrsomonas	ammonia	0.13-0.35 (0.2)	3-10 (3.5)	0.3-2.0 (0.7)	0.2-2.0		0.05	Mecalf &Eddy 1991

To design cometabolic reactor systems, organisms capable of conducting cometabolic transformations must be identified and cultured. Medium conditions and toxicity related to the target compounds and their transformation products should also be evaluated. Substrate competition should be minimized. Growth and nongrowth substrates may be competing for the same active site. If the growth substrate is supplied at a high concentration or has high affinity for the enzyme, transformation of nongrowth substrate may be inhibited or prevented altogether. To reduce the effects of competitive inhibition, target compounds and growth substrates may be supplied in different time periods, at different locations, or at concentrations that allow for simultaneous cell growth and cometabolism.

Product toxicity may affect the long-term stability of cometabolism. Before adaptation to a nongrowth substrate can occur, loss of microorganisms and diminished transformation can be expected. Transformation capability could be lost entirely. For TCE, toxicity is believed to be due to interaction of TCE reaction byproducts with cell macromolecules (Alvarez-Cohen and McCarty 1991b; Henry and Grbic-Galic 1991). Cells that do not transform TCE do not suffer toxic effects when exposed to TCE itself. As a result, populations with the capability for TCE degradation might be expected to lose that capability as the TCE-transforming cells within the population die. Pure cultures are likely to be especially susceptible because byproducts can accumulate (Little et al. 1988; Uchiyama et al 1992). In a well-balanced consortium, the products of cometabolism may be further degraded by consortium members (Uchiyama et al. 1992). More extensive biodegradation and reduced toxicity are possible in mixed culture systems. On the other hand, the selective pressure imposed by TCE toxicity may enhance the competitive advantages of non-TCE degraders.

For mixed culture systems, the survival of cometabolic species and the balance between different populations are important. Cometabolic species may be unable to

compete with non-cometabolizing species due to product toxicity. The effects of product toxicity are most severe when reactive intermediates exert their toxic effect by reacting with cell macromolecules. Cometabolizing cells can be damaged, providing an advantage to organisms that do not transform TCE. However, if product toxicity is caused by other TCE transformation products, like trichloroacetic acid (TCA) or dichloroacetic acid (DCA), toxic effects may be more nonspecific. Populations capable of degrading the TCA or DCA may be favored.

2.9 Choice of microbial systems for cometabolism of TCE

Many factors can influence the choice of a system for cometabolism of TCE. Ideally, the cometabolizing microorganisms should be easily grown, using growth substrate efficiently. The transformation should be fast and stable. Growth substrate should be cheap, easy to handle and non-toxic or hazardous. End products from transformation of growth and non growth substrates should be non-hazardous or easily handled for further treatment. None of the major TCE-cometabolizing microbial groups (nitrifiers, methanotophs, and aromatic degraders) satisfies all of these requirements. A comparative summary is provided in Table 2-6. Because nitrifiers are autotrophs, they have low yields and grow slowly. They are also sensitive to environmental conditions, with a narrow pH optimum (7.5-8.6) and a need for relatively high levels of dissolved oxygen. They are also susceptible to a variety of inhibitors. Their oxidation products, nitrite or nitrate, are potential common groundwater contaminants, and may require further treatment. As to methanotrophs, the growth substrate, methane, is flammable and explosive in high concentration. Methane also has low solubility in the aqueous phase (24 mg/L at 20°C, Weast, 1992) complicating its delivery. Costs involved in methane mass transfer limitations may hinder its usage as a growth substrate. The common aromatic growth substrates for cometabolism are phenol and toluene. Application of toluene is limit because of its volatility and toxicity. Phenol is less toxic and has high water

solubility. Although phenol is also a regulated compound, it is readily biodegradable. It is often found in leachant of hazardous waste landfills and in the industrial wastes of the coke, petroleum and the chemical industries. Where wastes contain both phenol and TCE, or where phenol is available from other waste stream, phenol is likely to be the favored candidate for growth substrate. In other situations, phenol may still be the favored choice because it is easy to handle and does not have the mass transformation limitations of toluene, methane or other gaseous substrates.

2.10 Choice of reactor systems for cometabolism of TCE

Reactor configurations that have been evaluated for cometabolism of TCE include conventional completely-stirred tank reactors (Folsom and Chapman 1991; Coyle et al., 1993), fixed beds (Arvin 1991; Bilbo et al., 1992; Strand et al., 1991; Strandberg et al., 1989) expended beds (Phelp et al., 1990) and multi-stage systems. Muti-stage systems are designed to deal with toxicity and substrate competition (Alvarez-Cohen and McCarty 1991b; Mcfarland et al., 1992; Speital and Leonord 1992).

Sequencing batch reactors (SBRs) are a multi-stage reactor system that seems well suited for the conduct of cometabolic reactions. Conventional SBR systems consist of one or more tanks, each capable of substrate biodegradation and solids separation. Each tank processes influent wastes through a success of five cyclic operating periods: fill, react, settle, draw and idle (see Figure 2-3). Completion of the five periods constitutes a cycle. During the fill period, the liquid volume inside the tank increases from a set minimum volume in response to a predetermined maximum volume. Mixing or aeration or both can be carried out during all or part of the fill period to provide distinct, selective growth conditions. During the react period, flow is discontinued either by cessation of wastewater generation or by diversion of flow to another tank. In aerobic SBRs, aeration is provided to complete substrate removal. During the settling period, energy inputs to the tank are stopped and the suspended solids are allowed to flocculate

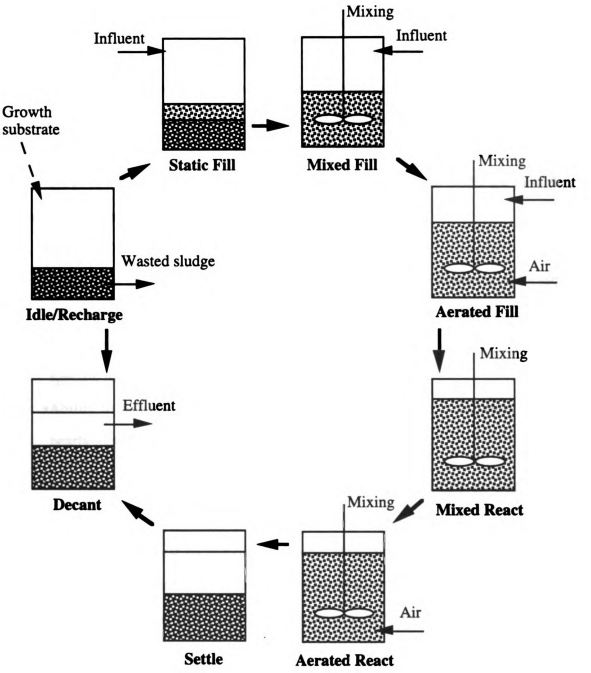

Figure 2-3 Typical SBR operating mode and its flexibilities in choosing or combining static fill, mixed fill, aerated fill, mixed react and aerated react. Proposed modification for cometabolic transformation was using idle period as the recharge stage that growth substrate was supplied to regenerate the cometabolic activity of cells.

and settle under quiescent conditions. The treated supernatant is then decanted to the minimum liquid volume level. Solids may be wasted from the tank as required to maintain the biomass at manageable levels. The tank remains as such either until wastewater production resumes (for a single tank system) or until other tanks making up the system are full and flow is diverted back to the first tank, initiating another cycle. An SBR accomplishes in time what traditional activated sludge systems accomplish in space in a series of continuous-flow reactors. The potential advantages of SBRs for hazardous waste treatment include

- •Ability of processes to handle periodic flows;
- •Possibility of tanks on- and off-lines to meet either short-term or seasonal variations;
- •Ability to periodically change environmental conditions, selecting or enriching specific microbial populations; and
- •Ability to better ensure biomass retention, as supernatant withdrawal occurs in nearly ideal quiescent conditions.

Conventional SBR operation can be modified for cometabolism by addition of a recharge stage after the decant period (see Figure 2-3). The recharge period rejuvenates cometabolism activity lost by toxicity or decay. During recharge, growth substrate is supplied to enrich or restore the cometabolizing populations. By incorporating a recharge stage, the SBR may be capable of stable and continuous cometabolism.

Literatures cited

Allsop, P. J. , M. Moo-Young , and G. R. Sullivan. "The dynamics and control of substrate inhibition in activated sludge." CRC Critic Reviews in Environmental Control 20 (1990): 115.

Alvarez-Cohen, L. M. and P. L. McCarty. "A cometabolic biotransformation model for halogenated aliphatic compounds exhibiting product toxicity,." Environ. Sci. Technol. 25 (1991a): 1381-1387.

Alvarez-Cohen, L. M. and P. L. McCarty. "Product toxicity and cometabolic competitive inhibition of chloroform and trichloroethylene transformation by methanotrophic resting cells." Appl. Environ. Microbiol. 57 (1991b): 1031-1037.

Alvarez-Cohen, L. M. and P. L. McCarty. "Two-stage dispersed-growth treatment of halogenated aliphatic compounds by cometabolism." Environ. Sci. Technol. 25 (1991c): 1387-1393.

Anderson, J. E. and P. L. McCarty. "Model for treatment of trichloroethylene by methanotrophic biofilms." Journal of Environmental Engineering 120 (2 1994): 379-400.

Anselmo, A. M., M. Mateus, J. M. S. Cabral, and J. M. Novais. "Degradation of phenol by immobilized cells of *Fusarium flocciferum*." Biotechnol. Letters 7 (12 1985): 889-894.

Arciero, D., T. Vannelli, M. Logan, and A. B. Hooper. "Degradation of trichloroethylene by the ammonia-oxidizing bacterium *Nitrosomonas europaea*." Bioch. and Bioph. Res. Commu. 159 (1989): 640-643.

Arvin, E. "Biodegradation kinetics of chlorinated aliphatic hydrocarbon in an aerobic fixed biofilm reactor." Wat. Res. 25 (7 1991): 873-881.

Auteinrieth, R. L., J. S. Bonner, A. Akgerman, and M. Okagun. "Biodegradation of phenolic wastes." Journal of Hazardous Materials 28 (1991): 29-53.

Bayly, R. C. and M. G. Barbour. "The degradation of aromatic compounds by the meta and genntistate pathways - biochemistry and regulation." In Microbial degradation of organic compounds, ed. D. T. Gibson. New York: Marcel Dekker, 1984.

Bayly, R. C., G. J. Wigmore, and D. I. McKenzie. "Regulation of enzymes of the *meta*-Cleavage pathway of *Pseudomonas putida*: the regulation is composed of two operons." J. Gen. Microbiol. 100 (1977): 71-79.

Beltrame, P., P. L. Beltrame, P. Carniti, and D Pitea. "Kinetics of phenol degradation by activated sludge in a continuous-stirred reactors." J. WPCF 52 (1 1980): 126-133.

Bilbo, C. M. , E. Arvin, H. Holst, and H. Spliid. "Modeling the growth of methane-oxidizing bacteria in a fixed biofilm." Wat. Res. 26 (3 1992): 301-309.

Blom, A., W. Harder, and A. Matin. "Unique and overlapping pollutant stress proteins of *Escherichia Coli*." Appl. Environ. Microbiol. 58 (1 1992): 331-334.

Bouwer, E. J., B. E. Rittmann, and P. L. McCarty. "Anaerobic degradation of halogenated 1- and 2-carbon organic compounds." Environ. Sci. Technol. 15 (1981): 596-599.

Bowman, J. P. and G. S. Sayler. "Optimization and maintenance of soluble methane monooxygenase activity in *Methylosinus trichosporium* OB3b." Biodegradation 5 (1994): 1-11.

Buswell, J. A. "Metabolism of phenol and cresols by *Bacillus stearothermophilus*." J. Bacteriol. 124 (3 1975): 1077-1083.

Conglio, W. A., K. Miller, and D. Mackeever. The occurrence of volatile organics in drinking water, criteria and standards. Environmental Protection Agent, 1980.

Criddle, C. S. "The kinetics of cometabolism." Biotechnol. Bioeng. 41 (1993): 1048-1056.

Criddle, C. S., J. T. Dewitt, and P. L. McCarty. "Reductive dehalogenation of carbon tetrachloride by *Escherichia coli* k-12." Appl. Environ. Microbiol. 56 (1990): 3247-3254.

D'Adamo, P. D. , A. F. Rozich, and A. F. Jr. Gaudy. "Analysis of growth data with inhibitory substrate." Biotechnol. Bioeng. 26 (1984): 397.

Dabrock, B., J. Riedel, J. Bertram, and G. Gottschalk. "Isopropylbenze (cumene) - a new substrate for isolation of trichloroethene-degrading bacteria." Archives of Microbiology 158 (1992): 9-13.

Dalton, H., S. D. Prior, D. J. Leak, and S. H. Stanley. "Regulation and control of methane monooxygenase." In Microbial growth on C1 compounds, ed. R. L. Crawford and R. S. Hanson. 75-82. Washington, DC: Ammerican Society for Microbiology Press, 1984.

Dalton, H. and D. I. Stirling. "Co-metabolism." Phil. Trans. R. Soc. 297 (1982): 481-496.

Ensign, S. A., M. R. Hyman, and Arp. D. J. "Cometabolic degradation of chlorinated alkenes by alkene monooxygenase in a propylene-grown *Xanthobacter* strain." Appl. Environ. Microbiol. 58 (9 1992): 3038-3046.

Ewers, J., D. Freier-Schroder, and H. J. Knackmuss. "Selection of trichloroethene (TCE) degrading bacteria that resist inactivation by TCE." Archives of Microbiology 154 (1990): 410-413.

Feist, C. F. and G. D. Hegeman. "Phenol and benzoate metabolism by *Pseudomonas putida*: regulation and tangential pathway." J. Bacteriol. 100 (2 1969): 869.

Fox, B. G., J. G. Borneman, L. P. Wackett, and J. D. Lipscomb. "Haloalkane oxidation by the soluble methane monooxygenase from *Methylosinus trichosporium* OB3b: mechanism and environmental implication." Biochemistry 29 (27 1990): 6419-6427.

Gaal, A. and H. Y. Neujahr. "Metabolism of phenol and resorcinol in *Trichosporon cutaneum*." J. Bacteriol. 137 (1 1979): 13-21.

Galli, R. and P. L. McCarty. "Biotransformation of 1,1,1-trichloroethane, trichloromethane, and tetrachloromethane by a *Clostridium* sp." Appl. Environ. Microbiol. 51 (1989): 720-724.

Henry, S, M. and D. Grbic-Galic. "Inhibition of TCE oxidation by the transformation intermediate carbon monooxide." Appl. Environ. Microbiol. 57 (1991): 1770-1776.

Henry, S. M. and D. Grbic-Galic. "Effect of mineral media on trichloroethylene oxidation by acquifer methanotrophs." Micrb. Ecol. 20, (1990): 151-169.

Josephson, J. "Implementing superfund." Environ. Sci. Technol. 20 (1 1986): 23.

Kamlet, M. J., R. M. Doherty, G. D. Veith, R. W. Taft, and M. H. Abraham. "Solubility properties in polymers and biological media. 7. an analysis of toxicant properties that influence inhibition of bioluminescence in photobacterium phosphoreum (The microtox test)." Environ. Sci. Technol. 20 (7 1986): 690.

Kotturi, G., C. W. Robinson, and W. E. Inniss. "Phenol degradation by a psychrotrophic strain of *Pseudomonas putida*." Applied Microbiology and Biotechnology 34 (1991): 539-543.

Little, C. D., A. V. Palumbo, S. E. Herbes, M. E. Lidstrom, R. L. Tyndall, and P. J. Gilmer. "Trichloroethylene biodegradation by a methane-oxidizing bacterium." Appl. Environ. Microbiol. 54 (4 1988): 951-956.

Mackay, D. and P. J. Leinonen. "Rate of evaporation of low-solubility contaminants from water bodies to atmosphere." Environ. Sci. Technol. 9 (13 1975): 1178.

Mcfarland, M. J., C. M. Vogel, and J. C. Spain. "Methanotrophic cometabolism of TCE in a two-stage bioreactor system." Wat. Res. 26 (2 1992): 259-265.

Miller, R. E. and F. P. Guengerich. "Oxidation of trichloroethylene by live microsomal P-450 evidence for chlorine migration state not involving trichloroethylene oxide." Biochemistry 27 (5 1982): 1090-1097.

Monod, J. "The growth of bacterial cultures." Annu. Rev. Microbiol. 3 (1949): 371-394.

Nelson, M. K., S. O. Montgomery, E. J. O'Neill, and P. H. Pritchard. "Aerobic metabolism of trichloroethylene by a bacterial isolate." Appl. Environ. Microbiol. 52 (2 1986): 383-384.

Nelson, M. J. K., S. O. Montgomery, W. R. Mahaffey, and P. H. Pritchard. "Biodegradation of trichloroethylene and involvement of an aromatic biodegradative pathway." Appl. Environ. Microbiol. 53. (5 1987): 949-954.

Nelson, M. J. K., S. O. Montgomery, and P. H. Pritchard. "Trichloroethylene metabolism by microorganism that degrade aromatic compounds." Appl. Environ. Microbiol. 54 (2 1988): 604-606.

Oldenhuis, R., R. L. J. M. Vink, D. B. Janssen, and B. Witholt. "Degradation of chlorinated aliphatic hydrocarbons by *Methylosinus trichosporium* OB3b expressing soluble methane monooxygenase." Appl. Environ. Microbiol. 55 (11 1989): 2819-2826.

Pawlowsky, P and J. A. Howell. "Mixed culture biooxidation of phenol. I. determination of kinetic parameters." Biotechnol. Bioeng. 15 (1973): 889-896.

Phelp, T. J., J. J. Niedzielski, R. M. Schram, S. E. Herbes, and D. C. White. "Biodegradation of trichloroethylene in continuous-recycle expended-bed bioreactor." Appl. Environ. Microbiol. 56 (1990): 1702-1709.

Rizzuti, L. and V. Augueliaro. "Kinetic parameter estimation in monoculture and monosubstrate biological reactors." Can. J. Chem. Eng. 60 (1982): 608.

Saez, P. B. and B. E. Rittmann. "Biodegraation kinetics of 4-chlorophenol, an inhibitory co-metabolite." Research Journal of the Water Pollution Control Fedration 63 ((6), 1991): 838-847.

Schaumburg, F. D. "Banning trichloroethylene: responsible reaction or overkill?" Environ. Sci. Technol. 24 (1 1990): 17-22.

Schmidt, S. K., S. Simkins, and M. Alexander,. "Models for kinetics of biodegradation of organic compounds not supporting growth." Appl. Environ. Microbiol. 50, (1985): 323-331.

Speitel, G. E. and J. M. Leonard. "A sequencing biofilm reactor for the treatment of chlorinated solvents using methanotrophs." Water Environment Research 64 (5 1992): 712.

SoKol, W. "Uptake rate of phenol by *Pseudomonas putida* grown in unsteady state." Biotechnol. Bioeng. 32 (1988): 1097-1103.

Stanley, S. H., S. D. Prior, D. J. Leak, and H. Dalton. "Copper stress underlies the fundamental change in intracellular location of methane mono-oxygenase in methane-oxidizing organisms: studies in batch and continuous cultures." Biotechnology Letter 5 (7 1983): 487-492.

Strand, S. E., J. V. Wodrivh, and H. D. Stensel. " Biodegradation of chlorinated solvents in a sparged, methanotrophic biofilm reactor." Research Journal WPCF 63 (6 1991): 859-867.

Strandberg, G. W., T. L. Donaldson, and L. L. Farr. "Degradation of trichloroethylene and trans-1,2-dichloroethylene by a methanotrophic consortium in a fixed-film, packed-bed bioreactor." Environ. Sci. Technol. 23 (1989): 1422-1425.

Szetela, P. W. and T. Z. Winnicki. "A novel method for determining the parameters of microbial kinetics." Biotechnol. Bioeng. 23 (1981): 1485-1490.

Templeton, L. L. and C. P. L. Grady. "Effect of culture history on determination of biodegradation kinetics by batch and fed batch techniques." J. WPCF 60 (1989): 651.

Tischler, L. F. and W. W. Jr. Eckenfelder. "Linear substrate removal in the activated sludge process." In Advances in Water Pollution Research, 361-374. 2. Oxford, England: Pergamon, 1969.

Tsien, H. C., G. A. Brusseau, R. S. Hanson, and L. P. Wackettet. "Biodegradation of trichloroethylene by *Methylosinus trichosporium* OB3b." Appl. Environ. Microbiol. 55 (12 1989): 3155-3161.

Vanilli, T., M. Logan, and A. B. Hooper. "Degradation of halogenated aliphatic compounds by the ammonia-oxidizing bacterium *Nitrosomonas europaes*." Appl. Environ. Microbiol. 56 (1990): 1169-1171.

Vogel, T. M., C. S. Criddle, and P. L. McCarty. "Transformation of halogenated aliphatic compounds." Environ. Sci. Technol. 21 (1987): 722-736.

Wacket, L. P., G. A. Brusseau, S. R. Householder, and R. S. Hanson. "Survey of microbial oxygenases: trichloroethylene degradation by propane-oxidizing bacteria." Appl. Environ. Microbiol. 55 (1 1989): 2960-2964.

Wackett, L. P. and D. T. Gibson. "Degradation of trichloroethylene by toluene dioxygenase in whole cell studies with *Pseudomonas putida* F1." Appl. Environ. Microbiol. 54 (1988): 1703-1708.

Wackett, L. P. and S. R. Householder. "Toxicity of trichloroethylene to *Pseudomonas putida* F1 is mediated by toluene dioxygenase." Appl. Environ. Microbiol. 55 (10 1989): 2723-2725.

Weast, R. C., ed. CRC handbook for chemistry and physics. 73 ed., Boca Raton, Florida: CRC Press, Inc., 1992.

Westrick, J. J., J. W. Mello, and R. F. Thomas. "The groundwater survey." J. Am. Water Works Assoc. 76 (1984): 52.

Wilson, J. T. and B. H. Wilson. "Biotransformation of trichloroethylene in soil." Appl. Environ. Microbiol. 49 (1985): 242-243.

Winter, R. B., K.-M. Yen, and B. D. Ensley. "Efficient degradation of trichloroethylene by a recombinant *Escherichia Coli*." Bio/Technology 7 (3 1989): 282.

Yang, R. D. and A. E. Humphrey. "Dynamic and steady state studies of phenol biodegradation in pure and mixed culture." Biotechnol. Bioeng. (1975): 1599-1615.

CHAPTER 3

USE OF NUMERICAL SIMULATION FOR DESIGN OF SEQUENCING BATCH REACTOR

3.1 Introduction

Sequencing batch reactors (SBRs) are established alternatives to conventional continuous flow systems. SBRs are flexible in design and operation, well-suited for nutrient removal, and give excellent solids separation (Irvine 1989) Substrate gradients are easily established, redox conditions changed, reaction periods modified, and substrates added as needed. These manipulations make it possible to enhance the growth of organisms that carry out useful functions such as nutrient removal, while preventing the growth of organisms that can cause problems, such as bulking. The creation of selective niches within SBRs offers exciting possibilities for innovative engineering design.

Current design procedures for SBRs are highly empirical - relying on rule-of-thumb criteria, such as hydraulic detention time and substrate loading rates (Arora and others 1985). Such approaches typically produce conservative designs, are limited in range of application, and lack predictive or simulation capabilities. Simulation capabilities are only achievable using dynamic models that distinguish between the different types of organisms, substrates, and solids that may enter or be produced within an SBR. Development and verification of such models is complex because SBRs are inherently non-steady state, and tools for the verification of changes in microbial community structure have been lacking. It now appears likely, however, that the latter

problem will be at least partially overcome by improved methods of microbial community analysis (signature molecules, gene probes, antibody probes, image analysis, etc.). These methods should provide insight into factors affecting the activity of key populations and the relationships between different microbial groups. If this understanding can be captured in verifiable kinetic expressions, computer simulations of a range of reactor design and operating scenarios seems possible.

In order to develop a reasonable computer simulation tool, a wastewater classification scheme is needed that distinguishes between substrates, microbial populations, and non-viable suspended solids. For demonstration purposes, we adopted a simplified version of the IAWPRC classification scheme (Henze and others 1987). Mass balance expressions are developed for each constituent and organism type. A solution representing long-term stable operation of the SBR is obtained by repeated numerical solution of the mass balance equations, repeated application of the selected solids wasting schedule, and repeated application of constraints on SBR operation. This long-term repeating pattern is used as the basis for SBR design. Predictions of changes in the concentration and age of specific cell types once the long term operating pattern is established should facilitate simulation of age-related enzyme activities within specific populations.

3.2 General approach

3.2.1 Constraints on SBR design

Time constraints

The operating cycle for a conventional SBR consists of five distinct time periods: fill (t_f), react (t_r), settle (t_s), decant (t_d) and idle (t_i), where:

$$t_c = t_f + t_r + t_s + t_d + t_i \qquad (3\text{-}1)$$

For N_r reactors treating a continuous stream of wastewater, the time required for the first reactor to complete its react, settle, decant and idle periods must equal the time required to sequentially fill the remaining N_r-1 reactors:

$$(N_r - 1)t_f = t_r + t_s + t_d + t_i \qquad (3\text{-}2)$$

Substituting equation 3-2 into equation 3-1,

$$t_f = t_c / N_r \qquad (3\text{-}3)$$

As indicated by equation 3-3, selection of cycle time and the number of reactors fixes t_f. React time depends upon the treatment requirements and the kinetics of degradation. Settling time depends upon the solids settling characteristics, with a normal value of 0.5 - 1 hour for aerobic municipal wastewater treatment. Settle and decant time should be chosen so that $t_s + t_d < 3\ hr$ to avoid sludge rising and undesired odor caused by anaerobic reactions. Sufficient idle time t_i is needed to accommodate changes in fill and react times when flow and substrate loadings vary or when solids are wasted. Typical values for each of the different time periods are provided in Table 3-1.

Table 3-1. Typical values of the required time for each operating stages in SBRs

Parameter	Unit	Typical value	Reference
t_f	hr	25% t_c	Arora et al. 1985.
t_r	hr	35% t_c 0.5 ~ 2*	Arora et al. 1985. Irvin 1989
t_s**	hr	0.5~1.5 20%t_c	Irvin 1989 Arora et al. 1985.
t_d**	hr	15% t_c	Arora et al. 1985.
t_i	hr	5% t_c	Arora et al. 1985.
θ	hr	12~50	Mecalf & Eddy.1991
θ_c	day	NA	
r	dimensionless	25~75 %	Irvin 1989.

* For domestic waste only.

** To avoid rising sludge, Irvine (1989) suggested $t_s + t_d < 3$ hr.

Volume constraints

Volume restrictions arise because each SBR vessel is both a reactor and as a settling tank. Consequently, part of the volume (V_o) is reserved for storage or "recycle" of settled solids from one cycle to the next. The recycled volume contains the settled solids after decanting. The total volume of a reactor is made up of the volume of settled solids and the wastewater volume added during the fill period:

$$V_{SBR} = t_f Q + V_o \tag{3-4}$$

where: V_{SBR} = reactor volume and Q = influent flowrate.

The relationship between V_o and V_{SBR} is given by:

$$V_{SBR} = V_o/r = Q(t_o + t_f) \tag{3-5}$$

where: $r = V_o/V_{SBR}$ = recycle ratio and $t_o = V_o/Q$ = the time theoretically required to fill the SBR to a volume V_o at a flowrate Q.

Substituting $Q = V_o/t_o$ into equation 3-5 and solving for t_o gives

$$t_o = t_f\left(\frac{r}{1-r}\right) \tag{3-6}$$

Substituting equation 3-6 into equation 3-5 gives:

$$V_{SBR} = \left(t_f + t_f\left(\frac{r}{1-r}\right)\right)Q \tag{3-7}$$

Equation 3-7 indicates that once t_f and r are chosen, the volume of an SBR is specified. Another volume relationship of interest in SBR design is the hydraulic residence time, θ. For an SBR system, θ can be defined as:

$$\theta = \frac{N_r V_{SBR}}{Q} = \frac{N_r t_f}{1-r} = \frac{t_c}{1-r} \tag{3-8}$$

Typical values for θ and r are provided in Table 3-1.

3.2.2 Mass balance equations

Success of the general design approach used in this work depends upon the development of accurate mass balance equations for dissolved and particulate matter entering the SBR, produced within it, or consumed within it. For the fill period, the mass balance expressions are:

$$\frac{dS_i}{dt} = \frac{Q(S_i^\circ - S_i)}{V} + r_{S_i} \qquad (3\text{-}9)$$

$$\frac{dX_j}{dt} = \frac{Q(X_j^\circ - X_j)}{V} + r_{X_j} \qquad (3\text{-}10)$$

where: X_j= concentration of suspended solid of type j , X_j° = influent concentration of X_j, Q = influent flowrate, r_{X_j} = rate of production or consumption of suspended solid of type j (mass of solid type j produced or consumed per unit volume per day), V = volume of water in the SBR. To solve equations 3-9 and 3-10, r_{S_i} and r_{X_j} must be specified, and initial conditions provided for S_i and X_j.

For the react period, the mass balance expressions are:

$$\frac{dS_i}{dt} = r_{S_i} \qquad (3\text{-}11)$$

$$\frac{dX_j}{dt} = r_{X_j} \qquad (3\text{-}12)$$

To solve equations 3-11 and 3-12, kinetic expressions for r_{S_i} and r_{X_j} must be defined, and initial conditions provided for S_i and X_j. Because the end of the fill period is the beginning of the react period, initial conditions for the react period are obtained from solution of equations 3-9 and 3-10 when $t = t_f$.

3.2.3 Use of the CSTR steady state solution to obtain initial condition estimates

The choice of initial conditions for equations 3-9 and 3-10 is not readily apparent. The initial conditions of interest are those that occur once the reactor has achieved a stable pattern of operation: at the beginning of each period of solids accumulation, just after a wasting event. Repeated solution of the mass balance equations along with repeated application of a specified solids wasting schedule eventually yields a repeating pattern. In the repeating solution, each solid type accumulates during the solids storage period, but is restored to its original mass at the beginning of the next solids storage period, immediately after wasting. If the first guess of initial concentrations at the beginning of the solids storage period is far from the values obtained for the repeating pattern, many computations will be needed to arrive at the repeating solution. To avoid this problem, a reasonable set of initial conditions is obtained by considering a limiting case, where t_c approaches zero and N_r approaches 1. Under such conditions, SBR operation approaches that of a continuous stirred tank reactor (CSTR). Solution of the steady state CSTR equations for solids and substrate at a specified solids residence time provides a reasonable first guess of initial conditions for the SBR. This approach has the added advantage of facilitating comparison of CSTR and SBR volume requirements. For a CSTR operating at a specified mean cell residence time, the steady state solution for each solid type is derivated in Appendix I and given by:

$$(X_j)_{ss} = \frac{\theta c}{\theta} X_j^o + \theta_c r_{xj} \qquad (3\text{-}13)$$

An initial guess for t_c can be obtained from the steady state CSTR solution by computing θ for the CSTR and relating it to t_c by equation 3-8:

$$(t_c)_{est} = \theta_{CSTR}(1\text{-}r) \qquad (3\text{-}14)$$

3.2.4 Mean solids retention time and wasting schedules

Solids tend to accumulate within an SBR and must be removed periodically. Assuming negligible loss of solids in the effluent, the mass of solids wasted at the end of a solids storage period must equal the mass of solids that accumulated over that same period. Mathematically, this can be expressed as:

$$Q^w X = \frac{wV_o X}{N_w t_c} \qquad (3\text{-}15)$$

where Q^w = equivalent daily wasting rate (wasting rate averaged over the entire storage period), w = volumetric fraction of settled solids wasted at the end of each solids storage period, N_w = number of cycles per solids storage period, so that $N_w t_c = t_{sp}$ = solids storage period. Equation 3-15 can be reformulated to give the mean solids retention time for an SBR (Irvine 1989):

$$SRT = V_o/Q^w = N_w t_c/w = t_{sp}/w \qquad (3\text{-}16)$$

If SRT, and solid storage time are known or specified, equation 3-16 can be used to calculate the fraction of the settled solids that must be wasted at the end of each solids storage period.

The frequency of solids removal events may vary from once a cycle to once a month or more. Wasting becomes mandatory if either of the following conditions occur: (1) solids concentration during the react period exceeds some maximum allowable concentration, X_{max}, (2) the settled solids volume, $V_{settled}$, exceeds the space available for solids storage, V_o. X_{max} exists because of limitations on oxygen mass transfer (Benefield and Randall 1980). A typical upper limit when oxygen is supplied by aeration is ~ 5000 mg/L; when oxygen is supplied by pure oxygen, X_{max} ~ 8000 mg/L (Metcalf & Eddy 1991). Limits on $V_{settled}$ can be predicted from settleability tests, such as the sludge volume index (SVI):

$$V_{settled} = \frac{SVI \bullet X}{10^6} V_{SBR} \qquad (3\text{-}17)$$

V_o must be greater than $V_{settled}$; otherwise, suspended solids will be lost from the reactor during the decant period.

3.2.5 Dynamic cell age

In a steady state CSTR with recycle, mean cell residence time θ_c is a constant and is controlled by solids wasting. Solids residence time and mean cell residence time are equal and constant for all types of organisms and suspended solids. In an SBR, the average age of a given microbial population varies with time: decreasing during periods of feast and growth and increasing during periods of famine and decay. Consequently, the concept of dynamic cell age is more meaningful measure of cell physiology than SRT. In principle, cell age can be linked to the level of expression of enzyme and/or RNA activities of a specific microbial population (Shu 1961).

In the present article, we use dynamic cell age *(A)* to describe the mean cell age of a designated microbial population. Vaccari et al. (1985) have previously described application of the dynamic sludge age *(DSA)* concept to non-steady state activated sludge systems. The derivation of equations for *DSA* is complex, and the reader is referred to the original references for details (Vaccari and others 1985; von Foerster 1959). As derived by Vaccari et al. (1988), computation of *A* for the case where no solids are wasted or lost over the period t is given by (Vaccari and others 1988):

$$A = (A_o + t/2)M_{ao}/M_a + t/2 \qquad (3\text{-}18)$$

where A = dynamic cell age at time t, A_o = dynamic cell age at time 0, M_{ao} = active biomass at time 0, M_a = activate biomass at time t. Equation 3-18 can be used to calculate A in the fill and react periods when M_{ao} and M_a are known. During the settle, decant, and idle periods, we assume that $M_{ao}/M_a = 1$ so that $A = A_o + t$.

Different microorganism types have different growth rates and different limits on cell age. A limiting age occurs when cells are growing at their maximum specific growth rate μ_m so that $dM_a/dt = \mu_m M_a$. A minimum age A_{min} occurs when the cells are growing at this rate. Its value can be computed by taking the time derivative of equation 3-18, setting it equal to zero, solving for A_o, then substituting the result back into equation 3-18. The resulting expression is:

$$A_{min} = \frac{1}{2\mu_m}\left(\frac{Mao}{Ma} + 1\right) + \frac{t}{2} \qquad (3\text{-}19)$$

In the limit, as t approaches 0 and M_a approaches M_{ao}, A_{min} approaches $1/\mu_m$:

$$(A_{min})_{lim} = \frac{1}{\mu_m} \qquad (3\text{-}20)$$

If a design choice for SRT is selected which is less than $(A_{min})_{lim}$ for a given desired microbial population, then that population will not be maintained in the SBR during long-term operation. Accordingly, design values for SRT should be chosen that are significantly larger than $(A_{min})_{lim}$ for the slowest growing population required for proper reactor performance. Table 3-2 summarizes $(A_{min})_{lim}$ values for common organisms types used in wastewater treatment.

3.2.6 Generic solution procedure

The flowchart of Figure 3-1 summarizes computational procedures used to obtain a repeating solution representing long-term SBR operation. Input parameters include waste characteristics, SBR operating parameters, and rate coefficients for degradation or production of solids and substrates. The CSTR steady state solution is calculated and used as the first guess for initial conditions to solve the differential equations describing solids and substrate concentrations during the fill and react periods. Wasting requirements are satisfied at the end of each cycle. The most recent calculations of solid and substrate concentrations are used to revise initial conditions, and the calculations are repeated.

Table 3-2 Minimum cell age for different group of microbial populations

Function of Microbial populations	μ_m (day^{-1})	$(A_{min})_{lim}$	Reference
Aerobic			
Organic removal	8	0.13	(1)
Nitrification	0.72	1.39	(2)
Sulfur oxidation	1.5	0.67	(3)
Ferrous oxidation	0.45	2.22	(3)
Hydrogen oxidation	1.8	0.56	(3)
Anaerobic			
Denitrification	0.3	3.3	(2)
Sulfate respiration	0.9	1.11	(2)
Methane fermentation			
Fats	0.26	3.85	(3)
Proteins	0.68	1.47	(3)
Carbohydrates	1.9	0.53	(3)
Sewage sludge	0.68	1.47	(3)

Reference: (1) Grady and Lim 1980, (2) Metcalf and Eddy 1992, (3) Lawrence and McCarty 1970.

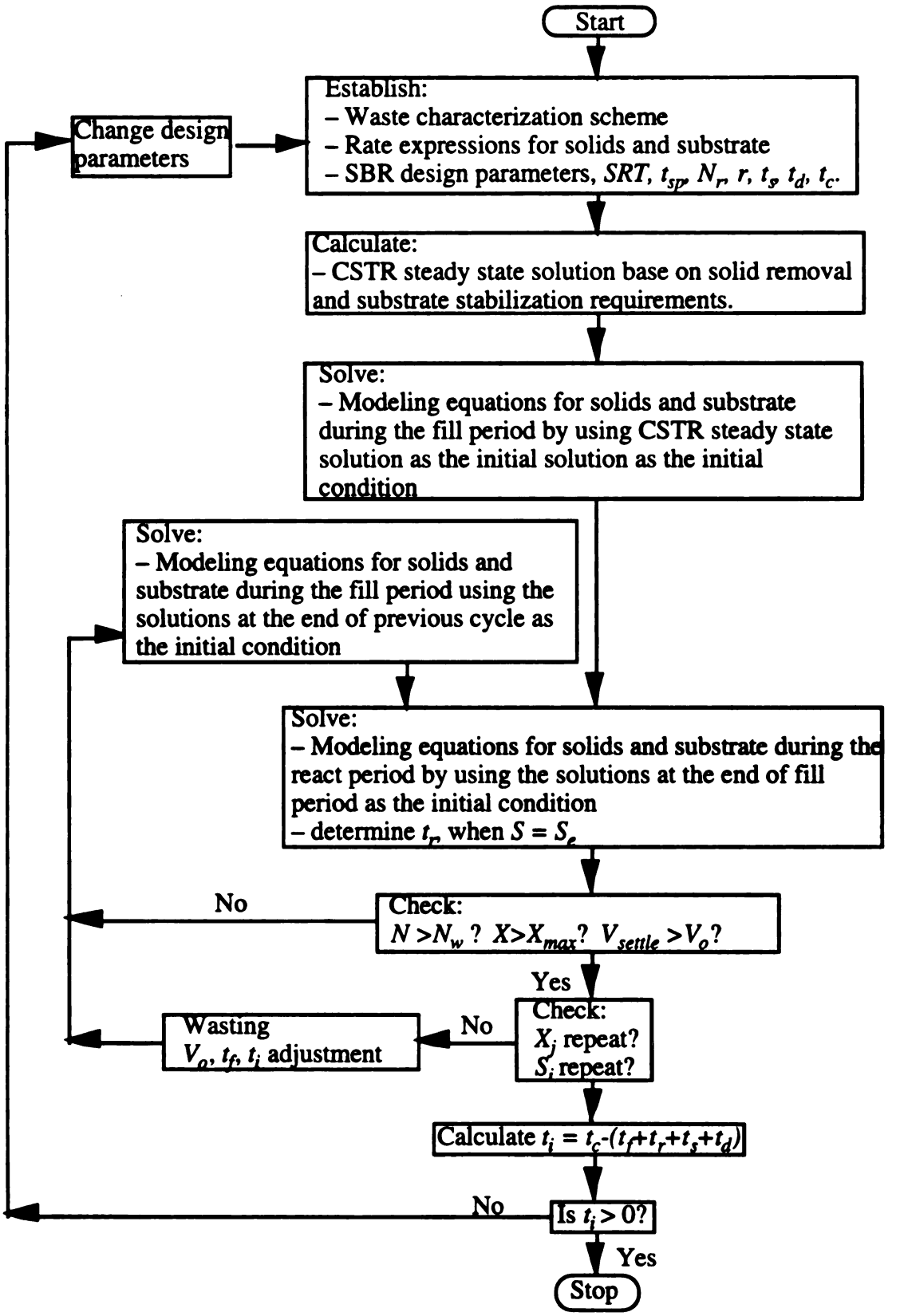

Figure 3-1 Flowchart for numerical simulation and design of an SBR system

Eventually, the solids and substrate concentrations at the beginning of a new solids storage period equal the solids and substrate concentrations at the beginning of the previous solids storatge period. This repeating solution represents the long-term stable pattern of operation.

Overall, two levels of iteration control are involved. The first is the number of operating cycles (N). Solid and substrate concentrations iterate until the wasting occurs (i.e., $N=N_w$). The second iteration control parameter is the solid and substrate concentrations that continue to iterate until the repeating solution is obtained.

3.3 Application to domestic wastewater treatment

3.3.1 Choice of wastewater classification scheme

In order to implement the solution strategy described in the previous sections, mass balances must be obtained on the different types of suspended solids and substrates within the SBR. Many possible classification schemes are possible, and the appropriate choice will depend upon the system under consideration. Figure 3-2 illustrates a scheme used for organics oxidation by aerobic heterotrophs, along with ammonia oxidation by nitrifiers. The classification approach used is similar to that of IAWPRC (Henze and others 1987). The first level of classification entails separation of suspended solids from dissolved matter. This distinction is made by filtration of the wastewater through glass fiber filters (APHA 1989). Suspended solids are further classified as either fixed or volatile by igniting them at 550°C for one hour in a muffle furnace (APHA 1989). In general, fixed suspended solids constitute the inorganic fraction of suspended solids (X_{in}) while the volatile suspended solids represent the organic portion of suspended solid.

Biodegradability is an important characteristic in the classification scheme of Figure 3-2. If dissolved organic matter is refractory, it passes through the biological

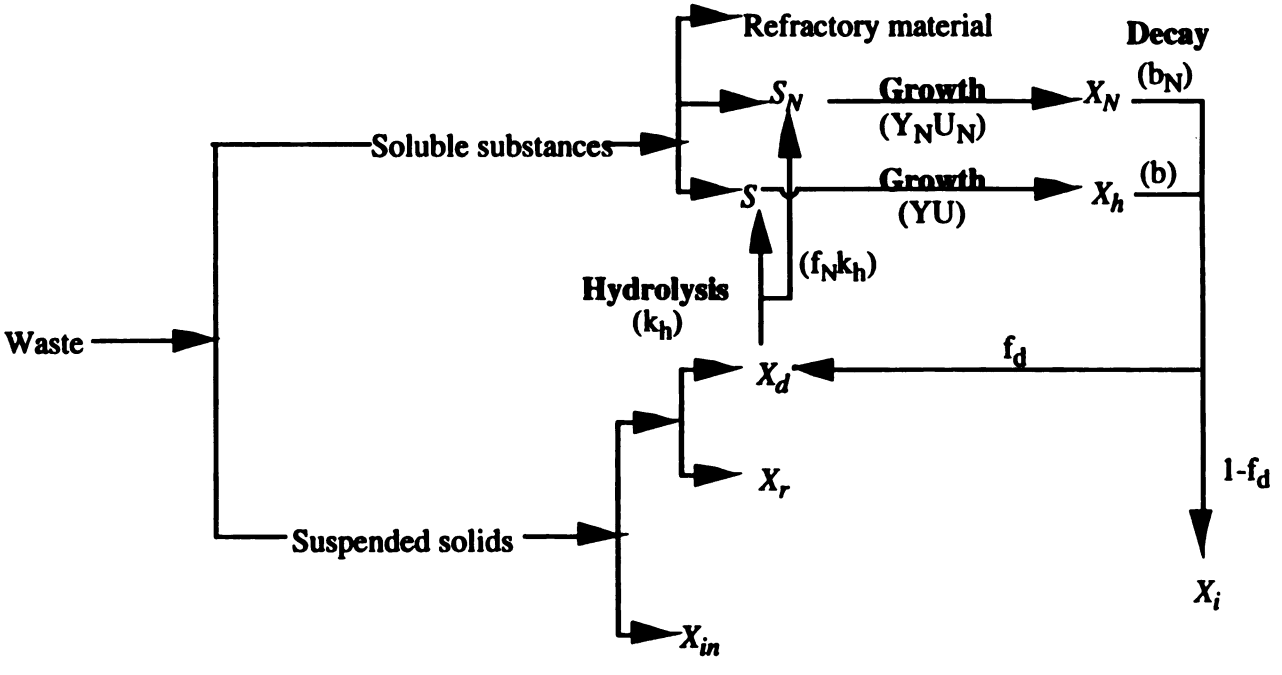

Figure 3-2 Waste characteristics and their conversions in biological processes. Where, S_i = inert substrate, S = readily biodegradable organic substrate, S_N = ammonia, X_h = active biomass ofheterotrophs; X_N = active nitrifying biomass, X_d = biodegradable suspended solids, X_r = refractory suspended solid, X_i = inert biomass from decay of X_a, X_{in} = inorganic suspended solid.

treatment process unchanged; if it is biodegradable, it is consumed for cell growth and maintenance. Degradable suspended solids (X_d) are removed by wasting and are converted into dissolved biodegradable substrate by the hydrolytic action of extracellular enzymes; refractory suspended solids (X_r) are only removed by wasting. Active heterotrophic biomass (X_h) is produced by growth on soluble biodegradable organics and is lost by decay. Active nitrifying biomass (X_N) is produced by growth on ammonia. Decay is treated as a lumped parameter, including endogenous decay, death, predation, and lysis. Decay is assumed to convert active biomass into biodegradable particulate matter (X_d) and inert particulate matter (X_i).

3.3.2 Choice of kinetic parameters

The selective pressures in an SBR are significant and can result in communities with kinetic properties that are not predictable. Accordingly, bench- and pilot-scale testing are recommended to establish appropriate kinetic expressions and coefficients.

For illustration purposes, we assumed saturation kinetics for substrate removal and first order kinetics for the hydrolysis and decay of suspended solids. Rate expressions for each type of solid and substrate are summarized in Table 3-3, and the corresponding differential equations for the fill and react periods are summarized in Tables 3-4 and 3-5, respectively. Steady state CSTR solutions are provided in Table 3-6. The steady state CSTR solutions are used as the initial conditions for fill period of the first cycle.

Although saturation kinetics are used in these examples, the design and simulation procedure outlined here is readily adaptable to different rate expressions, appropriate to the system under consideration. Mass balance equations are obtained by substituting the appropriate rate equation into equations 3-9 - 3-12.

Table 3-3 Assumed rate expressions for each type of solids and substrate categorized in Figure 3-2.

Wastewater constituent	Rate expression
X_r	0
X_{in}	0
X_d	$-k_h X_d + f_d b X_h + f_d b_N X_N$
X_h	$-bX_h + \frac{YkSX_h}{K_s + S}$
X_i	$(1-f_d)bX_h + (1-f_d)b_N X_N$
X_N	$-b_N X_N + \frac{Y_N k_N S_N X_N}{K_N + S_N}$
S	$-\frac{kSX_a}{K_s + S} + k_h X_d$
S_N	$-\frac{k_N S_N X_N}{K_N + S_N} + f_N k_h X_d$

Table 3-4 Mass balance equations and solutions for SBR in fill period

Component	Mass balance equation
X_r	$\frac{dX_r}{dt} = \frac{X_r^o - X_r}{t + t_o}$
X_{in}	$\frac{dX_{in}}{dt} = \frac{X_{in}^o - X_{in}}{t + t_o}$
X_d	$\frac{dX_d}{dt} = \frac{X_d^o - X_d}{t + t_o} - k_h X_d + f_d b X_h + f_d b_N X_N$
X_h	$\frac{dX_h}{dt} = \frac{X_h^o - X_h}{t + t_o} - bX_h + \frac{YkSX_h}{K_s + S}$
X_N	$\frac{dX_N}{dt} = \frac{X_N^o - X_N}{t + t_o} - b_N X_N + \frac{Y_N k_N S_N X_N}{K_N + S_N}$
X_i	$\frac{dX_i}{dt} = \frac{X_i^o - X_i}{t + t_o} + (1-f_d)bX_h + (1-f_d)b_N X_N$
S	$\frac{dS}{dt} = \frac{S^o - S}{t + t_o} - \frac{kSX_h}{K_s + S} + k_h X_d$
S_N	$\frac{dS_N}{dt} = \frac{S_N^o - S_N}{t + t_o} - \frac{k_N S_N X_N}{K_N + S_N} + f_N k_h X_d$

Table 3-5 Mass balance equations and solutions for SBR in react period

Component	Mass balance equation
X_r	$\frac{dX_r}{dt} = 0$
X_{in}	$\frac{dX_{in}}{dt} = 0$
X_d	$\frac{dX_d}{dt} = -k_h X_d + f_d b X_h + f_d b_N X_N$
X_h	$\frac{dX_h}{dt} = -bX_h + \frac{YkSX_h}{K_s + S}$
X_N	$\frac{dX_N}{dt} = -b_N X_N + \frac{Y_N k_N S_N X_N}{K_N + S_N}$
X_i	$\frac{dX_i}{dt} = (1 - f_d) b X_h + (1 - f_d) b_N X_N$
S	$\frac{dS}{dt} = -\frac{kSX_h}{K_s + S} + k_h X_d$
S_N	$\frac{dS_N}{dt} = -\frac{k_N S_N X_N}{K_N + S_N} + f_N k_h X_d$

Table 3-6. Steady-state solutions for solids and substrate in a CSTR with sludge recycle

Solids or substrate	Steady-state solution
X_r	$\frac{\theta_c}{\theta} X_r^\circ$
X_{in}	$\frac{\theta_c}{\theta} X_{in}^\circ$
X_d	$\frac{\theta_c}{\theta}\left[\frac{X_d^\circ}{(1+k_h\theta_c)} + \frac{f_d b\theta_c Y(S^\circ - S)}{(1+k_h\theta_c)(1+b\theta_c)} + \frac{f_d b_N \theta_c Y_N (S_N^\circ - S_N)}{(1+k_h\theta_c)(1+b_N\theta_c)}\right]$
X_h	$\frac{\theta_c}{\theta}\left[\frac{Y(S^\circ - S)}{1+b\theta_c}\right]$
X_N	$\frac{\theta_c}{\theta}\left[\frac{Y_N(S_N^\circ - S_N)}{1+b_N\theta_c}\right]$
X_i	$\frac{\theta_c}{\theta}\left[\frac{Y(S^\circ - S)(1-f_d)b\theta_c}{1+b\theta_c} + \frac{Y_N(S_N^\circ - S_N)(1-f_d)b_N\theta_c}{1+b_N\theta_c}\right]$
S	$\frac{(1+b\theta_c)K_s}{\theta_c(Yk-b)-1}$
S_N	$\frac{(1+b_N\theta_c)K_N}{\theta_c(Y_N k_N - b_N)-1}$
MLSS	$\sum X$

3.3.3 Choice of treatment objectives

Treatment criteria include effluent standards and requirements for stabilization. Effluent standards for domestic wastewater typically include standards for BOD removal, ammonia removal, and suspended solids removal. For an SBR, the effluent suspended solids standards are typically satisfied without difficulty. As a result, soluble substrate removal and overall waste biological stabilization are the critical design objectives. The efficiency of substrate removal (E_s) is calculated from the expression:

$$E_s\,(\%) = 100(S^o - S_e)/S^o \qquad (3\text{-}21)$$

Overall waste biological stabilization (E) can be defined as the percentage of biodegradable material removed during treatment (including soluble and suspended forms). In general terms,

$$E = \frac{100\,[(\text{input total COD}_b + \text{input NOD}) - (\text{output total COD}_b + \text{output NOD})]}{\text{input total COD}_b + \text{input NOD}}$$

Total COD_b is total ***biodegradable*** soluble and suspended COD. For a CSTR,

$$E_{CSTR}(\%) = \frac{100\left[Q(S_o + X_d^o\gamma_{Xd}) - \frac{V}{\theta_c}(X_d^o\gamma_{Xd} + X_a^o\gamma_{Xa}) - QS_e\right]}{Q(S_o + X_d^o\gamma_{Xd})} \qquad (3\text{-}22)$$

where: γ_{Xd} = COD to weight ratio for biodegradable suspended solids (mg COD /mgVSS); γ_{Xa} = COD to weight ratio for biomass = 1.42 mg COD/mg VSS.

For an SBR,

$$E_{SBR}(\%) = \frac{100\left[Qt_fN_w(S^o + X_d^o\gamma_{Xd}) - (\sum_{N=1}^{N=N_w} Qt_fS_e + wV_o(X_d\gamma_{Xd} + X_a\gamma_{Xa}))\right]}{Qt_fN_w(S^o + X_d^o\gamma_{Xd})} \qquad (3\text{-}23)$$

3.3.4 Program development and execution

A computer program based on the computational procedures of Figure 3-1 and the classification scheme of Figure 3-2 was developed using QuickBasic. The system of differential equations for the fill and react periods are solved using fourth-order Runge-Kutta approximations. The program is initiated from an interactive input screen. Simulation results are saved as a text file and can be exported to a spreadsheet program for data manipulation. Information provided from the simulation output includes concentrations of different types of solids and substrates, reactor size, required time for each operating stage and mean cell ages of specific microbial groups.

Input parameters

Input parameters that must be specified include the number of reactors N_T (=2, 3, 4...), r ($=V_o/V_{SBR}$), SVI, t_s, t_d, t_c, X_{max}, SRT and t_{sp}. Empirical values for those parameters are summarized in Table 3-1.

Initial conditions

Design of an SBR is an iterative process, but concentrations are needed for X_j and S_i at the beginning of the fill period to initate calculations. A reasonable set of initial conditions can be obtained from the steady state CSTR solution. When solids residence time and effluent concentrations for a CSTR are chosen, the designer can calculate $(X_j)_{ss}$ and a hydraulic residence time (θ) after selecting a desired mixed liquor suspended solids concentration (X):

$$\theta_{CSTR} = \frac{\theta_c}{X}\left[\begin{array}{l} X_{in}^o + X_r^o + \dfrac{X_d^o}{1+\theta_c k_h} + \dfrac{f_d b\theta_c Y(S^o - S)}{(1+k_h\theta_c)(1+b\theta_c)} + \dfrac{f_d b_N \theta_c Y_N (S_N^o - S_N)}{(1+k_h\theta_c)(1+b_N\theta_c)} + \dfrac{Y(S^o - S)}{1+b\theta_c} \\ + \dfrac{Y_N(S_N^o - S_N)}{1+b_N\theta_c} + (1-f_d)b\theta_c \dfrac{Y(S^o - S)}{1+b\theta_c} + (1-f_d)b_N\theta_c \dfrac{Y(S_N^o - S_N)}{1+b_N\theta_c} \end{array}\right] \quad (3\text{-}25)$$

As indicated by equation 3-14, the value of θ_{CSTR} obtained from equation 3-25 can be used to estimate an upper bound for t_c . In general, a reasonable working range for for t_c is defined by:

$$\frac{t_s + t_d}{1 - 1/N_r} \leq t_{c,max} \leq \theta_{CSTR}(1 - r) \qquad (3\text{-}26)$$

Calculation steps

The following calculations are performed in sequence:

1. Calculate t_f using equation 3-3.

2. Calculate t_o using equation 3-6.

3. Calculate V_o (= Qt_o) and V_{SBR} (= V_o/r). The total volume is $N_r V_{SBR}$.

4. The volumetric sludge wasting fraction (w) is calculated from $w = t_{sp}/SRT$. The number of operating cycle between two sludge wasting events (N_w) is obtained from $N_w = t_{sp}/t_c$.

5. Calculate the substrate and solids concentrations throughout fill period (until $t = t_f$) by solving the mass balance equations for the fill period (Table 3-4). To solve the mass balance equations, initial conditions are first calculated using the CSTR steady state solution (Table 3-6). The CSTR steady state solution for solids concentrations is divided by r to estimate the initial solids concentration for the first cycle. Dynamic cell age, A, is calculated throughout the fill period using equation 3-18.

6. Calculate solids and substrate concentrations throughout the react period by solving the differential equations for the react period. The substrate and solid concentrations at the end of fill period are the initial conditions for the react period. Calculations continue

until all treatment objectives are satisfied, where $t = t_r$. Dynamic cell age, A, is calculated throughout the react period using equation 3-18.

7. If solids are not scheduled for wasting, a new operating cycle is initiated by repeating steps 5 to step 6, where the initial concentrations for a new operating cycle are the concentrations at the end of the previous operating cycle, adjusted for settling (divided by r). Between wasting events, biomass accumulates as it is carried over from one cycle to the next, making it possible to satisfy the treatment objectives with a shorter t_r. In practice, however, a constant t_r is used. Consequently, t_r is computed for the first cycle and maintained constant thereafter. This results in some excess level of treatment in cycles after the first cycle of the solids storage period.

8. Wasting is executed when one of the following conditions is satisfied: (1) the operating cycle N equals the wasting cycle N_w, (2) $X > X_{max}$, or (3) $V_{sludge} > V_o$. Assuming solids are removed during the idle period, the volume to be wasted (V_{waste}) is

$$V_{waste} = wV_o \tag{3-27}$$

After wasting, the liquid volume is reduced from V_o to $V_o - V_{waste}$. Because V_o is changed, t_f and t_o also change. Idle time, t_i , decreases to cover the increase of t_f. Because t_i is intended to provide operating flexibility and safety, a decrease in t_i will not affect reactor operation, provided that peak flows can be accomodated and $t_i > 0$. After mathematically altering V_o to account for wasting, the reactor is ready for another solids storage period.

9. Divide suspended solids and substrate concentration obtained from step 8 by r and use them as the initial condition for next cycle calculation.

10. Calculate t_i from $t_i = t_c-(t_f+t_r+t_s+t_d)$. If $t_i < 0$, calculations should be repeated using a longer cycle time.

11. Compute oxygen requirements for the repeating solution. Oxygen utilization is proportional to substrate utilization:

$$r_{O_2}=\gamma_{s_i} f_e r_s \qquad (3\text{-}28)$$

where r_{O_2} = oxygen utilization rate, mg O_2/L-d, γ_{s_i} = COD to weight ratio for the substrate, mg O_2/ mg S, r_s = substrate utilization rate, mg S/L-d, $f_e = 1 - 1.42\frac{dX_a}{dS} =$ fraction of electrons removed from substrate and transferred to oxygen for energy. The oxygen requirement is obtained by multiplying r_{O_2} by the reactor volume, where $V(t) = V_o + Qt$ for the fill period and $V(t) = V_{SBR}$ for the react period.

12. Compute nutrient requirements. The accumulation of active biomass can be computed during each solids storage period, between wasting events. Nitrogen and phosphorus requirements are estimated by assuming the cell contain 2% of phosphorus and 12% of nitrogen in the basis of dry weight.

Many possible design configurations can satisfy the treatment goals. Thus, a range of conditions should be explored. The final design decision should consider capital and operating costs, space requirements, flexibility, etc.

3.3.5 Simulation results

Two design examples were evaluated to illustrate the proposed design procedure. Conditions and design comeouts for both examples are summarized in Table 3-7. The first example is for aerobic heterotrophs removing biodegradable organics. Changes in substrtate concentration and DSA during the repeated solution are shown in Figures 3-3. As indicated in Figure 3-3, substrate concentration increased in the fill period and rapidly decreased during react period. Suspended solids concentrations increase during the fill period, and remain constant or undergo slight changes during the react stage. Dynamic cell age decreases during the fill period, decreases until substrate is removed during the

react period, and increases after substrate is removed. Figure 3-4 demonstrtated the accumulation of different type of solids during reactor operatiion. Solids concentration accumulated during the normal operating cycle and decreased when sludge wasting took place.

The second design example was for an SBR containing both heterotrophs for organics removal and nitrifiers for ammonia oxidation. The scheme of waste characterization and the system of modeling equations for this case were similar to the first example except some extra terms derived from nitrification were added. Figures 3-5 and 3-6 summarize changes in substrate concentration, DSA, and each type of solids.. Trends for substrate removal, solid accumulation, and dynamic cell age variation were similar to the first example, but longer t_f, t_r and t_c are required. The required reactor volume and dynamic cell age are also larger.

In the proposed SBR design procedure, the designer specifies *SRT and* t_{sp} to determine solid wasting parameters (N_w and w). The effects of these parameters on SBR behavior were evaluated by executing the program under a default condition in which only one parameter was changed. Simulation results are summarized in Figures 3-7 and 3-9. For low values of w, the SBR accumulated more solids, and required less reactor volume and a shorter cycle time (Figure 3-7). Higher values for N_w also had the same effect on the concentration of accumulated solids, reactor volume and cycle time (Figure 3-9). Choosing a higher N_w or lower w in SBR design results in older cell ages but the cell age never exceeds the design *SRT*. This result is ensured by selection of an *SRT* that is sufficiently greater than $(A_{min})_{lim}$ for the slowest growing population that is needed for efficient reactor operation.

Table 3-7. Summary of input parameters and design outputs for design examples

Carbon oxidation and nitrification		Carbon oxidation	Carbon oxidation and nitrification		Carbon oxidation
****Kinetic Parameters****			**Influent Waste Characters**		
$K_S(g/m^3)$	60	60	$Q(m^3/d)$	10000	10000
$K_N(g/m^3)$	0.4	NA*	$S^o(g/m^3)$	300	300
$k(d^{-1})$	5	5	$S_N^o(g/m^3)$	40	40
$k_N(d^{-1})$	1	NA*	$X_a^o(g/m^3)$	0	0
$k_h(d^{-1})$	0.06	0.06	$X_N^o(g/m^3)$	0	0
$b(d^{-1})$	0.06	0.06	$X_d^o(g/m^3)$	130	130
$b_N(d^{-1})$	0.02	0.02	$X_i^o(g/m^3)$	0	0
Y(g/g)	0.6	0.6	$X_{in}^o(g/m^3)$	60	60
$Y_N(g/g)$	0.36	0.36	$X_r^o(g/m^3)$	40	40
$f_d(g/g)$	0.8	0.8			
**** Design Parameters****					
E(%)	10	10	N_r	4	4
$E_S(\%)$	90	90	r	0.5	0.5
$E_{SN}(\%)$	90	NA*	t_s (d)	0.04	0.04
Xmax(mg/l)	8000	8000	t_d (d)	0.04	0.04
SVI(ml/g)	50	50	t_c (d)	0.48	0.23
***** Wasting Strategy *****					
SRT(day)	6.4	3	t_{sp}(day)	1.9	0.9
Outputs for design examples					
Required time			Volume and wasting requirement		
$t_f(d)$	0.0564	0.1193	N_w	4	4
$t_r(d)$	0.0482	0.2380	w	0.3	0.3
$t_o(d)$	0.0564	0.1193	$V_O(m^3)$	564	1193
$t_i(d)$	0.04	0.04	$V_{SBR}(m^3)$	1127	2387

* NA = Not apply.

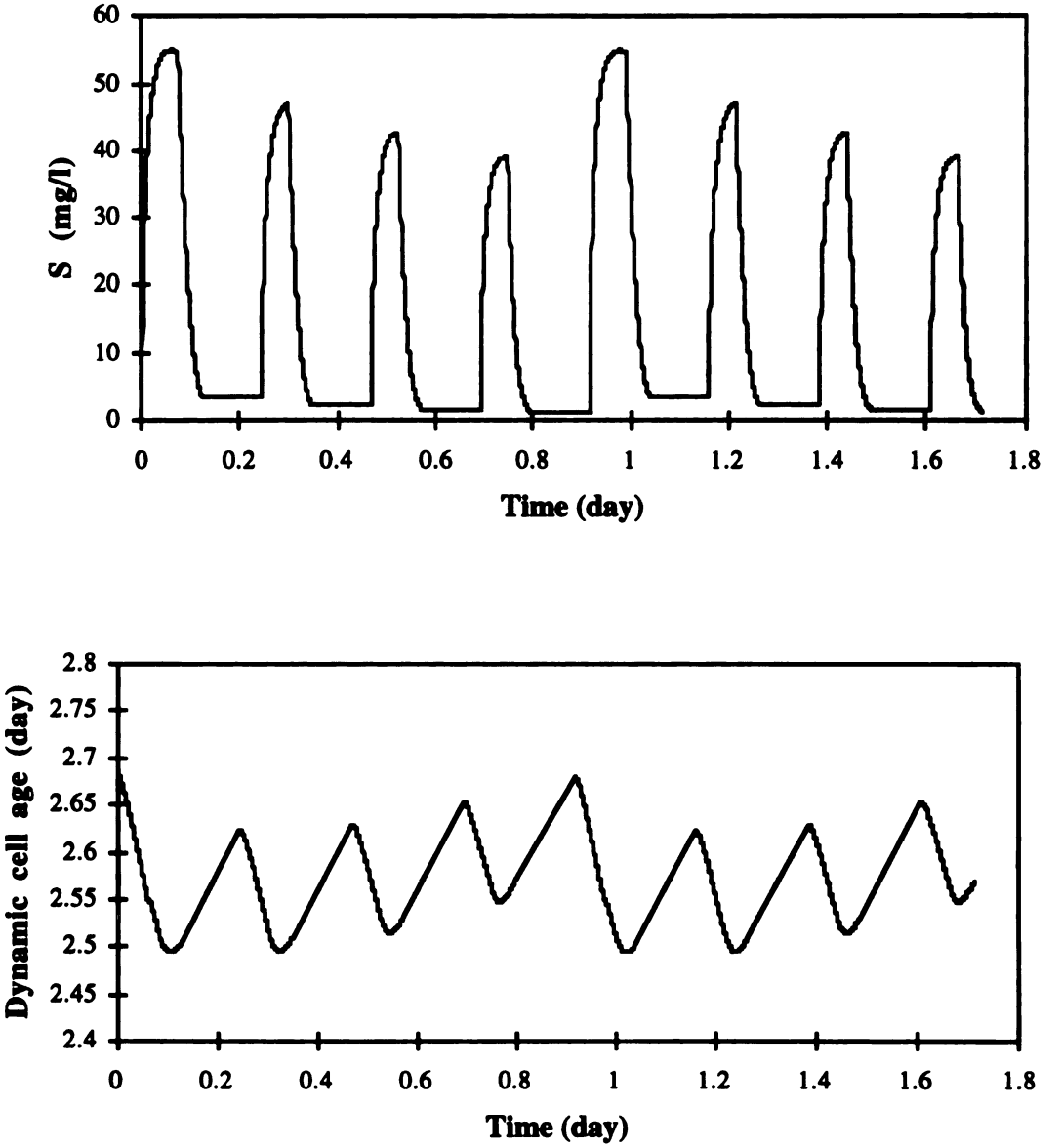

Figure 3-3 Repeating solution for dynamic cell age and substrate concentration in an SBR system designed for carbon oxidation (example 1)

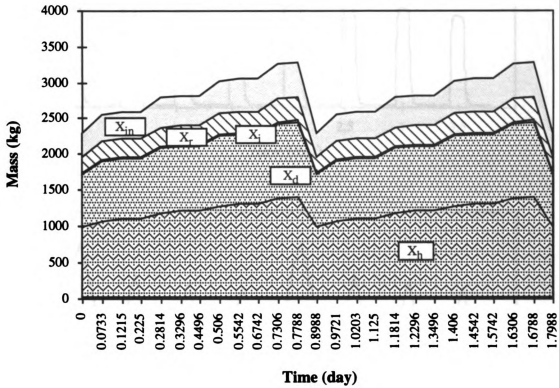

Figure 3-4 Repeating solution for mass of each type of solids present during two solid storage periods.

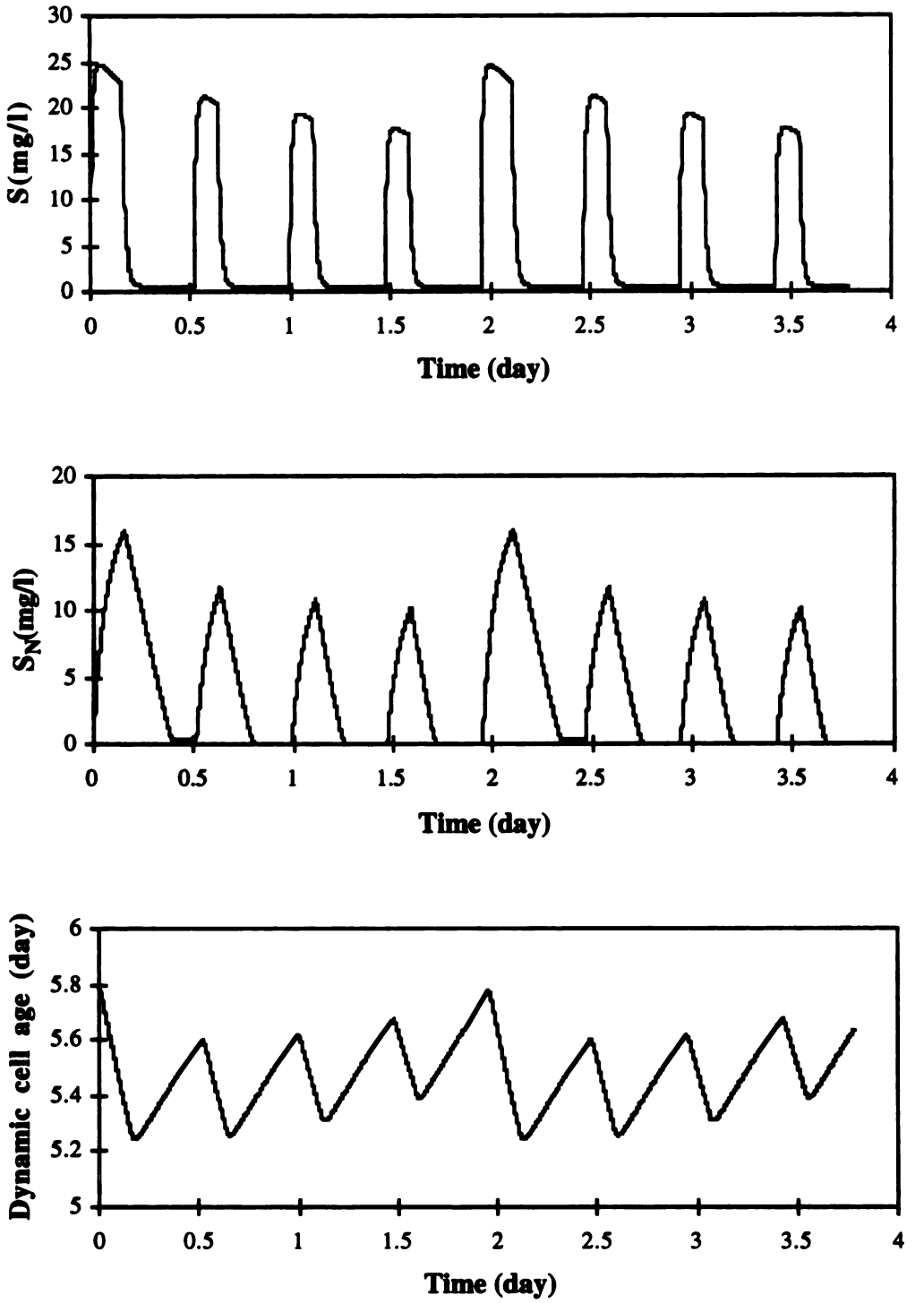

Figure 3-5 Repeating solution for substrate concentration and dynamic cell age in an SBR system designed for simultaneous oxidation of organic matter removal and ammonia .

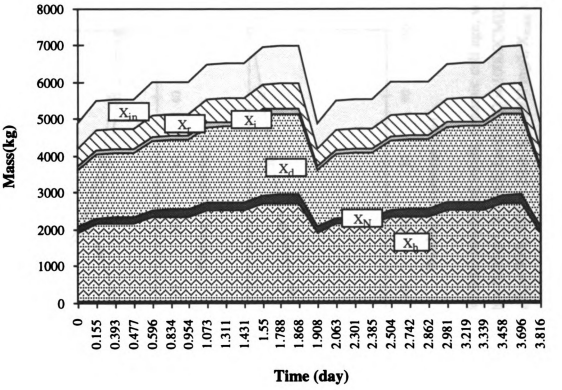

Figure 3-6 Repeating solution for mass of each type of solids accumulated during two solids storage periods.

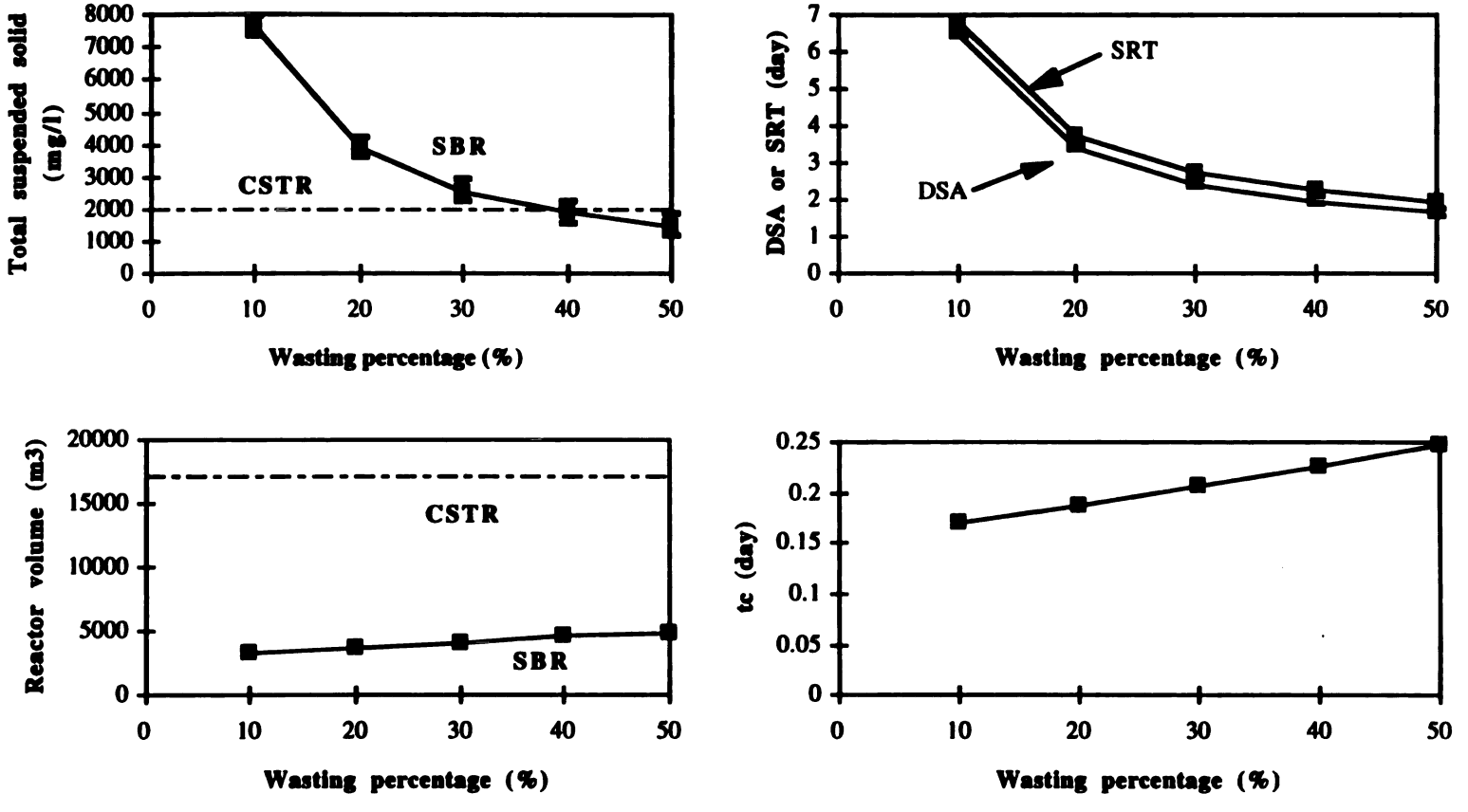

Figure 3-7. Effects of solids wasting percentage (W) on the repeating solution for total suspended solids, dynamic cell age, volume and cycle time. Parameters used in simulation are K_s = 60 mg/l, k = 5 d-1, k_h = b = 0.06 d^{-1}, Y = 0.6, f_d= 0.8, Q = 10000CMD, So = 300 mg/l, $X_{ao} = X_{io}$= 0, X_{do} = 130 mg/l, X_{ino}= 60 mg/l, X_{ro} = 40 mg/l, E_x = 10%, E_s = 90%, SRT = 10 d, X = 2000 mg/l, X_{max} = 8000 mg/l, SVI = 50 mg/l, N_r = 4, r = 0.5, $t_s = t_d = t_i$ = 0.04 d, N_w = 4.

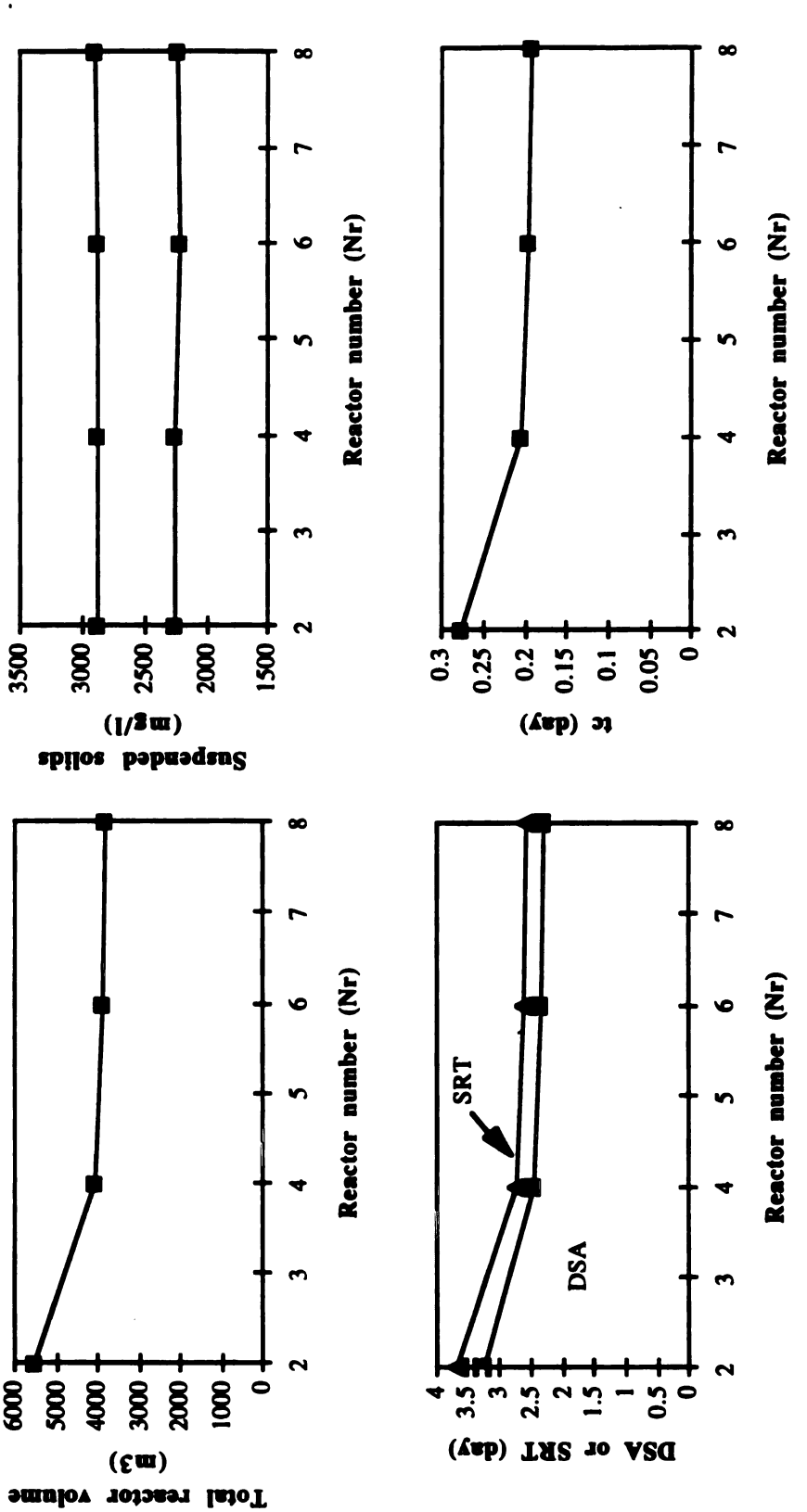

Figure 3-8 Effects of the number of reactor (Nr) on the repeating solution for total suspended solids, dynamic cell age, and reactor volume. Parameters used in simulation are K_s = 60 mg/l, k = 5 d-1, k_h = b = 0.06 d^{-1}, Y = 0.6, f_d= 0.8, Q = 10000CMD, So = 300 mg/l, $X_{so} = X_{io} = 0$, X_{do} = 130 mg/l, X_{ino}= 60 mg/l, X_{no} = 40 mg/l, E_x = 10%, E_s = 90%, SRT = 10 d, X = 2000 mg/l, X_{max} = 8000 mg/l, SVI = 50 mg/l, r = 0.5, $t_s = t_d = t_i$ = 0.04 d, N_w = 4, W = 30%.

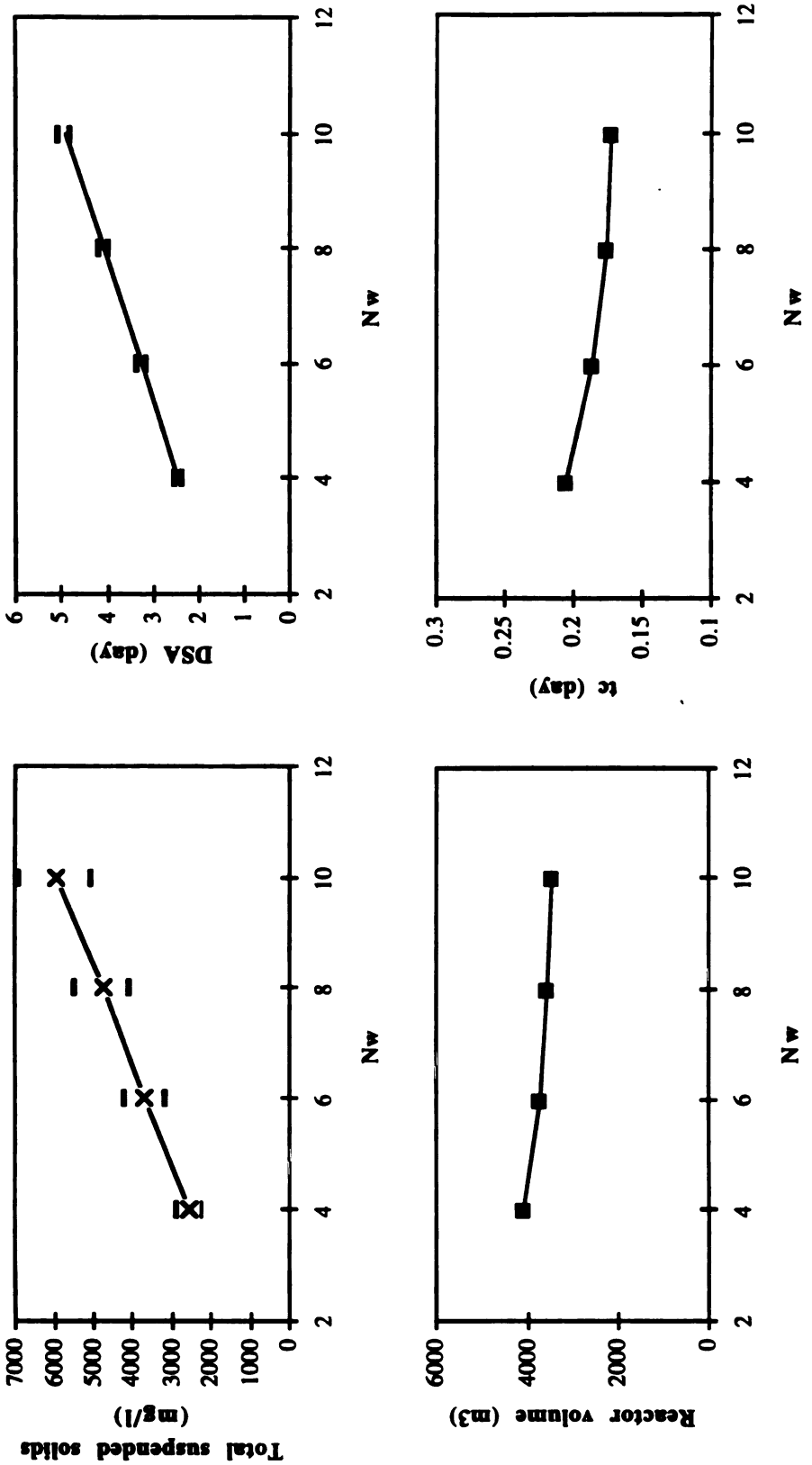

Figure 3-9. Effects of solid wasting frequency ($1/N_w$) on the repeating solution for total suspended solids, dynamic cell age, volume and cycle time. Parameters used in simulation are K_s = 60 mg/l, k = 5 d-1, k_h = b = 0.06 d^{-1}, Y = 0.6, f_d= 0.8, Q = 10000 CMD, So = 300 mg/l, X_{so} = X_{io}= 0, X_{do} = 130 mg/l, X_{ino}= 60 mg/l, X_{ro} = 40 mg/l, E_x = 10%, E_s = 90%, SRT = 10 d, X = 2000 mg/l, X_{max} = 8000 mg/l, SVI = 50 mg/l, N_r = 4, r = 0.5, t_s = t_d = t_i = 0.04 d, W = 30%.

Increasing the number of SBRs reduces the total volume requirement, required *SRT*, and cycle time (Figure 3-8). This is because the SBR performs more like a plug flow reactor as N_r increases. The decrease of total reactor volume is not so apparent when $N_r > 4$. This is because the dilution of substrate becomes more pronounced during the fill period (reducing the initial substrate concentration) as t_f decreases. As expected, the SBR required significantly less volume than a comparable CSTR system.

3.4 Summary

Numerical simulation appears to be an effective tool for SBR design and simulation. The ability to simulate substrate and solids concentrations, and to predict oxygen utilization rates and nutrient requirements enables improved understanding of the complex interactive processes within the SBR and should facilitate design and operation. The dynamic cell age fluctuations of active microbial populations was constrained by the choice of SRT. Monitoring of cell age provides a means whereby cell age-dependent phenomena might be simulated and controlled.

Literatures cited

APHA. Standard methods for the examination of water and wastewater. 17th ed., Washington, D. C.: APHA, 1989.

Arora, M. L., E. F. Barth, and M. B. Umphres. "Technology evaluation of SBRs." J. WPCF 57 (8 1985): 867-875.

Benefield, L. D. and C. W. Randall. Biological process design for wastewater treatment. 1st ed., Englewood Cliffs, New Jersey: Prentice-Hall, Inc., 1980.

Grady, C. P. L. and H. C. Lim. Biological wasterwater treatment. New York: Marcel Dekker, Inc., 1980.

Henze, M., C. P. L. Grady, W. Gujer, G. V. R. Marais, and T. Matsuo. Activated Sludge model no. 1. IAWPRC, 1987.

Irvine, R. L. "SBR for biological wastewater treatment." CRC Critical Reviws in Environmental Control 18 (4 1989): 255-266.

Lawrence, A. W. and P. L. McCarty. "Unified basis for biological treatment design and operation." Journal of the Sanitary Engineering Division, ASCE 93 (SA 3 1970): 757-778.

Metcalf & Eddy, Inc. Wastewater engineering: treatment, disposal and reuse. 3 rd. ed., McGraw-Hill series in water resources and environmental engineering, ed. R. Eliasen, P. H. King, and R. K. Linsley. New York: McGraw-Hill, Inc., 1991.

Shu, P. "Mathematical models for product accumulation in microbiology processes." J. Biochem. Microbiol. Technol. Eng. 3 (1 1961): 95-100.

Vaccari, D. A., A. Cooper, and C. Christodoulatos. "Feedback control of activated sludge waste rate." J. of WPCF 60 (11 1988): 1979-1985.

Vaccari, D. A., T. Fagedes, and J. Longtin. "Calculation of mean cell residence time for unsteady-state activated sludge systems." Biotechnol. Bioeng. 27 (5 1985): 695-703.

von Foerster, H. "Some remarks on changing populations." In The kinetics of cellular proliferation, ed. F. Stohlman. 382-407. New York: Grune & Stratton, Inc., 1959.

CHAPTER 4

EFFECTS OF GROWTH SUBSTRATE FEEDING PATTERN ON COMMUNITY STRUCTURE AND COMETABOLISM

4.1 Introduction

A wide range of chemicals can be detoxified by cometabolism. To sustain cometabolic reactions, a growth substrate must be added, either continuously or periodically. In mixed cultures, it is not clear how different methods of growth substrate addition will affect community structure and cometabolic populations within the community. The pattern and timing of growth substrate addition is likely to change the structure of the microbial community and its propensity for cometabolism. This could be of particular importance in the design and operation of reactor systems for cometabolism. To explore this issue, trichloroethylene (TCE) was selected as nongrowth substrate, and phenol as the growth substrate. Certain phenol- and toluene-degrading *Pseudomonas* species rapidly cometabolize TCE (Coyle et al., 1993; Nelson et al., 1988; Nelson et al., 1987; Shields et al., 1986; Shields et al., 1991; Wackett and Gibson 1988), but this ability is not common to all phenol- and toluene-degraders (Dabrock et al., 1992). Consequently, enrichments that are fed phenol or toluene may differ in their capabilities for cometabolism due to differences in the species present. To test this hypothesis, phenol and TCE degradation activities were monitored in four reactors fed the same daily mass of phenol, but with different feeding patterns (frequency and feeding rate). The structure and composition of microbial community for these four reactor was subsequently analyzed.

4.2 Materials and methods

4.2.1 Chemicals

Trichloroethylene (TCE, 99% purity) was obtained from Aldrich Chemical Co., Milwaukee, Wisconsin. Chemicals for preparation of media and analyses were ACS reagent grade and were purchased from Aldrich or Sigma Chemical Co.

4.2.2 Medium and culture

Phenol feed medium contained (per liter of deionized water): 2 g of phenol, 2.13 g of Na_2HPO_4, 2.04 g of KH_2PO_4, 1 g of $(NH_4)_2SO_4$, 0.067 g of $CaCl_2$ $2H_2O$, 0.248 g of $MgCl_26H_2O$, 0.5 mg of $FeSO_4$ $7H_2O$, 0.4 mg of $ZnSO_4$ $7H_2O$, 0.002 mg of $MnCl_2$ $4H_2O$, 0.05 mg of $CoCl_2$ $6H_2O$, 0.01 mg of $NiCl_2$ $6H_2O$, 0.015 mg of H_3BO_3, and 0.25 mg of EDTA. The pH of the medium was 6.8.

4.2.3 Reactors and reactor operating conditions

Four glass vessel reactors were used to examine the effects of phenol addition: a pulse fed reactor (reactor P); a continuously fed reactor (reactor C); and two semi-continuously fed reactors (reactors SC2 and SC5). Each reactor received 200 mL of phenol feed medium daily, resulting in a phenol loading rate of 0.2 g per liter per day and an average dilution rate of 0.1 d^{-1} (hydraulic residence time of 10 days). Each reactor was operated so as to maintain a constant liquid volume of 2 L. For reactor P, 200 mL medium was provided as a single daily pulse immediately after removing the same volume of liquid from the reactor. For reactor C, 200 mL of medium was supplied continuously. Reactor SC5 received phenol semi-continuously - alternating between 5 hours of feed and 3 hours of no feed. Reactor SC2 alternated between 2 hours of feed and 6 hours of no feed.

Reactor vessels (Wheaton 2-L Double-Sidearm Celstir, Wheaton No. 356806) were vigorously stirred by teflon paddles attached to a spinning shaft and driven by a teflon-

coated stir rod coupled magnetically to a magnetic stir plate under the vessel (Figure 4-1). Defined phenol medium was provided by syringe pumps. An air pump supplied oxygen (dissolved oxygen maintained > 2 mg/L) through a glass diffusion tube. All reactors were operated at 21.5±1.0 °C.

4.2.4 Inoculum

Each reactor was inoculated on the same day with a subsample from the same phenol-degrading enrichment. The enrichment was obtained by seeding a chemostat with activated sludge from a municipal wastewater treatment plant (East Lansing, Michigan) and providing phenol feed medium for two months at a dilution rate of 0.1 d^{-1}. The enrichment was maintained at 21.5±1.0 °C. Microscopic examination revealed a diverse microbial community, including flocs of spherical and rod shaped bacteria, filaments, and distinctive predators, including protozoa and rotifers.

4.2.5 Evaluation of TCE transformation kinetics

Samples were periodically removed from the 4 phenol-fed reactors just before the beginning of feed to evaluate TCE transformation activity. Two to five milliliters of culture was transferred to a 20 mL glass vial, crimp-sealed with Teflon coated butyl rubber stoppers, and spiked with 10~50 μL of aqueous TCE stock solution to give the desired initial TCE concentration. Vials were incubated at room temperature on a rotatory shaker at 120 rpm. Periodically, 0.1 mL of headspace gas was withdrawn using a Precision gas tight syringe and injected into the injection port of a Hewlett-Packed 5890A gas chromatograph equipped with a 30 m (L), 0.53 mm (ID) DB624 capillary column (Alltech No. 93532) and a flame ionization detector (helium carrier flowrate of 12 mL/min). The GC oven was operated isothermally at 90 °C, and both the detector and the injector were maintained at 250°C. TCE concentrations were determined by comparing the peak areas of samples to the peak areas of external standards. Aqueous phase TCE concentrations were calculated

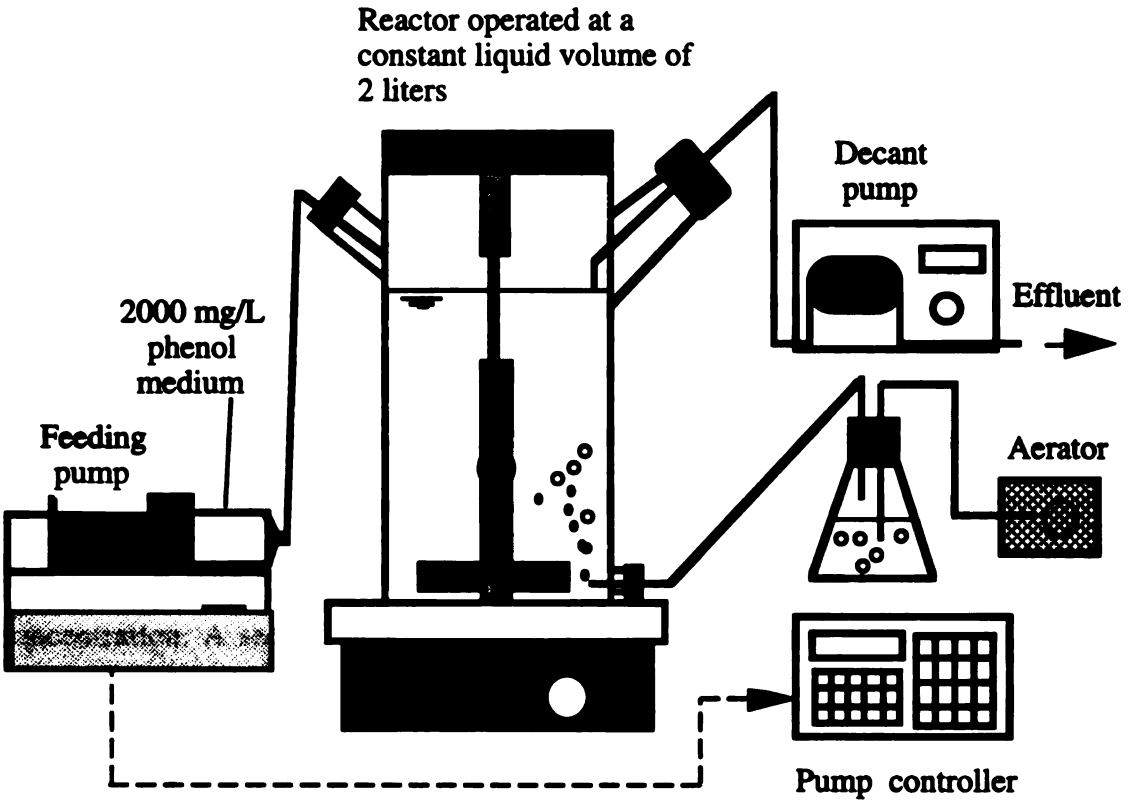

Figure 4-1 Schematic of experimental setup

using a dimensionless Henry's law constant of 0.333 at 21°C (Gossett 1987). The initial concentration of TCE added was estimated from triplicate sterile controls after equilibration. The total sample volume withdrawn from each vial was less than 5% of the total headspace volume. In general, the coefficient of variance on TCE measurements was 1 to 5% for triplicate samples.

Data from the above assays were fit to three different kinetic models using the statistical package SYSTAT 5.2.1. A first-order rate expression (first order in TCE concentration) fit the data for each of the four reactors with an average $r^2 > 0.95$; a zero-order rate expression did not fit the data; and saturation kinetics only applied at high TCE transformation rates. Typical curve fitting results for TCE degradation kinetics were provided in Appendix B. Transformation rates were also proportional to the biomass concentration. Based on these observations, TCE transformation kinetics are assumed to be first-order with respect to TCE concentration and first order with respect to biomass concentration. A second-order rate coefficient k_c' (first order with respect to TCE and biomass concentrations) was used for comparison of TCE transformation rates. The corresponding mass balance expression was:

$$\frac{dC}{dt} = -k_c' CX \qquad (4\text{-}1)$$

where C = concentration of TCE in the aqueous phase and X = concentration of biomass. Assuming that cell concentration does not change appreciably during the assay, the integrated form of equation 4-1 is:

$$\ln C = \ln C_o - k_c' Xt \qquad (4\text{-}2)$$

where C_o = initial concentration of aqueous TCE.

4.2.6 Measurement of pH, dissolved oxygen, optical density, phenol, and MLSS

Dissolved oxygen, pH, and optical density (absorbance at 600 nm) were routinely monitored with a dissolved oxygen probe (Orion model 97-08), pH meter (Orion 720) and spectrophotometer (Shimadru UV-160), respectively. Phenol was assayed by liquid chromatograph on a Gilson HPLC (Gilson Medical Electronics, Inc., Middleton, Wisconsin) equipped with a 250 mm (L) x 4.6 mm (ID) Whatman C-18 column (Alltech NO. 46211502). The flow rate of the mobile phase (40% acetonitrile + 60% deionized water containing 0.1% H_3PO_4) was 1 mL/min. A 20 μL injection loop was used for injecting sample. Phenol was detected by a UV detector at 235 nm. The detection limit was 0.5 mg/L. A typical coefficient of variance for phenol measurement for 5 samples was less than 5%. Suspended solids were measured by dry weight according to the procedure of Standard Methods (APHA 1989), but 0.2 μm membrane filters were substituted for glass fiber filters in the filtration step.

4.2.7 Identification and quantification of filaments

Identification of filaments was performed according to the identification keys of Eikelboom and van Buijsen (1981) and Storm and Jenkins (1984). Filamentous organisms were quantified by total extended filament length (TEFL), as Sezgin and Jenkins (1978) suggested.

4.2.8 Rotifer enumeration

Rotifers are distinguished from protozoa by their size (100~500 μm) and morphological characteristics (Calaway 1968). To enumerate rotifers, a 10 μL cell suspension was evenly spread over an area of 1.5 cm^2 on a glass slide and examined under 100x magnification by a phase contrast microscope (Olympus BH2) equipped with micrometer scale in ocular. The numbers of rotifers present in 0.5 cm^2 viewing area were counted. The number of rotifer in 1 mL sample (#/mL) was calculated and corrected for

viewing area and dilution factor. For triplicate samples, this method gave an average coefficient of variation of 30% for the number of rotifers in a sample containing 1,000 to 10,000 per mL.

4.2.9 Enumeration of phenol utilizers and TCE degraders

A most probable number (MPN) procedure was developed to estimate the number of phenol and TCE degraders. Phenol utilizers were identified by their ability to grow on phenol, and TCE degraders were identified by their ability to degrade TCE after growth on phenol. It was assumed that all TCE degraders are phenol utilizers. Some support for this assumption was obtained in preliminary test results: phenol-grown cells degraded TCE, but catechol-grown cells from the same inoculum did not. To enumerate cells by MPN, 10 milliliters of cell suspension were removed from the reactors at the end of the phenol feeding period and briefly sonicated (30 sec, 25 watt) to disperse floc and to dislodge attached cells from the filaments (Banks and Walker 1977). Dilutions (10^{-3} to 10^{-8}) of the dispersed cell suspension were then prepared in mineral medium. A one milliliter inoculum was added to a 20-mL glass vial with 9 mL of phenol feed medium (phenol conc. = 100 mg/L). TCE was added to give 1 mg/L in the aqueous phase. Vials were sealed with Teflon-coated septa and incubated at 21°C on a rotary shaker at 120 rpm. Control vials were prepared with sterile medium. After 10 days, optical density at 600 nm, phenol concentration, and TCE concentration were measured. A vial was scored "phenol positive" when $OD_{600} > 0.1$ or more than 50% of the phenol had disappeared. A vial was scored "TCE positive" when the remaining TCE in vials was over 50% less than that in the control vials.

4.2.10 Pure culture isolation and characterization

Ten milliliters of samples were collected from each of the four reactors on day 425. The samples were diluted in phosphate buffer (K_2HPO_4, 1.0 g and KH_2PO_4, 0.75 g; pH

= 7.2). Ten-fold dilutions were prepared in a total volume of 10 mL. The samples were vortexed for five minutes before diluting. The samples were also vortexed for one minute at each dilution step before transfer. The dilutions were plated on R2A agar and incubated for four days at 25°C. Representatives of the various morphologies were counted, picked, and transferred to R2A plates for isolation. To ensure the purity of each isolate, colonies were transferred five times before REP-PCR was performed. Each isolate with a different REP-PCR pattern was regrown in 20-mL glass vials with 10 mL mineral medium containing 100 mg/L phenol and 1 mg/L TCE for 10 days. Increase in optical density at 600 nm over the incubation period was used to determine whether the isolate can grow on phenol. TCE cometabolism was evaluated by monitoring TCE removal. For the phenol and TCE degradation assays, each isolate was regrown and tested in five vials.

4.2.11 Assay for catechol ring fission pathway

The production of the yellow product, α-hydroxymuconic semialdehyde (α-HMS), from catechol was used as a test for the presence of a catechol *meta* ring fission pathway (Folsom et al., 1990; Gerhardt 1994). Ten milliliters of cell suspension was concentrated to two milliliters (~ 5000 mg/L) by centrifugation at 4,000 rpm. Concentrated cells (0.5 mL) were resuspended in 2 mL of 0.2 M Tris buffer (pH = 8), supplemented with 0.5 mL toluene to solubilize the cell membranes, and shaken with 0.2 mL of a 1.0 M catechol solution. Appearance of a yellow color within a few minutes is indicative of *meta* cleavage activity.

Production of ß-ketoadipate from catechol was used as a test for the presence of a catechol *ortho* ring fission pathway (Folsom et al., 1990; Gerhardt 1994). Ten milliliters of cell suspension was concentrated to 2 mL (~5000 mg/L) by centrifugation at 4,000 rpm. Concentrated cells (0.5 mL) were resuspended in 2 mL of 0.2 Tris buffer (pH = 8), supplemented with 0.5 mL toluene to solubilize the cell membranes, and spiked with catechol (1.0M, 0.2 mL). After 1 hr of incubation at 30°C, the following chemicals were

added: 1 g of $(NH_4)_2SO_4$, 1 drop of 1% sodium nitroprusside (nitroferricyanide) and 0.5 mL of ammonia solution (28 to 30%). A purple color indicates *ortho* cleavage activity.

4.3 Results and Discussions

4.3.1 TCE transformation

The reactor communities displayed significantly different TCE removal rates during the period of operation (Figure 4-2). TCE degradation rates in reactor P increased over time. For the initial 75 days, k_c' was as low as 0.00535±0.00108 L/mg-day. From day 75 to 220, k_c' doubled to 0.01104±0.00101 L/mg-day. After day 250, removal rates increased tenfold to k_c'= 0.1134±0.0260 L/mg-day. At this point, saturation kinetics (k_c' = 0.1036±0.03174 mg TCE/mg cell d.w.-day and K_s = 0.35 +/- 0.08 mg/L provided a more accurate description of TCE transformation kinetics. Degradation rates observed after day 250 were comparable to rates of methanotrophic consortia (Arciero et al., 1989; Henry and Grbic-Galic 1990). During the period of increasing TCE transformation rates, biomass concentration did not increase.

For reactor C, during the initial 25 days, cells exhibited moderate TCE degradation rates (k_c'= 0.01349±0.004398 L/mg-day). After 25 days, transformation rates decreased, with k_c'=0.003586±0.001817 L/mg-day, and rates remained low for the remainder of the operating period. The rates ultimately observed in reactor C were far below than those observed in reactor P. From days 25 to 40, reactor C changed color from white to yellow, and biomass decreased from 750 mg/L to 250 mg/L. The yellow color may be due to the accumulation of α-hydroxymuconic semialdehyde (α-HMS), a yellow intermediate of phenol degradation. After two more weeks operation, the yellow color disappeared. The yellow color was not removed over a 3 day period when a filtered sample of reactor C was incubated with cells drawn from other reactors (reactor P, SC2 and SC5). Brief interruptions in aeration to reactor C also triggered appearance of a yellow color. These

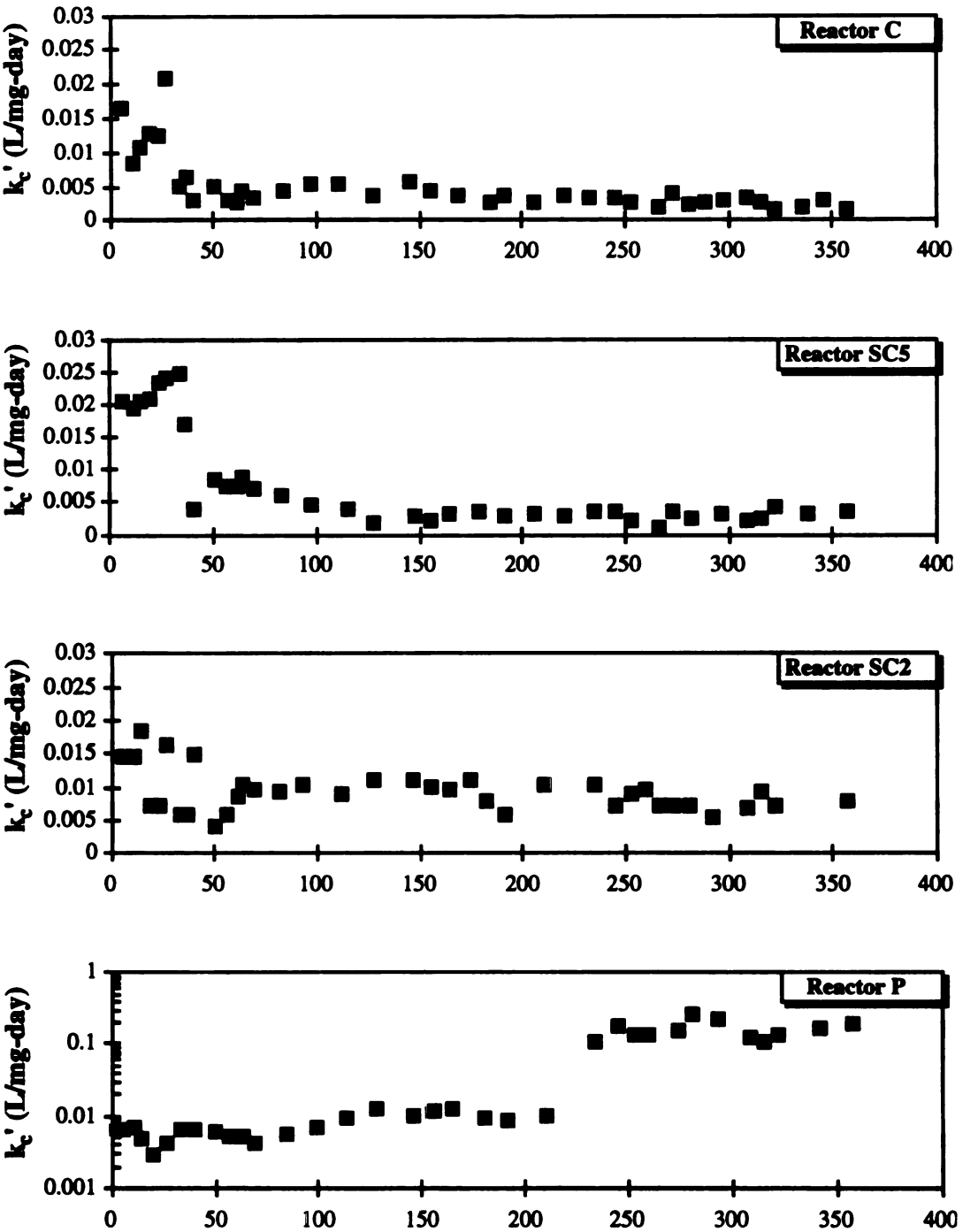

Figure 4-2 Second-order TCE removal coefficients for cells from different feeding pattern reactors

observations suggest that the yellow color resulted from incomplete oxidation of phenol. Appearance of the yellow color correlated with decreases in cell concentration and TCE transformation rate, possibly indicating some form of product toxicity.

For cells harvested from reactor SC2, k_c' for TCE removal varied from 0.015 to 0.005 L/mg-d (average 0.011 L/mg-d). Changes in TCE removal rates (k_c' s) roughly correlated with changes in biomass concentration. For organisms from reactor SC5, removal of TCE was optimal from day 10 to day 35 with k_c'= 0.02119±0.00266 L/mg-day. After day 35, TCE degradation rates and biomass levels decreased. After day 80, k_c' decreased to 0.002625±0.000906 L/mg-day, and biomass concentration varied cyclically from 500 mg/L to 1000 mg/L. TCE transformation rates were low and maintained at 0.002 to 0.003 L/mg-day after day 80. Second order rate coefficients for reactor SC5 were similar to those of reactor C.

Typical TCE degradation curves for each reactor community after day 250 are illustrated in Figure 4-3. TCE was transformed at high rates by cells from reactor P, at intermittent rates by cells from reactor SC2, and at low rates by cells from reactors C and SC5.

4.3.2 Biomass variation

As shown in Figure 4-4, total biomass concentrations remained relatively stable in reactors P (suspended solids concentration of 913±126 mg/L) and SC2 (suspended solids concentration of 990±170 mg/L). In contrast, significant fluctuations were observed in reactors C (suspended solids concentration range of 300 to 1400 mg/L, with an average of 835±248 mg/L) and SC5 (850±200) Reductions in the concentration of suspended solids were accompanied by decreased TCE degradation rates in reactors C, SC2 and SC5. Possible explanations for these differences include toxicity of phenol degradation intermediates or bacterial predation by protozoa and rotifers. Evidence that predation was

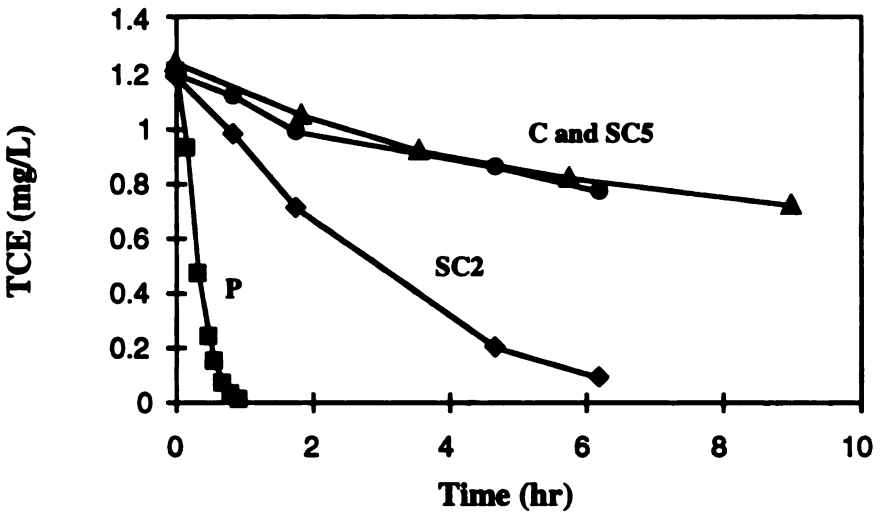

Figure 4-3 TCE degradation observed in batch experiments using cells from different feeding pattern reactors

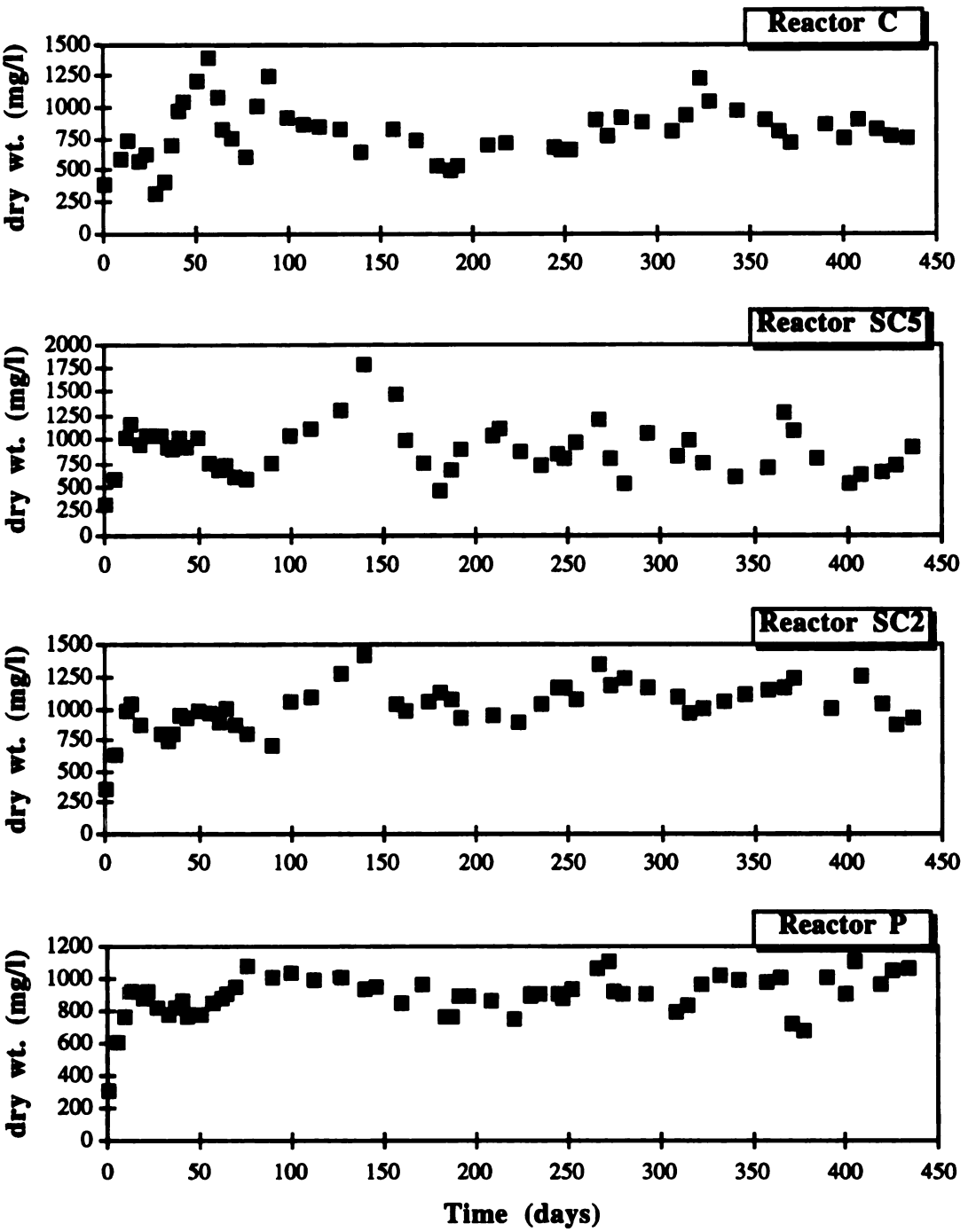

Figure 4-4 Changes of biomass during reactor operating period, each sample was taken at the end of growth substrate fill period.

important was subsequently obtained by microscopic analysis. High levels of protozoa and rotifers were observed in reactors SC5 and C.

4.3.3 Phenol degradation

Results of the catechol ring fission assay indicate that phenol degradation proceeded by the *meta*-cleavage pathway. The occasional appearance of α-HMS in the reactors supported this observation. Phenol concentrations in the continuous-fed reactor (reactor C) and the two semi-continuously-fed reactors (SC2 and SC5) were below the phenol detection limit (below 0.5 mg/L). In the pulse-fed reactor (reactor P), phenol concentration decreased from 200 mg/L to 0 mg/L in 2~6 hours after the pulse. On day 30, phenol degradation in reactor P was zero-order in phenol concentration (Figure 4-5) with a rate constant of 0.051 ± 0.008 hr^{-1} and $r^2 > 0.99$ (Table 4-1). After day 250, the rate constant of phenol degradation in reactor P had increased to 0.135 ± 0.010 hr^{-1}. The zero-order pattern of phenol utilization in reactor P was similar to the results of Tischler and Eckenfelder (1969). Substrate inhibition kinetics, such as those reported by Grady (1985), were not observed.

Repeated spikes of phenol into reactor P did not affect the ability of the community to degrade phenol, in contrast with the results of Okaygun et al. (1992). In their studies, each spike of phenol delayed the degradation of subsequent phenol spikes (Okaygun and Akgerman 1992) Apparently, the pattern of phenol addition in reactor P selected for organisms with high phenol utilization rates and resistance to phenol toxicity. Phenol degraded repeatedly without any detectable inhibition.

4.3.4 Phenol utilization patterns for reactors with different feeding pattern

Control of phenol feeding pattern appeared to select for cells with higher specific substrate utilization rates. On day 155, 100 mL of culture was removed from each reactor, spiked to an initial phenol concentration of 100 mg/L, and monitored for phenol utilization.

Table 4-1. Curve fitting results for estimating zero-order phenol degradation kinetic coefficients.

Exp. No	X_o (mg/L)	S_o (mg/L)	n	Y	k^o (hr^{-1})	r^2
1st	700	202.95	8	0.8790	0.05526	0.9949
2nd	840	209.44	10	0.8790	0.05071	0.9890
4th	920	196.74	11	0.8790	0.03712	0.9981
7th	660	212.58	12	0.8790	0.05732	0.9920
8th	650	207.32	9	0.8790	0.05427	0.9897
Avg.	754	205.81	10	0.8790	0.05094	0.9927
Stdev.	107	5.51	1.41	-	0.00809	0.0034

X_o = initial microorganism concentration, mg/L.

S_o = initial phenol concentration, mg/L.

n = sample number in curve fitting procedure.

Data obtained on days 31 to 38.

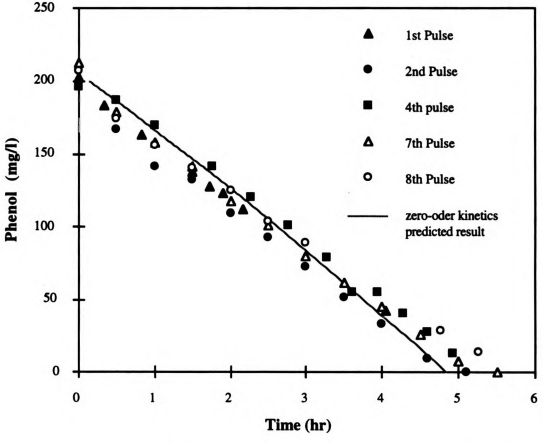

Figure 4-5. Phenol degradation in reactor P for daily spiking with phenol from day 31 to 38.

As shown in Figure 4-6, organisms from reactor P degraded phenol faster than organisms from the other reactors. Cells obtained from continuously and semi-continuously fed reactors exhibited a lag phase and slow rates of phenol degradation. these observations might be explained by differences in community structure or in the enzymes present. A lag period for phenol degradation was also observed for cells harvested from reactor P when the spiked phenol concentration was greater than 400 mg/L. In general, a lag period occurred whenever cells were exposed to phenol concentrations that were significantly greater than the levels to which the cells were preadapted.

4.3.5 Effect of phenol feeding pattern on reactor pH and dissolved oxygen

There was little difference in the pH values of the four reactor communities. During startup, pH decreased from 6.9 to 6.3. After 50 days, pH values stabilized as follows: reactor C – 6.47±0.10; reactor SC5 – 6.51±0.06; reactor SC2 – 6.60±0.08; reactor P – 6.51±0.09. The pH decrease is probably explained by the acidic character of phenol and its transformation products. Ammonia-oxidizing bacteria can also contribute to pH reduction and TCE removal, but their role was apparently minor, as indicated by the low levels of nitrate (~ 0-10 mg/L) and nitrite (~ 0-3 mg/L) detected in the reactors.

Aeration levels for all reactors sustained dissolved oxygen levels in excess of 2 mg/L at all times. These levels are considered sufficient to avoid oxygen limitation (Bailey and Ollis 1986). However, variations in phenol feeding patterns did mirror changes in dissolved oxygen (DO) concentrations. As shown in Figure 4-7, the continuously fed reactor had the highest and most stable DO of 7.5 mg/L. DO levels in the other reactors varied from 7.5 to 2.0 mg/L depending on the operating mode. The lower DO concentrations were observed during periods of phenol feed.

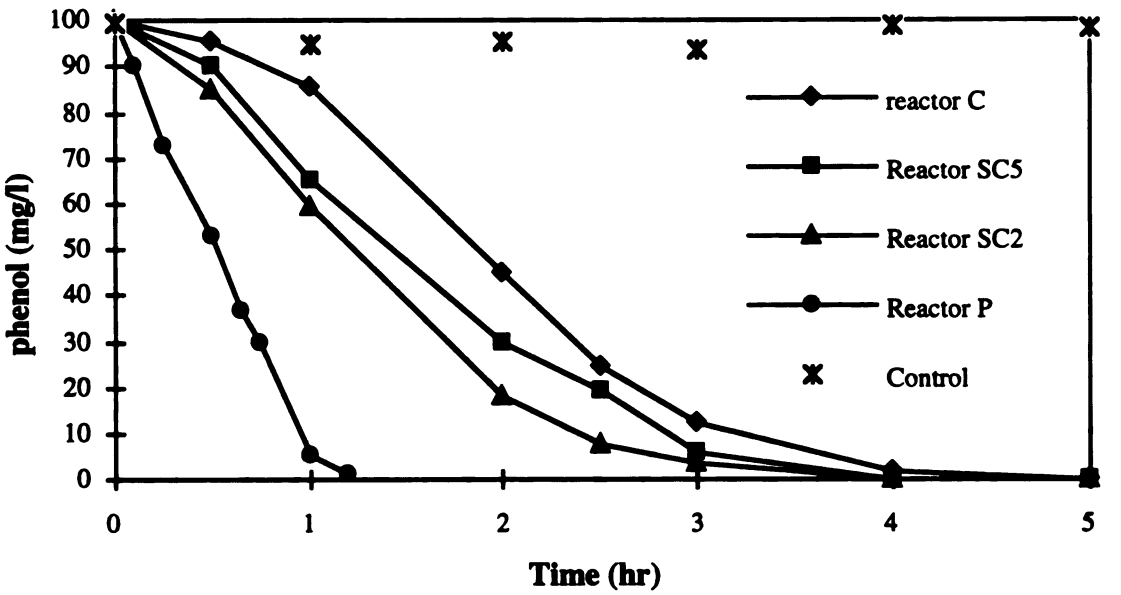

Figure 4-6 Effects of phenol feeding pattern on phenol degradation in batch system. Experiments were conducted in 250 mL bottle filled with 100 mL of cells obtained from each reactor at the end of feeding stage on 3-24-94. Control bottle contained mineral medium only. Initial suspended solid concentration in each bottle was adjusted to 1000±50 mg/L.

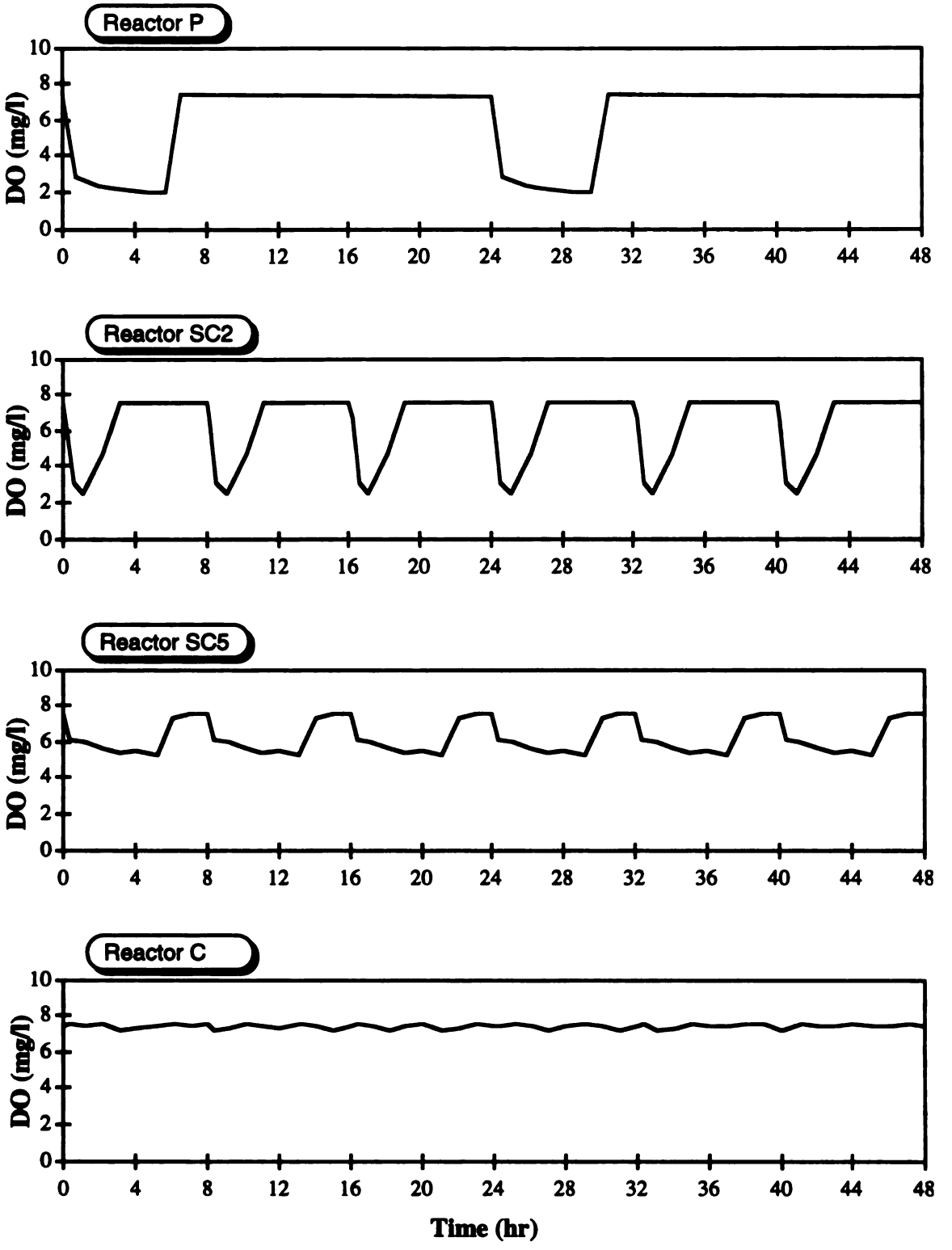

Figure 4-7 Effect of feeding pattern on dissolved oxygen concentration

4.3.6 Microscopic inspection

The microbial community of all four reactors contained bacteria, fungi, protozoa and rotifers. The microbial community of reactor P was predominantly flocculent; those of the other reactors were predominantly filamentous. Shifts in community structure were established by monitoring functional changes and changes in the morphology of dominant species.

Prior to day 35, the dominant species in reactor SC5 were unattached 1-2 μm motile gram negative rod-shaped bacteria. After day 80, the dominant organisms were filaments with an average length of 500-900 μm, 2-4 μm in diameter with visible septa and true branches (Figure 4-8). Some bacteria were attached to the filaments. During the transition period (days 35 - 80), flocculate biomass appeared. For reactors C and SC2, a similar morphological change was observed. A color switch occurred in reactors C and SC2. Reactor C changed from white to yellow then back to white. In reactor SC2, the color switched from straw yellow to white, and floc structure changed from flocculent to filamentous (from day 35 to day 40). After day 50, reactors SC5, C and SC2 were dominated by filamentous microorganisms (Figure 4-8 ~ 4-10). The filamentous organisms were identified as fungi. The filaments present in reactors were comprised of real branches, straight or slightly bent, > 200 μm in length, sheathless with visible crosswalls and containing rectangular cells, > 2.5 μm in diameter, with a negative Neisser stain. The prevalence of fungi might have been due to the slightly acidic conditions. In reactor P, fungi were much less common, and a distinctive floc structure was observed (Figure 4-11).

Fungi were quantified by measuring the total extended filaments length (TEFL). As shown in Table 4-2, the TEFLs for reactors ranged from 1.7×10^7 to 2.21×10^8 μm/mg of dry weight. Reactor C and SC5 had 10 times higher TEFL values than reactor P. The estimated mass filaments comprised 70% or 95% of the total biomass in reactor C and

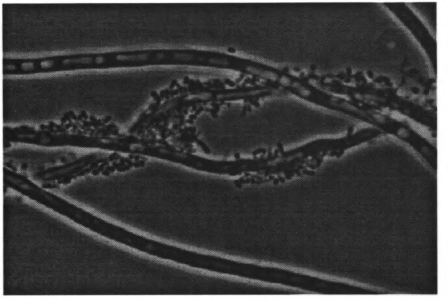

Figure 4-8 Microphotograph of sludge in reactor SC5

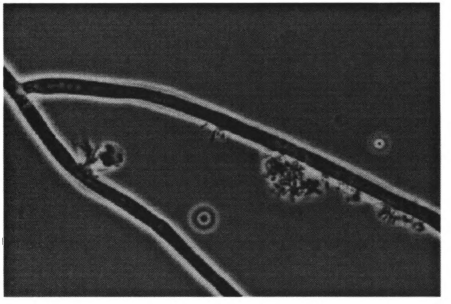

Figure 4-9 Microphotograph of sludge in reactor C

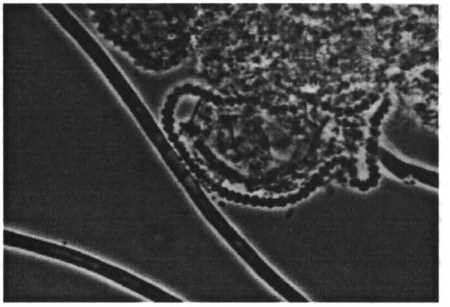

Figure 4-10 Microphotograph of sludge in reactor SC2

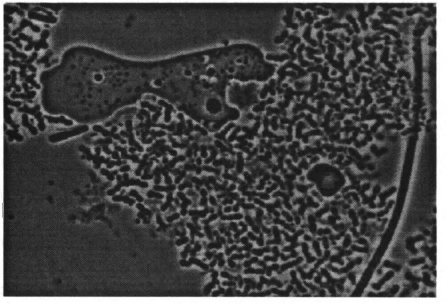

Figure 4-11 Microphotograph of sludge in reactor P

Table 4-2. Results for quantification of filaments and rotifers in reactors (sample was collected on day 275 and day 290)

Parameter	Reactor P	Reactor SC2	Reactor SC5	Reactor C
Total Filament, no./mg	1.9 +/- 0.5 x 10^4	1.7 +/- 0.7 x 10^5	2.2 +/- 0.6 x 10^5	2.87 +/- 0.7 x 10^5
Total Filament Length, μm/mg	1.7 +/- 0.5 x 10^7	8.03 +/- 4.2 x 10^7	2.21 +/- 1.02 x 10^8	1.7 +/- 0.5 x 10^8
Filament length, μm	900 +/- 400	500+/- 400	1000 +/- 700	600 +/- 300
% of filaments mass in total biomass[a]	5 - 10	30 - 50	70 - 95	60 - 95
Rotifer no./mL	820 +/- 350	2500 +/- 750	4100 +/- 1300	11600 +/- 2100

a The % of filaments in total biomass was estimated using culture dry weight and an estimation for fungal dry weight assuming filament diameters of 2 - 3 μm and density of 1 g/L.

SC2, 30-50 % of the total biomass in reactor SC2, and 5-10 % of the total biomass in reactor P.concentration, and cyclic changes were observed. Rotifers, principally of the order Bedellodia, were present in a relative stable number (1,000 to 100,000 per mL) depending on the feeding pattern. As indicated in Table 4-2, rotifers were present in much higher concentrations in reactors C, SC2 and SC5 than in reactor P. This might explain the biomass stability of reactor P in comparison with reactors C, SC5 and SC2. The stable suspended solids concentration of reactor P might be attributed to a temporal substrate gradient flavoring flocculent (bacterial) growth over filamentous growth or to the inhibitory action of high phenol concentrations on predators.

4.3.7 Enumeration of phenol utilizers and TCE degraders

Most Probable Number (MPN) values for phenol utilizers ranged from 2.2 x 10^6 to 60 x 10^6 mL^{-1} for all reactors, and the MPN values for TCE degraders ranged from 0.34 x 10^6 to 40 x 10^6 mL^{-1} (Table 4-3). The percentage of TCE degrading phenol-degraders Protozoa and rotifers were present in all reactors. Their existence might be responsible for

the fluctuation of biomass and TCE transformation. The dominant protozoa were ciliates and their population varied (10^2 ~ 10^7 per mL) over the period of operation. The number of ciliates appeared to be inversely proportional to total suspended solids ranged from 7 to 70%. Reactor P had the highest number of phenol utilizers and TCE degraders (~10-100 time higher than other reactors). Reactors C, SC2 and SC5 were not significantly different, with approximately 2 x 10^6 mL^{-1} phenol utilizers and 0.3 x 10^5 mL^{-1} TCE utilizers. MPN enumeration results were consistent with the measured TCE transformation rates. Reactors with highest TCE transformation rates also had highest concentration of TCE degraders. The MPN method provided an approach for estimating the number of cometabolizing organisms, but the method was time consumed and required exhaustive effort to draw statistically valid conclusions. For samples with same order of magnitude MPN value, each dilution required 10, 20 or even 100 tubes to provide statistically distinguishable results. MPN measurements for reactor C, SC2 and SC5 were indistinguishable in the typical 5 tube counting procedure recommended by Standard Methods (APHA 1989). A further disadvantage of the MPN method was the need for a completely dispersed sample for dilution. This was problematic for filamentous or flocculent growth.

Table 4-3 Numbers of phenol and TCE degraders in mixed liquid from different feeding pattern reactors (sampling on day 192)

Reactor	MPN (cells/g of dry wt.)			
	Phenol degraders		TCE degraders	
	Cell no.	95 % CI[a]	Cell no.	95 % CI[a]
P	6.7 x 10^{10}	2.2 x 10^{10} - 2.0 x 10^{11}	4.5 x 10^{10}	1.5 x 10^{10} - 1.4 x 10^{11}
C	5.4 x 10^9	1.8 x 10^9 - 1.6 x 10^{10}	1.7 x 10^9	5.4 x 10^8 - 5.1 x 10^{10}
SC2	3.3 x 10^9	1.1 x 10^9 - 1.0 x 10^{10}	2.2 x 10^8	7.3 x 10^7 - 6.6 x 10^8
SC5	3.3 x 10^9	1.1 x 10^9 - 1.0 x 10^{10}	4.5 x 10^8	1.5 x 10^7 - 1.4 x 10^9

[a]CI, confidence interval.

4.3.8 Pure culture isolation and characterization

Fifty bacterial isolates with distinct Rep-PCR patterns were obtained. Reactors P and SC2 reactors appeared to have more diverse microbial communities than reactors C and SC5 reactors (Table 4-4). Only 13 isolates possessed the ability to degrade phenol. Of the phenol utilizers, 10 were also able to cometabolize TCE. Three species from reactor P (P-4, P-21 and P-23) had the highest TCE transformation rates. The three TCE-degrading isolates from SC5 and C (C-1, C-2 and SC5-1) grew slowly in phenol medium and transformed only 10~15% of the TCE present in the TCE transformation assay. Isolates C-1 and SC5-1 are similar in Rep-PCR pattern as well as in phenol and TCE degradation rates and cell morphology (filament). Similar REP-PCR pattern isolates among reactors are rare. As indicated in Figure 4-12, the REP-PCR patterns for isolates from reactor C and P are entirely different.

Characterization of isolates from the four reactors indicates that the microbial communities in the four reactors are different and complex. As summarized in Table 4-4 and Figure 4-13, only 20% of the community members were capable of transforming TCE (10 out of 50). Even the ability to utilize phenol was uncommon (13 out of 50). Over 75 % of isolates were unable to grow with phenol as the carbon source in mineral medium. Several explanations are possible for this observation. It is possible that organisms that were unable to degrade phenol in the assay used in this work might still be able to degrade phenol under other assay conditions, for example if growth factors provided by other community members were available, or if the phenol concentration used in the assay were reduced. The phenol concentration used might have been excessive for some isolates, especially those from reactors C and SC5 because these communities were not adapted to high concentrations of phenol. Finally, it is possible that some of the isolates were unable to use phenol because they use other substrates for growth, such as intermediates in the phenol degradation pathway or substances released by cell lysis.

Table 4-4. Characteristics of isolates from different reactor communities.

Reactor	Rep-PCR pattern	Colony morphology	Number of isolate	Phenol[a,c] utilization	TCE[b,c] degradation
Continuous	C-1	white, pearl[d]	10	+	13%
	C-2	white, small	3	+	11%
	C-3	white, small	5	-	< 5%
	C-4	yellow	3	-	< 5%
	C-5	yellow	1	-	< 5%
	C-6	yellow	1	-	< 5%
	C-7	yellow	3	-	< 5%
	C-8[e]	peachy/orange	1	-	< 5%
	C-9	white, large	3	-	< 5%
	C-10	orange	1	-	< 5%
	C-11	white,brown center	1	-	< 5%
Pulse	P-1	white, large	2	+	11%
	P-2	yellow	2	-	< 5%
	P-3	white,brown center, hard[d]	1	-	< 5%
	P-4	white,brown center, hard[d]	5	+	95%
	P-5	white, peal	2	-	<5%
	P-6	white, small	1	-	<5%
	P-7	white, small	1	-	<5%
	P-8	white, small	1	-	<5%
	P-9	white, small	1	-	<5%
	P-10	white, small	1	-	<5%
	P-11	yellow	2	-	<5%
	P-12	clear, small orange	1	-	<5%
	P-13	clear, small orange	1	-	<5%
	P-14	white, large	1	-	<5%
	P-15	white, large	1	-	<5%
	P-16	yellow	1	-	<5%
	P-17	small,white brown	1	-	<5%
	P-18	small,white brown	7	-	<5%
	P-19	orange	2	-	<5%
	P-20	white, small	1	-	<5%
	P-21	white, large	6	+	94%
	P-22	large, pearl, hard	11	-	<5%
	P-23	white, large	1	+	54%

Table 4-4. (cont'd)

Reactor	Rep.PCR pattern	Colony morphology	Number of isolate	Phenol[a,c] utilization	TCE[b,c] degradation
SC2	SC2-1[e]	peach/orange	6	-	<5%
	SC2-2	yellow, pinpoint	2	-	<5%
	SC2-3	white,large[d]	3	+	45%
	SC2-4	white,large[d]	3	+(yellow)	<5%
	SC2-5	white,small	4	-	<5%
	SC2-6	white,small	1	+	38%
	SC2-7	clear, small, waxy	4	+	<5%
	SC2-8	white, spreading	2	+(yellow)	<5%
	SC2-9	opaque	4	+	15%
	SC2-10	opaque	2	-	<5%
	SC2-11	buffy/ yellowish,large	4	-	<5%
	SC2-12	buffy,large	2	-	<5%
	SC2-13	white,small	1	-	<5%
	SC2-14	white,large	1	-	<5%
SC5	SC5-1[e]	white,pearl[d]	5	+	15%
	SC5-2[e]	yellow[d]	5	-	<5%
	SC5-3	yellow,small	2	-	<5%

a. Phenol utilization and TCE degradation assays were conducted in 20 mL glass vials. Each vial filled with 10 mL phenol medium (phenol concentration = 80 mg/L) and spiked to 1.0 mg/L of TCE. One loopful inoculum was transferred from R2A agar to vials and incubated on a 120 rpm rotatory shaker under room temperature for 10 days. Phenol utilization ability was determined by measuring the changes of optical density before and after incubation.

b. TCE degradation capacity was determined by monitoring TCE disappearance in a 10-day incubation period.

c. Each isolate was tested in triplicate.

d. Dominant colony morphology.

e. Similar REP-PCR patterns for isolates between reactor: C-1 and SC5-1, C-4 and SC5-2, C-8 and SC2-1.

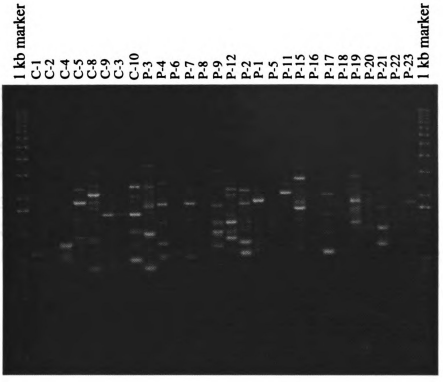

Figure 4-12 REP-PCR patterns of isolates from reactor P and C

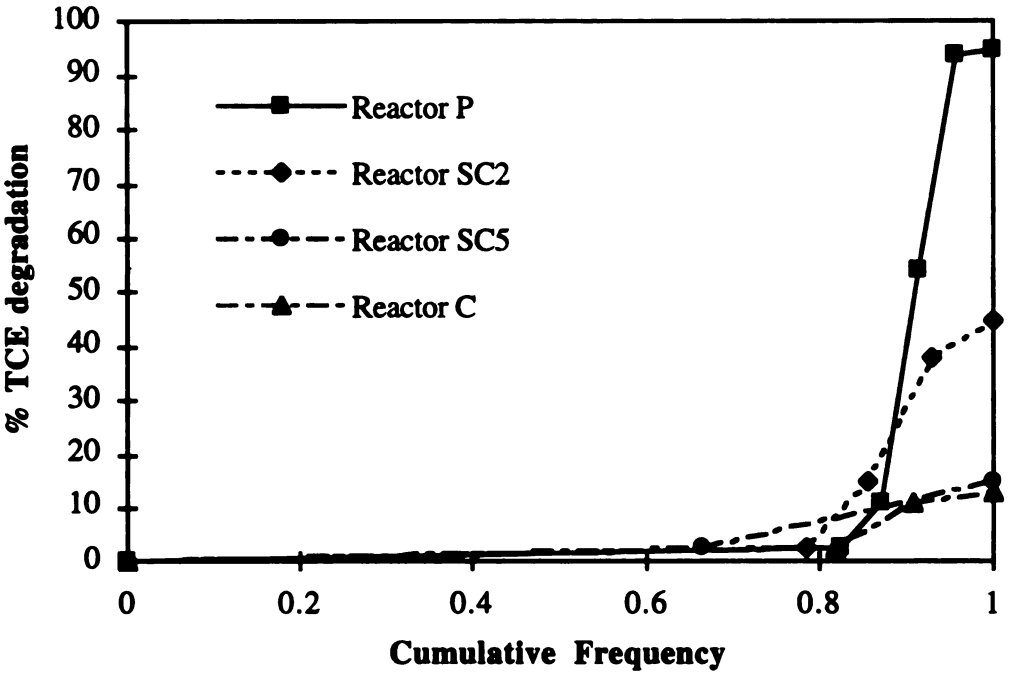

Figure 4-13 TCE transformation capacity profiles of isolated from different feeding pattern reactors.

The results of the isolates studies were consistent with measures of community function, such as TCE transformation and phenol utilization. The microbial communities of reactors P and SC2 exhibited higher rates of TCE and phenol degradation than reactors SC5 and C; the same pattern was observed in the bacterial isolates.

We conclude that communities enriched with continuous or protracted feeding intervals (reactor P and SC5) exhibited limited long-term capacity for TCE transformation. Microbial communities enriched under conditions of pulse or abbreviated feeding intervals (reactors P and SC2) maintained higher TCE transformation rates. An unexplained increase in TCE transformation rates was observed in reactor P. In addition, cyclic changes in TCE transformation rate and biomass were observed in reactor SC2.

4.4 Conclusions

Based on the above results, the following conclusions can be made

1. Growth substrate feeding patterns can have a profound effect on the selection of microorganism types and concentrations, and can dramatically change the cometabolic capabilities of a microbial community.

2. During start-up, conditions in reactors C and SC5 were initially favorable for the selection of TCE degraders. However, this feeding pattern also selected for filamentous microorganisms. Loss of TCE degradation activity during long term operation was probably due to the outgrowth of fungi which did not degrade TCE or did so slowly.

3. The pulse feeding pattern resulted in a more stable biomass concentration and a higher long-term capacity for TCE degradation.

4. The feeding pattern affected the reactor substrate level, DO profile, prevalence of predators and biomass yield. All of these factors may contribute to the final community structure and function .

5. Complex communities formed in the phenol fed reactors: many of the isolates (~70%) failed to degrade both phenol and TCE under the conditions of the assay. The pulse fed reactor exhibited higher diversity and had isolates with higher TCE transformation rates.

Literatures cited

APHA. Standard methods for the examination of water and wastewater. 17th ed., Washington, D. C.: APHA, 1989.

Arciero, D., T. Vannelli, M. Logan, and A. B. Hooper. "Degradation of trichloroethylene by the ammonia-oxidizing bacterium *Nitrosomonas europaea*." Bioch. and Bioph. Res. Commu. 159 (1989): 640-643.

Bailey, J. E. and D. F. Ollis. Biochemical Engineering Fundamentals. 2 nd ed., New York: McGraw-Hill, Inc., 1986.

Banks, C. J. and I. Walker. "Sonication of activated sludge flocs and the recovery of their bacteria on solid media." Journal of General Microbiology 98 (1977): 363-368.

Calaway, W. T. "The metazoa of waste treatment processess - rotifers." Journal of WPCF 40 (11 1968): R415.

Dabrock, B., J. Riedel, J. Bertram, and G. Gottschalk. "Isopropylbenze (cumene) - a new substrate for isolation of trichloroethene-degrading bacteria." Archives of Microbiology 158 (1992): 9-13.

Eikelboom, D. H. and H. J. J. van Buijsen. Microscopic sludge investigation manual. Deft, Neth.: TNO Res. Inst. Environ. Hygiene, 1981.

Folsom, B. R., P. J. Chapman, and P. H. Pritchard. "Phenol and trichloroethylene degradation by *Pseudomonas cepacia* G4: kinetics and interactions between substrates." Appl. Environ. Microbiol. 56 (1990): 1279-1285.

Fox, B. G., J. G. Borneman, L. P. Wackett, and J. D. Lipscomb. "Haloalkane oxidation by the soluble methane monooxygenase from *Methylosinus trichosporium* OB3b: mechanism and environmental implication." Biochemistry 29 (27 1990): 6419-6427.

Gerhardt, P., ed. Methods for general and molecular bacteriology. Washington, DC: American Society for Microbiology, 1994.

Gossett, J. M. "Measurement of Henry's law constants for C1 and C2 chlorinated hydrocarbons,." Environ. Sci. Technol. 21 (1987): 202-208.

Grady, C. P. L. Jr. "Biodegradation: Its measurement and Microbiological basis." Biotechnol. Bioeng. 27 (May 1985): 660-674.

Henry, S. M. and D. Grbic-Galic. "Effect of mineral media on trichloroethylene oxidation by acquifer methanotrophs." Microb. Ecol. 20, (1990): 151-169.

Hopkins, G. D. and P. L. McCarty. "Field evaluation of in situ aerobic cometabolism of trichloroethylene and three dichloroethylene isomers using phenol and toluene as the primary substrate." Environ. Sci. Technol. 29 (6 1995): 1628-1637.

Maltoni, C. and G. Lefemine. "Carcinigenicity bioassays of vinyl chloride." Environ. Res. 7 (1974): 387-398.

Nelson, M. J. K. , S. O. Montgomery, W. R. Mahaffey, and P. H. Pritchard. "Biodegradation of trichloroethylene and involvement of an aromatic biodegradative pathway." Appl. Environ. Microbiol. 53 (5 1987): 949-954.

Okaygun, M. S. and A. Akgerman. "Microbial dynamics in a continuously stirred tank reactor with 100% cell recycle." Water Environ. Res. 64 (6 1992): 811-816.

Oldenhuis, R., R. L. J. M. Vink, D. B. Janssen, and B. Witholt. "Degradation of chlorinated aliphatic hydrocarbons by *Methylosinus trichosporium* OB3b expressing soluble methane monooxygenase." Appl. Environ. Microbiol. 55 (11 1989): 2819-2826.

Sezgin, M. and D. Jenkins. "A unified theory of filamentous activated sludge bulking." J. WPCF (Feb. 1978): 362-381.

Storm, P. F. and D. Jenkins. "Identification and significance of filamentous microorganisms in activated sludge." J. WPCF 56 (5 1984): 449-458.

Tsien, H. C., G. A. Brusseau, R. S. Hanson, and L. P. Wackettet. "Biodegradation of trichloroethylene by *Methylosinus trichosporium* OB3b." Appl. Environ. Microbiol. 55 (12 1989): 3155-3161.

Vanilli, T., M. Logan, and A. B. Hooper. "Degradation of halogenated aliphatic compounds by the ammonia-oxidizating bacterium *Nitrosomonas europaes*." Appl. Environ. Microbiol. 56 (1990): 1169-1171.

Vogel, T. M. and P. L. McCarty. "Biotransformation of tetrachloroethylene to trichloroethylene, dichloroethylene, vinyl chloride, and carbon dioxide under methanogenic conditions." Appl. Environ. Microbiol. 49 (1985): 1080-1083.

Wackett, L. P. and D. T. Gibson. "Degradation of trichloroethylene by toluene dioxygenase in whole cell studies with *Pseudomonas putida* F1." Appl. Environ. Microbiol. 54 (1988): 1703-1708.

Westrick, J. J., J. W. Mello, and R. F. Thomas. "The groundwater survey." J. Am. Water Works Assoc. 76 (1984): 52.

CHAPTER 5

EFFECTS OF TCE TOXICITY ON CELL VIABILITY

5.1 Introduction

Aerobic TCE biodegradation can be mediated by methanotrophs (Alvarez-Cohen and McCarty 1991a; Henry and Grbic'-Galic' 1991; Oldenhuis et al., 1989; Tsien et al., 1989), propane oxidizers (Wacket et al., 1989), ethylene oxidizers (Henry and Grbic'-Galic' 1991), toluene, phenol, or cresol oxidizers (Folsom et al., 1990; Harker and Kim 1990; Shields et al., 1986), and ammonia oxidizers (Hyman and Arp 1992; Hyman et al., 1995; Rasche et al., 1991). These organisms possess catabolic oxygenases with broad substrate specificity and can catalyze fortuitous oxygenation of TCE when stimulated by their respective substrate.

Regardless of the microorganism type, certain features of oxygenase-mediated cometabolism must be considered in any engineered system: competitive inhibition, intermediate and product toxicity, and reductant supply. For oxygenase systems, TCE and the growth substrate are competitive inhibitors at the active cite of the oxygenase. For methanotrophs, TCE concentrations in the range of 50 mg/l are toxic, inhibiting TCE transformation and methane utilization (Henry and Grbic'-Galic' 1991; Oldenhuis et al., 1989). In pure and mixed cultures studies with methanotrophs, Henry and Grbic'-Galic' (1991) observed that oxidation of 6 mg/L TCE reduced subsequent methane utilization and decreased the number of viable cells in the pure culture by an order of magnitude. They hypothesized that toxicity was caused by the attack of reactive intermediates on cellular macromolecules, not from TCE itself or its degradation intermediates.

In evaluating TCE oxidation by *Pseudomonas putida* F1, Wacket and Gibson (1988) found evidence of toxicity and proposed that a toxic intermediate was responsible (Wackett and Gibson 1988). Wacket and Householder (1989) concluded that the toxic effects of TCE oxidation in *P. putida* F1, such as decreased growth rate and increased death rate, depended upon metabolic activation of TCE by toluene dioxygenase. In *E. coli*, TCE exposure led to increased doubling time and induction of stress proteins (Blom et al., 1992). The TCE concentration causing a 50% inhibition of growth (IC50) for *Nitrosomonas*, methanogens, and aerobic heterotrophs were 0.81 mg/L, 13 mg/L and 130 mg/L, respectively (Blum and Speece 1991). By comparison, LC50 values for fathead mirrows and the Microtox assay were 44 and 960 mg/L, respectively. Apparently, TCE is more toxic to *Nitrosomonas* rather than to methanogens and aerobic heterotrophs.

Broholm et al. (1990) suggested that competitive inhibition by TCE may reduce methane consumption rates (Broholm et al., 1990). Another factor affecting rates is toxicity. To estimate toxic effects, Alvarez-Cohen and McCarty (1991) introduced the idea of a limited transformation capacity (T_c) by resting cells. The concept is that a given mass of cells has a finite capacity for transformation of a nongrowth substrate, such as TCE. By coupling the idea of a finite transformation capacity with saturation kinetics, a kinetic expression was obtained that could account for product toxicity and limited reductant supply (Alvarez-Cohen and McCarty 1991b).

In the following section, we evaluate the viability of TCE-amended phenol utilizers. Viability of cells exposed to TCE is found to be dependent upon TCE degradation and the microbial species evaluated. Modeling efforts were taken to evaluate the loss of cells during TCE cometabolism. After selection of a model for estimatiion of the loss of cells, the required time and growth substrate for cell recharge can be determined and applied to design of the recharge stage for SBRs. The purpose of the studies was to verify TCE

toxicity effects and to explore possible models fort loss of cells during the TCE transformation.

5.2 Background

The mechanism of oxygenase catalyzed oxidation is similar to that of cytochrome p-450 catalyzed oxidation: both produce the same reactive species of oxygen (Miller and Guengerich 1982). Monooxygenase-mediated TCE oxidation results in epoxide formation, which is chemically and biologically converted to mineral end products:

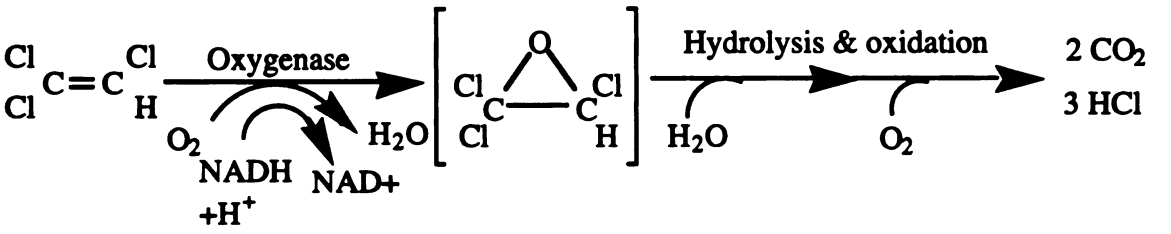

TCE epoxide is an extremely short-lived (~ 20 sec), highly reactive molecule that is toxic in mammalian systems. Thus it appears likely that the toxicity to whole cells observed during TCE transformation results from the epoxide or its degradation products rather than TCE itself.

Upon transforming ^{14}C–TCE, methanotrophs generate radiolabeled cellular protein (Oldenhuis et al., 1991). Wacket (1991) demonstrated ^{14}C incorporation into DNA, RNA, small molecules and lipids. Soluble methane monooxygenase and ammonia monooxygenase were radiolabeled during ^{14}C-TCE degradation (Hyman and Arp 1992; Oldenhuis et al., 1991). These observations suggest that nonspecific covalent binding of degradation products to cellular molecules causes the TCE-mediated inactivation of cells.

The mechanisms of TCE transformation toxicity can be more clearly understood by considering the minimal steps involved in a suicidal inactivation of an enzyme, as shown in Figure 5-1.

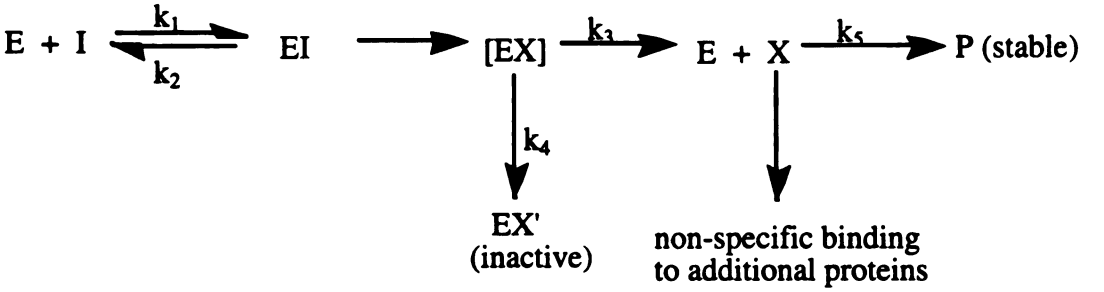

Figure 5-1 The minimal steps involved in a suicidal inactivation of an enzyme (Hyman and Arp 1991)

The initial reversible binding of the inhibitor (I) to the enzyme (E) to form an enzyme inhibitor complex (EI) is followed by a catalytic step (EI—>EX) which transforms the inhibitor to an activated reactive species (X). This reactive species can either bind to the enzyme to produce a covalently modified inactive enzyme complex (EX') or it can fully dissociate from the enzyme to give free X and active enzyme. As the free form of the reactive species diffuses from the active site of the enzyme it may either react with other cellular components or undergo further transformations to a stable unreactive product (P). The ratio of inhibitor activation events to the enzyme inactivation events is known as the partitioning ratio and is normally defined by the ratio of k_3/k_4. An ideal suicide substrate would have a partitioning ratio of 0. TCE can be regard as a nonspecific suicide substrate so the partitioning ratio should be larger than 0. The activated TCE degradation product covalently modifies numerous polypeptides or cellular components.

The loss of cells during cometabolism has been modeled by first order decay (Saez and Rittman 1989), transformation capacity (Alvaez-Cohen and McCarty 1991) and an unified model proposed by Criddle (1991). The expressions used in these models were summarized in equations 5-1, 5-2 and 5-3 respectively.

$$\frac{dX}{dt} = -b'X \qquad (5\text{-}1)$$

$$\frac{dC}{dX} = T_c \tag{5-2}$$

$$\frac{dX}{dt} = -bX - \frac{q_c}{T_c} X \tag{5-3}$$

Where X = active cells, b' = first order cell decay coefficient, include endogenous decay, and product toxicity (time^{-1}), b = endogenous decay coefficient (time $^{-1}$). T_C = transformation capacity (mg nongrowth substrate/mg cell) and q_C = specific transformation rate for nongrowth substrate (time^{-1}). These models are all empirical and can be applied to estimate the loss of cells during cometabolism.

5.3 Material and methods

5.3.1 Organisms and conditions

Pseudomonas cepacia G4 and *Pseudomonas putida* F1 were obtained from the laboratory of Dr. James Tiedje. Strain P2 was isolated from the phenol pulse fed reactor, as described in chapter 4. Strain P2 was able to use phenol but was unable to cometabolize TCE. Strains G4, F1, and P2 were batch cultured in a defined phenol medium. The composition of the medium was (per liter of deionized water): 100 mg of C_6H_5OH, 2.13 g of Na_2HPO_4, 2.04 g of KH_2PO_4, 1 g of $(NH_4)_2SO_4$, 0.067 g of $CaCl_2$ $2H_2O$, 0.248 g of $MgCl_26H_2O$, 0.5 mg of $FeSO_4$ $7H_2O$, 0.4 mg of $ZnSO_4$ $7H_2O$, 0.002 mg of $MnCl_2$ $4H_2O$, 0.05 mg of $CoCl_2$ $6H_2O$, 0.01 mg of $NiCl_2$ $6H_2O$, 0.015 mg of H_3BO_3, and 0.25 mg of EDTA. The pH of the medium was 6.8. Cells used in toxicity and viability studies were harvested in the stationary stage.

5.3.2 Assays of TCE and phenol concentrations and cell viability

TCE concentration was assayed by injecting a 1 mL headspace gas sample into a Hewlett-Packed 5890 gas chromatograph equipped with a 30 m (L), 0.53 mm (ID) DB624

capillary column (Alltech No. 93532) and a flame ionization detector. The flowrate of helium carrier was 12 mL/min. The GC oven was operated isothermally at 90°C. Sampling injection port and detector temperatures were both 250°C. Liquid phase TCE concentrations were calculated assuming equilibrium between TCE concentrations in the gas and liquid phases. A dimensionless Henry's law constant of 0.333 was determined for the growth medium at 21°C. The initial concentration of TCE was estimated from triplicate sterile controls after equilibration. In general, the coefficient of variance of TCE determination was 1 to 5% for triplicate samples. Phenol was analyzed by the 4-aminoantipyrene method (Martin 1949).

Viability experiments were conducted in triplicate using a series of 10-fold dilutions and R2A spread plates. Diluted cell culture was placed onto each plate and incubated for one week under 21°C. Colony forming units were counted daily until a constant number was obtained. In general, a 3 to 5 days incubation was required to obtain a constant reading.

5.3.3 Toxicity effects experiment

One hundred milliliters of cells were grown in a 250 ml glass vessel containing 100 mg/L phenol medium, capped and sealed with a Mininert valve. Periodically, grown cells were withdrawn and assayed for phenol concentration. As phenol concentration decreased to nondetectable levels, 10 mL of cell suspension was transferred to a 20 mL glass vial and spiked with TCE, and sealed with teflon-coated septa. The vials were then incubated at 21 °C in an 120 rpm shaker. After specified incubation periods, cell viability and TCE concentration were assayed. Two sets of control vials were prepared: TCE-free vials as controls for cell viability and sterile vials as controls for abiotic TCE losses.

5.3.4 TCE transformation capacity measurement

Ten milliliters of cell suspension (biomass concentration = 50 ~ 100 mg dry wt /L) was spiked with 2 mg TCE sealed with mininert valve in 20 mL vials. Those vials were incubated at 21°C in an 120 rpm shaker. TCE concentrations were periodically monitored until TCE degradation ceased. The viable cell concentrations before and after TCE degradation were measured by spread plating cell suspensions on R2A agar. Controls that without TCE addition were used to correct for loss of viable cells due to endogenous decay. The ratio of the degraded TCE to the decreased number of viable cells was the TCE transformation capacity. For unit conversion, it was assumed 1 g cell (as dry wt) is approximately equivalent to 2×10^{12} cell.

5.4 Results and discussions

5.4.1 Effects of TCE concentration on cell viability

P. cepacia G4 (10 mL of culture at cell concentration of 50 mg/l) were incubated in the presence of aqueous phase TCE concentrations ranging from 0 to 13 mg/L. Cell viability after 16 μg of TCE had been transformed. The concentrations of viable cells are summarized in Figure 5-2. A 56 % to 65% decrease in viable cells was observed for all TCE concentrations examined. Apparently, for strain G4, cell viability was independent of the applied TCE concentration over the range examined.

5.4.2 Effects of cell type on viability following TCE transformation

The role of TCE transformation in toxicity was established by comparing TCE -transforming strains - *P. cepacia* G4 and *P. putida* F1, with the phenol-degrading isolate P2. Strain P2 does not degrade TCE. All cultures were amended with an aqueous phase concentration of TCE of 2.5 mg/L and incubated for 24 hours. The concentration of viable cells remaining was determined. Results are provided in Figure 5-3. *P. putida* F1 was

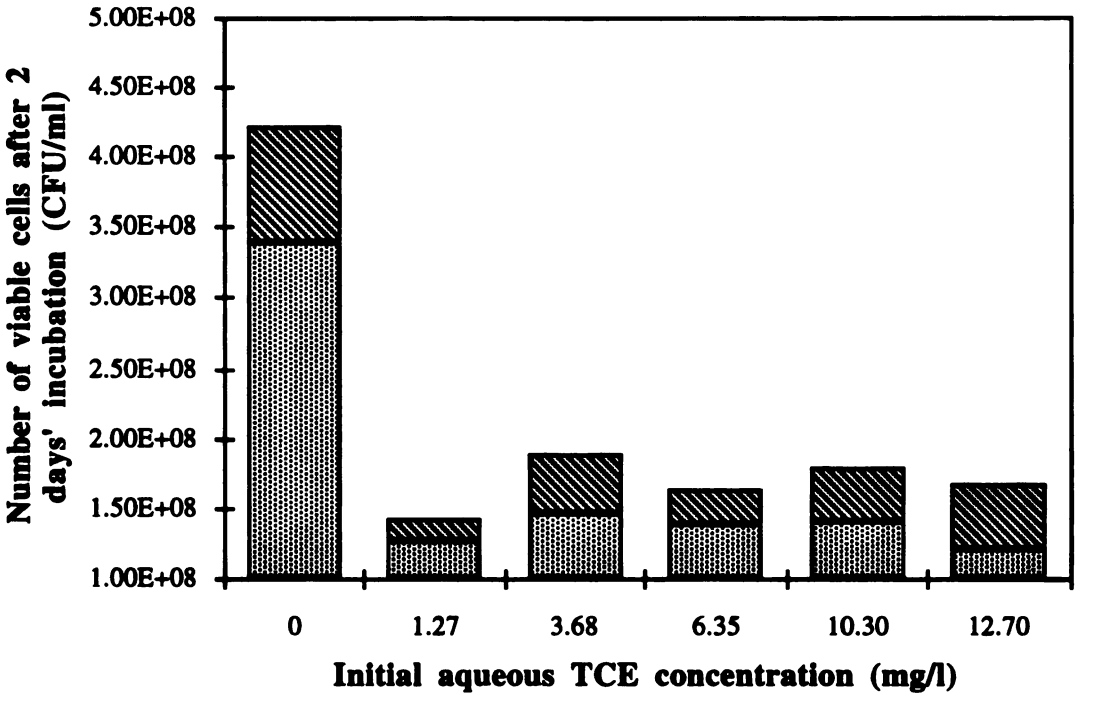

Figure 5-2. Concentration of viable *P. cepacia G4*after exposure to different initial TCE concentrationsd. ▨ represent average viable cell concentration +/- standard derviation.

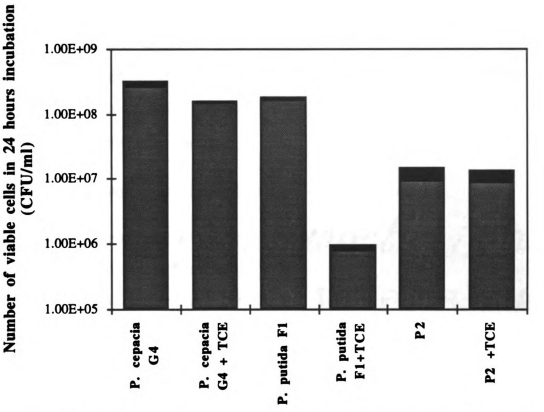

Figure 5-3. Concentration of different cell typesafter exposure to 2.5 mg/l of aqueous TCE in a 24 hours incubation period.■ represents average concentration of viable cell +/- one standard derviation.

highly sensitive to TCE, experiencing a 99.5% decrease in viable cells. *P. cepacia* G4 was less sensitive, with a 47% decrease in viable cells. Strain P2 did not undergo an appreciable loss. These results were supportive of the generally held view that: (1) TCE toxicity is linked to TCE transformation, inasmuch as strain P2 cells exhibited no loss of cell viability and (2) TCE toxicity is species dependent. *P. cepacia* G4 was more resistant to TCE transformation toxicity than *P. putida* F1.

5.4.3 Quantification and modeling of TCE toxicity on *P. cepacia* G4

The transformation capacity of *P. cepacia* G4 was also measured to assess decrease in active organisms during TCE transformation. A T_c of (2.67±0.42) x 10^{-11} mg TCE / cell was obtained for cell concentrations ranges from 10^8 to 10^9. Assuming 1 g cell dry weight approximately to 2 x 10^{12} cells, a T_c of 0.0534±0.0084 mg TCE / mg cell dry wt. was obtained. This value is similar to experimental values (~ 0.06) and is higher than the reported transformation capacity of methanotrophs (0.036 mg TCE / mg cell (Alvaez-Cohen and McCarty 1991)) and *Nitrosomonas* (0.004 mg TCE / mg cell (Hyman 1995)). A summary of measured T_c for different cultures is provided in Table 5-1. As indicated in Table 5-1, (1) the transformation capacity model adequately predicted the loss of viable cell during TCE transformation, and (2) phenol enrichment from pulse fed reactor and *P. cepacia* G4 have higher TCE transformation capacities compared to methanotrophs, *P. putida* F1 and *Nitrosomonas*.

5.5 Conclusions

For the TCE concentrations range of 1 to 10 mg/L, degradation of TCE causes the loss of viable cells. Results indicated that TCE transformation resulted in cell death, or at least a loss of culturability on spread plates. It might be argued that the loss of cell culturability is the result of damage to critical cell enzyme systems, and that repair of those

systems would enable regrowth. In these experiments, however, there was no evidence of damaged cells, capable of slowly growing on spread plates.

Table 5-1 TCE transformation capacity of different cultures

Culture	T_C (mg TCE /mg cell[a])
phenol enrichment	0.12 +/- 0.015
P. cepacia G4	0.054 +/- 0.008
P. putida F1	0.012 +/- 0.002
methaotrophs	0.036[b]
Nitrosomonas europaea	0.004[c]

[a] mg cell as dry wt
[b] Alvarez-Cohen and McCarty, 1991
[c] Hyman et al., 1993

The degree of TCE toxicity evaluated by cell reproduction ability was species dependent. Two TCE degraders -*P. cepacia* G4 and *P. putida* F1- exhibited different sensitivity to TCE toxicity. *P. cepacia* G4 might be advantageous for bioremediation applications. Death of *P. cepacia* G4 resulting from TCE transformation was well modeled by use of a transformation capacity term and was log-linearly related to the number of cell that were not exposed to TCE. Thus, it appears that modeling and quantification efforts may be applied to assess the loss of active cells during TCE cometabolism. To compensate for TCE toxicity, additional growth substrate must be supplied for regeneration, and models are needed to predict the required time for cell regeneration or regrowth.

Literatures cited

Alvarez-Cohen, L. and P. L. McCarty. "TCE transformation by a mixed methanotrophic culture - effects of toxicity, aeration and reductant supply." Appl. Environ. Microbiol. 57 (1 1991a): 228-235.

Alvarez-Cohen, L. M. and P. L. McCarty. "A cometabolic biotransformation model for halogenated aliphatic compounds exhibiting product toxicity." Environ. Sci. Technol. 25 (1991b): 1381-1387.

Blom, A., W. Harder, and A. Matin. "Unique and overlapping pollutant stress proteins of *Escherichia Coli*." Appl. Environ. Microbiol. 58 (1 1992): 331-334.

Blum, D. J. W. and R. E. Speece. "A database of chemical toxicity to environmental bacteria and its use in interspecies comparisons and correlations." Research Journal WPCF 63 (3 1991): 198-207.

Broholm, K., B. K. Jensen, T. H. Christensen, and L. Olsen. "Toxicity of 1, 1, 1-trichloroethane and trichloroethene on a mixed culture of methane-oxidizing bacteria." Appl. Environ. Microbiol. 56 (8 1990): 2488-2493.

Folsom, B. R., P. J. Chapman, and P. H. Pritchard. "Phenol and trichloroethylene degradation by *Pseudomonas cepacia* G4: kinetics and interactions between substrates." Appl. Environ. Microbiol. 56 (1990): 1279-1285.

Harker, A. R. and Young Kim. "Trichloroethylene degradation by two independent aromatic degrading pathways in *Alcaligene eutrophus* JMP134,." Appl. Environ. Microbiol. (1990): 1179-1181.

Henry, S. M. and D. Grbic-Galic. "Influence of endogenous and exogenous electron donors and trichloroethylene oxidation toxicity on trichloroethylene oxidation by

methanotrophic cultures from a groundwater aquifer." Appl. Environ. Microbiol. 57 (1 1991): 236-244.

Hyman, M. R. and D. J. Arp. "$^{14}C_2H_2$- and $^{14}CO_2$-labeling studies of de nova synthesis of polypeptides by *Nitrosomonas europaea* during recovery from acetylene and light inactivation of ammonia monooxygenase." J of Bio. Chem. 267 (3 1992): 1534-1545.

Hyman, M. R., S. A. Russell, R. L. Ely, K. J. Williamson, and Arp. D. J. "Inhibition, inactivation, and recovery of ammonia-oxidizing activity in cometabolism of trichloroethylene by *Nitrosomonas europaea*." Appl. Environ. Microbiol. 61 (4 1995): 1480-1487.

Miller, R. E. and F. P. Guengerich. "Oxidation of trichloroethylene by live microsomal P-450 evidence for chlorine migration state not involving trichloroethylene oxide." Biochemistry 27 (5 1982): 1090-1097.

Oldenhuis, R., J. Y. Oedzes, and D. B. Janssen. "Kinetics of chlorinated hydrocarbon by *Methylosinus trichosporium* OB3b and toxicity of trichloroethylene." Appl. Environ. Microbiol. 57 (1 1991): 7-14.

Oldenhuis, R., R. L. J. M. Vink, D. B. Janssen, and B. Witholt. "Degradation of chlorinated aliphatic hydrocarbons by *Methylosinus trichosporium* OB3b expressing soluble methane monooxygenase." Appl. Environ. Microbiol. 55 (11 1989): 2819-2826.

Rasche, M. E., M. R. Hyman, and D. J. Arp. "Factors limiting aliphatic chlorocarbon degradation by *Nitrosomonas europaea*: cometabolic inactivation of ammonia monooxygenase and substrate specificity." Appl. Environ. Microbiol. 57 (10 1991): 2986-2994.

Shields, M. S., S. O. Montgomery, P. J. Chapman, S. M. Cuskey, and P. H. Pritchard. "Novel pathway of toluene catabolism in the trichloroethylene-degrading bacterium G4." Appl. Environ. Microbiol. 55 (6 1986): 1624-1629.

Tsien, H. C., G. A. Brusseau, R. S. Hanson, and L. P. Wackett. "Biodegradation of trichloroethylene by *Methylosinus trichosporium* OB3b." Appl. Environ. Microbiol. 55 (12 1989): 3155-3161.

Wackett, L. P., G. A. Brusseau, S. R. Householder, and R. S. Hanson. "Survey of microbial oxygenases: trichloroethylene degradation by propane-oxidizing bacteria." Appl. Environ. Microbiol. 55 (1 1989): 2960-2964.

Wackett, L. P. and D. T. Gibson. "Degradation of trichloroethylene by toluene dioxygenase in whole cell studies with *Pseudomonas putida* F1." Appl. Environ. Microbiol. 54 (1988): 1703-1708.

Wackett, L. P. and S. R. Householder. "Toxicity of trichloroethylene to *Pseudomonas putida* F1 is mediated by toluene dioxygenase." Appl. Environ. Microbiol. 55 (10 1989): 2723-2725.

CHAPTER 6

EXPERIMENTAL EVALUATION AND NUMERICAL SIMULATION OF TRICHLOROETHYLENE COMETABOLISM BY A PHENOL-FED ENRICHMENT IN SEQUENCING BATCH REACTORS

6.1 Introduction

Many hazardous compounds can be detoxified by cometabolic reactions. Use of such reactions will likely lead to novel wastewater treatment and groundwater remediation processes. To date, however, development of engineered systems for cometabolism has proceeded slowly. In part, this can be attributed to challenges inherent to cometabolic transformations, including competition for enzyme between the growth and nongrowth substrates, the requirement for continual or periodic inputs of growth or energy substrate, and loss of activity due to product toxicity.

Sequencing batch reactors (SBRs) offer several advantages for cometabolic transformations. An SBR can alternate between periods of growth on growth substrates and periods of cometabolism of nongrowth substrates, eliminating the possibility of competitive inhibition for enzyme between the growth and nongrowth substrates. In an SBR, growth substrates can be added as needed to rejuvenate the cometabolizing biomass and to select for microbial populations with favorable transformation kinetics and settling properties. The ability to mix during the fill period is a favorable feature for cometabolism and for hazardous waste treatment. Chemicals entering during this period are readily diluted and degraded by a concentrated microbial suspension. This enables

treatment of contaminants at concentrations that would be toxic in many other reactor configurations.

For the bench-scale SBR described in this chapter, cometabolic oxygenase activity was induced by the addition of phenol as growth substrate. Phenol and trichloroethylene (TCE), the nongrowth substrate, were provided in separate stages, preventing competitive inhibition. Addition and degradation of phenol occurred during the "recharge" period, a period that replaces the idle period of the conventional SBR sequence of operations. Periodic phenol addition rejuvenated and sustained TCE cometabolism during the fill and react periods.

Design of SBRs for cometabolism is not obvious or straight forward. We adopted a mechanistic approach using mass balance relationships. In this paper, we illustrate the development and verification of these procedures for a bench-scale SBR. The proposed approach is shown to successfully describe cometabolism and volatilization in this system.

6.2 Modeling considerations

6.2.1 Substrate removal mechanisms

Mechanisms of contaminant removal include biodegradation, air stripping, and sorption. Not all of these mechanisms are significant for every compound. The relative importance of the different removal mechanisms depends upon the kinetics of biodegradation, mass transfer coefficients, Henry's constant, and solid partition coefficients. As indicated in Table 6-1, for volatile substrates, such as TCE, the major removal mechanisms in an aerated SBR are biodegradation and air stripping, with minor removal by sorption. Less volatile substrates, such as phenol, are removed by biodegradation, and negligible phenol is removal by air stripping and sorption. Mathematical expressions must accurately account for both physical and biological

removal to successfully simulate biomass and substrate concentrations. Development of these expressions is described in the following sections.

Table 6-1 Biodegradability, Henry's constant and solid partition coefficient of phenol and TCE

Compounds	phenol	TCE
Biodegradability	Readily biodegraded in acclaimed activated sludge (1)	Cometabolism by some oxygenase system (2)
Henry's constant H (L water/ L gas)	1.64×10^{-5} at 25°C (3)	0.33 at 21°C (4)
Partition coefficient in activated sludge K_p $(\frac{mg/Kg\ VSS}{mg/L\ water})$	95 at 25°C (5)	295 at 25°C (5)

Reference (1) D'Adamo et al., 1984), (2) Oldenhuis et al., 1989; Wacket et al., 1989, (3) Mackay and Shiu 1981, (4) Gossett 1987, (5) Estimate from log K_p $=1.14 + 0.58 \log K_{ow}$ (Dobbs et al., 1989).

Biodegradation

For hazardous contaminants, experimental evaluation of kinetic expressions is recommended. Batch experiments on the phenol-fed enrichment of the SBR operated in this study established that removal of phenol was zero-order with respect to phenol concentration and first order with respect to biomass concentration for phenol concentrations less than 200 mg/L. Thus, $r_s = -k^o X_a$, where r_s = phenol removal rate (mg/L-d), k^o = maximum specific rate of phenol utilization (mg/mg-d) and X_a = active biomass concentration (mg/L). This result is similar to the findings of Thischler and Eckenfielder (1969) and Rizzuti et al. (1982).

For cometabolism of TCE, saturation kinetics provided the best description of degradation :

$$r_c = -\frac{k_c C X_a}{K_c + C} \qquad (6\text{-}1)$$

where C = aqueous TCE concentration (mg/L), k_c = maximum specific rate of TCE transformation (mg/mg-d), and K_c = half saturation coefficient for TCE (mg/L). At low TCE concentration ($C << K_c$):

$$r_c = -k_c' C X_a \qquad (6\text{-}2)$$

where k_c' = second-order rate coefficient (l/mg-d).

Air stripping

Delivery of oxygen by aeration results in the mass transfer of volatile compounds (TCE, in this case) to the gas phase:

$$r_{st} = K_L a(C - C^*) \qquad (6\text{-}3)$$

where C = aqueous phase contaminant concentration (mg/L); C^* = aqueous phase contaminant concentration at equilibrium (mg/L); and $K_L a$= overall mass transfer coefficient (d^{-1}).

Sorption

Sorption of contaminants by microorganisms is a relatively rapid process (Matter-Muller et al., 1980). For a liquid/solid system at equilibrium, the concentration of a contaminant on a solid sorbent can be expressed as $C_s = K_p C_L$, where K_p = sorption partition coefficient (L/kg), C_s = concentration of contaminant on the solid (mg/kg) and C_L = concentration of contaminant in the liquid (mg/L). This relationship is generally valid at the low contaminant concentrations, such as those encountered in wastewater

treatment. Sorption partition coefficients can be related to octanol/water partition coefficients (K_{ow}). For activated sludge the following relation was proposed:

$$\log K_p = 0.67 \log K_{ow} - 2.61 \text{ (Matter-Muller et al., 1980)} \quad (6\text{-}4a)$$

$$\log K_p = 0.58 \log K_{ow} + 1.14 \text{ (Dobbs et al., 1989)} \quad (6\text{-}4b)$$

For a given K_p, the percentage of contaminant partitioning into solids (P) can be estimated by:

$$P(\%) = \frac{K_p X \times 10^{-6}}{K_p X \times 10^{-6} + 1} \times 100 \quad (6\text{-}5)$$

where X = suspended solid concentration, mg/L.

6.2.2 Mass balance equations

Equations describing removal of nongrowth substrate were obtained by performing a mass balance on nongrowth substrate for the fill and react stages. Negligible nongrowth substrate was removed during the settle, decant, and recharge periods.

Mass balance on TCE

Because TCE is volatile (H_c = 0.33 at 21°C, Gossett, 1987), TCE mass balance expressions are needed for both the gas and liquid phases. Theoretical considerations indicate that adsorption of TCE into biomass is insignificant, and this was confirmed experimentally. The following liquid and gas phase TCE mass balance equations were derived for the fill period:

$$(V_o + Q^o t)\frac{dC_L}{dt} + Q^o C_L = Q^o C^o - K_L a_{,TCE}(C_L - \frac{C_g}{H_c})V_L - r_c V_L \quad (6\text{-}6)$$

$$\frac{dV_g C_g}{dt} = K_L a_{,TCE}(C_L - \frac{C_g}{H_c})V_L - Q_g C_g \quad (6\text{-}7)$$

where V_o = reactor liquid volume (mL) at the beginning of the fill period (t = 0), V_g = gas phase volume (mL), Q_g = air flowrate (mL/min), Q^o = influent flowrate (mL/min), C_L =

liquid phase TCE concentration (mg/mL), C^o = influent TCE concentration (mg/mL), $K_L a_{,TCE}$ = TCE overall mass transfer coefficient (min^{-1}), C_g = gas phase TCE concentration (mg/mL), and t_f = fill time (min). Rearranging equations 6-6 and 6-7 gives:

$$\frac{dC_L}{dt} = \frac{Q^o}{(V_o + Q^o t)}(C^o - C_L) - K_L a_{,TCE}(C_L - \frac{C_g}{H_c})V_L - \frac{k_c C_L X_a}{(K_c + C_L)} \qquad (6\text{-}8)$$

$$\frac{dC_g}{dt} = -\frac{C_g}{(V_T - V_L)}(Q_g - Q^o) + \frac{V_L}{(V_T - V_L)} K_L a_{,TCE}(C_L - \frac{C_g}{H_c}) \qquad (6\text{-}9)$$

where V_T = total reactor volume, including both liquid phase and gas phase (mL), and V_L = liquid volume of reactor (mL). Substituting $t_o = V_o / Q^o$, $V_L = V_o + Q^o t$ and $t_g = (V_T - V_o)/Q^o$ into equations 6-8 and 6-9 gives:

$$\frac{dC_L}{dt} = \frac{C^o - C_L}{t_o + t} - K_L a_{,TCE}(C_L - \frac{C_g}{H_c}) - \frac{k_c C_L X_a}{K_c + C_L} \qquad (6\text{-}10)$$

$$\frac{dC_g}{dt} = -\frac{C_g}{t_g - t}(Q_g / Q^o - 1) + \frac{t_o + t}{t_g - t} K_L a_{,TCE}(C_L - \frac{C_g}{H_c}) \qquad (6\text{-}11)$$

Assuming that the influent contains an insignificant concentration of cells and that decay of active cells is first-order with a decay coefficient b, then the biomass mass balance equation is:

$$\frac{dX_a}{dt} = -\frac{X_a}{t_o + t} - bX_a \qquad (6\text{-}12)$$

Integrating equation 6-12, gives

$$X_a = X_{ao} e^{-\ln(\frac{t_o + t}{t_o}) - bt} \qquad (6\text{-}13)$$

where X_{ao} = active biomass concentration at the beginning of fill (mg/L). When $bt << ln[(t_O+t)/t_O]$, equation 6-13 simplifies to

$$X_a = \frac{t_o}{t_o + t} X_{ao} \qquad (6\text{-}14)$$

For the react stage, mass balance expressions for substrate and biomass in the liquid phase are:

$$\frac{dC_L}{dt} = -K_L a_{,TCE}(C_L - \frac{C_g}{H_c}) - \frac{k_c C_L X_a}{K_c + C_L} \quad (6\text{-}15)$$

$$X_a = X_{ao} e^{-bt} \quad (6\text{-}16)$$

Substituting equations 6-16 into equation 6-15 gives:

$$\frac{dC_L}{dt} = -K_L a_{,TCE}(C_L - \frac{C_g}{H_c}) - \frac{k_c C_L X_{ao} e^{-bt}}{K_c + C_L} \quad (6\text{-}17)$$

For substrate in gas phase, the mass balance is:

$$\frac{dC_g}{dt} = K_L a_{,TCE}(\frac{V_L}{V_g})(C_L - \frac{C_g}{H_c}) - \frac{Q_g C_g}{V_g} \quad (6\text{-}18)$$

Mass balance on phenol

During the recharge period, phenol was fed for a fixed interval (30 minutes) to the settled biomass. Due to the low Henry's law constant for phenol (~1.64 x 10^{-5} at 25°C (Weast 1992)), removal of phenol by air stripping can be neglected. During recharge, the mass balance for phenol is:

$$\frac{dS}{dt} = \frac{S^o - S}{t_o + t} + r_s \quad (6\text{-}19)$$

For biomass,

$$\frac{dX}{dt} = \frac{-X}{t_o + t} + r_x \quad (6\text{-}20)$$

After completion of phenol addition, phenol degradation and biomass variation is described by:

$$\frac{dS}{dt} = r_s \quad (6\text{-}21)$$

$$\frac{dX}{dt} = r_x \quad (6\text{-}22)$$

6.3 Materials

6.3.1 Chemicals

Trichloroethylene (TCE, 99+%) was obtained from Aldrich Chemical Co., Milwaukee, Wis. Chemicals for preparation of media and analyses were ACS reagent grade from Aldrich or Sigma.

6.3.2 Bioreactor

A 3.7 L water jacketed Pyrex reactor was operated sequentially in fill, react, settle, decant and recharge modes (Figure 6-1). Mixing during the fill, react and recharge periods was accomplished using a magnetic stir plate set at 100 rpm. Temperature was maintained constant at 23 ± 1°C. Concentrated aqueous TCE (concentration = 12.5 mg/L ~ 125 mg/L) was delivered by a syringe pump and in-line mixed with mineral medium stream that was delivered by a peristaltic pump. The combined flow was then supplied to the reactor during the fill period. TCE volatilization losses were reduced by introducing TCE into the reactor below the liquid level. Oxygen was supplied by bubbling air through the reactor during the fill, react, and recharge periods. Phenol was fed by a syringe pump during the recharge period. During the decant period, supernatant was withdrawn by a peristaltic pump. A programmable timer was connected to the power supply to control the on-off status of pumps, the aerator, and the mixer. The solids retention time of the enrichment was maintained at 10 days by daily wasting of 10% of the reactor liquid volume during the recharge period. All tubing and fittings in contact with TCE were made of teflon, glass, or stainless steel to reduce losses of TCE. Before initiating reactor operation, all fittings and connections were leak tested by pressurizing the reactor.

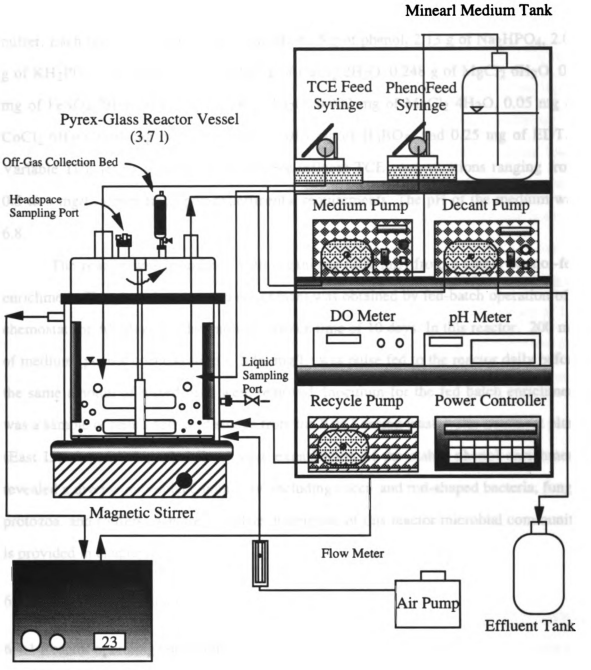

Figure 6-1 Experimental setup for bench-scale SBR

6.3.3 Media and inoculum preparation

The influent media contained phenol, macro and micronutrients, and phosphate buffer. Each liter of deionized water contained: 5 g of phenol, 2.13 g of Na_2HPO_4, 2.04 g of KH_2PO_4, 1 g of $(NH_4)_2SO_4$, 0.067 g of $CaCl_2$ $2H_2O$, 0.248 g of $MgCl_2$ $6H_2O$, 0.5 mg of $FeSO_4$ $7H_2O$, 0.4 mg of $ZnSO_4$ $7H_2O$, 0.002 mg of $MnCl_2$ $4H_2O$, 0.05 mg of $CoCl_2$ $6H_2O$, 0.01 mg of $NiCl_2$ $6H_2O$, 0.015 mg of H_3BO_3, and 0.25 mg of EDTA. Variable TCE levels were added to achieve influent TCE concentrations ranging from 0.5 to 5 mg/L, depending upon experimental requirements. The pH of the medium was 6.8.

The reactor was inoculated with organisms (200 mL) from a stable phenol-fed enrichment. The phenol acclimated enrichment was obtained by fed-batch operation of a chemostat for 300 days at a hydraulic residence time of 10 days. In this reactor, 200 mL of medium (phenol concentration = 2000 mg/L) was pulse fed to the reactor daily before the same amount of mixed cells were removed. Inoculum for the fed batch enrichment was a sample of return activated sludge from the East Lansing wastewater treatment plant (East Lansing, Michigan). Microscopic examination of the stable phenol enrichment revealed a diverse microbial community, including cocci- and rod-shaped bacteria, fungi, protozoa, and rotifers. A more complete description of this reactor microbial community is provided in chapter 4.

6.4 Experimental conditions

6.4.1 Reactor operating conditions

Behavior of the SBR can be divided into three distinct operating phases: (1) a start-up period in which the community adapted to cyclic SBR operation in the absence of TCE, (2) a period of acclimation to TCE addition, and (3) stabilized TCE removal. During start-up, TCE was not added for over 100 cycles (2 months). The reactor was

operated with 2 cycles per day. Each cycle consisted of a 1 hr fill period, 3 hr react period, 1 hr settling period, 1 hr decant period, and 6 hr recharge period. After the reactor had stabilized with respect to biomass and phenol concentrations, TCE feed was initiated during the fill period. At the beginning of the fill period, the liquid volume was 1250 mL. TCE and mineral medium was supplied at a flowrate of 20.8 mL/min to give a final liquid volume of 2500 mL at the end of the fill period. Oxygen was provided by bubbling air through the reactor at 220 ~ 280 mL/min (flowrate decreased slightly as liquid level increased). During the react stage, aeration continued, but no additional influent entered the reactor. During the settling period, air flow and mixing ceased. After one hour of settling, a decant pump was activated to withdraw supernatant from the reactor at a rate of 19.3 mL/min. Aeration and mixing resumed during the recharge step. At the beginning of the recharge period, a 5 g/l phenol solution was supplied to the reactor at a flowrate of 1.5 mL/min for 30 min. Mixing and aeration continued for 5.5 hrs to completely remove the added phenol. The operating pattern and parameters are summarized in Table 6-2 and Figure 6-2.

TCE, phenol, pH, dissolved oxygen (DO) and mixed liquid suspended solids (MLSS) were monitored periodically. TCE transformation activity was evaluated using cells removed for control of the solids residence time.

6.4.2 Batch assay of TCE transformation activity

Batch TCE transformation assays were conducted in 20 mL glass vials sealed with teflon coated butyl rubber stoppers and aluminum crimp caps. A 5 mL volume of cell suspension was dispensed into the vial, sealed, and spiked with 10~50 μl of aqueous TCE stock solution. The vial was incubated in an 120 rpm rotatory shaker under 23°C. Periodically, 0.1 mL gas phase samples were withdrawn and injected into a Hewlett-Packed 5890A gas chromatograph (GC) equipped with a DB624 capillary column (Alltech No. 93532) and a flame ionization detector. The flowrate of carrier gas, helium,

Table 6-2. Summary of bench-scale SBR operating parameters

Parameter	value
Reactor Volume	
Total volume, V_T	3700 mL
Liquid volume, V_L	1250 mL - 2500 mL
Headspace volume, V_g	1200 mL - 2450 mL
Initial volume, V_o	1250 mL
Flow rate	
Influent flow rate, Q^o	20.83 mL/min
TCE concentration, C^o	0.5 - 5 mg/L
Recharge flow rate, Q_{RC}	1.5 mL/min
phenol concentration, S^o	5000 mg/L
Airflow, Q_g	220 - 280 mg/L
Minimum oxygen concentration in reactor	2 mg/L
Operating mode	
Fill time, t_f	1 hr
React time, t_r	3 hr
Settle time, t_s	1 hr
Decant time, t_d	1 hr
Recharge time, t_{rc}	6 hr
-phenol feed mode	0.5 hr
-phenol react mode	5.5 hr
operating cycle time, t_c	12 hr/cycle
Sludge age, SRT	10 day

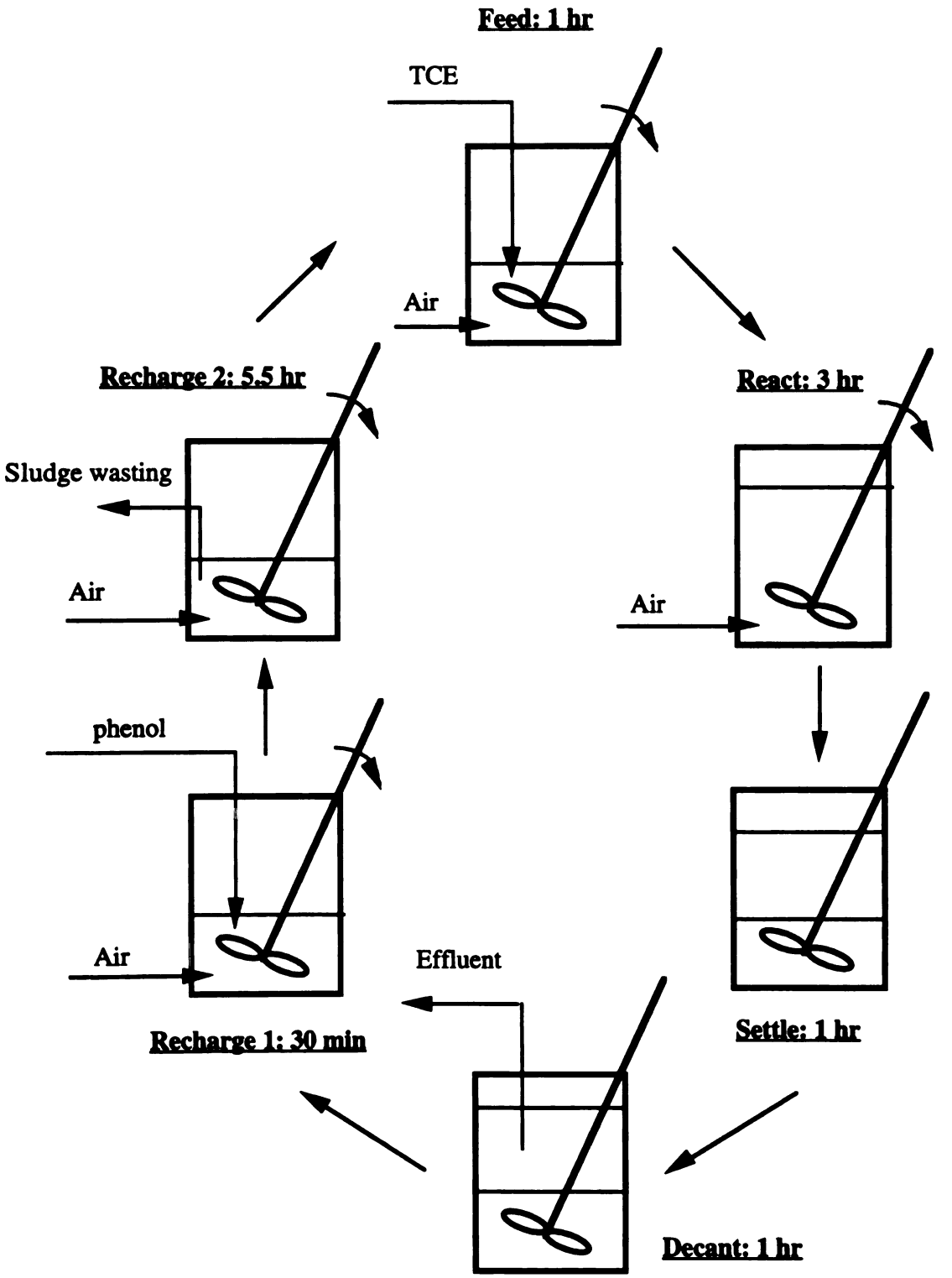

Figure 6-2 Operating mode of bench-scale SBR for TCE cometabolis

was 12 mL/min. Oven temperature was 90 °C, and detector and injector temperatures were 250 °C. TCE concentrations were determined by comparing the peak areas of samples to the peak areas of standards. The coefficient of variance ranged from 1 to 5% for triplicate samples. The total sampled volume for each vial was less than 5% of the total headspace volume. All reported TCE concentrations are aqueous concentrations calculated under the assumption that TCE concentrations in gas and liquid phases were in equilibrium. A dimensionless Henry's law constant of 0.355 at 23 °C was used in liquid phase TCE calculation (Gossett 1987). The initial mass of TCE added to the vial was estimated from triplicate uninoculated controls calculated using Henry's law. Preliminary work (Clowater 1992) established that equilibrium was achieved after 30 seconds of hand shaking and 3 min incubation in an 120 rpm rotatory shaker.

6.4.3 Measurement of pH, dissolved oxygen, phenol, and MLSS

Culture pH and dissolved oxygen were measured with a pH meter (Orion 720) and a dissolved oxygen probe (Orion model 97-08), respectively. Phenol was measured by the 4-aminoantipyrene derivative method (Martin 1949). The detection limit for phenol was approximately 0.5 mg/L. Coefficients of variance for 5 samples were typically less than 5%. Suspended solids were measured by the dry weight method of Standard Methods (APHA 1989) but a 0.2 μm membrane filter was used instead of a glass fiber filter.

6.4.4 Measurement of TCE in reactor off-gas

A modification of National Institute for Occupational Safety and Health (NIOSH) method for measuring airborne contaminants was used to measure TCE concentration in reactor off-gas. NIOSH approved glass tubes containing coconut-shell derived activated carbon was attached to the off-gas line to capture volatilized TCE. The adsorbed TCE was extracted with carbon disulfide, diluted into isooctane, and injected into a gas

chromatograph (Hewlett-Packard 5890) equipped with a DB5 capillary column (J&W Scientific). The flowrate of carrier gas (nitrogen) was 1.5 mL/min. Detection was accomplished with a ^{63}Ni electron-capture detector. The GC oven temperature program was: 1 min at 45°C increasing at 5°C/min to 70°C with a final holding period of 1 min at 70°C. Injection port temperature was 250°C, and detector temperature was 350°C.

Known quantities of TCE were injected onto activated carbon in off-gas collection tubes to determine TCE recovery efficiency. 95 ± 5% of the TCE was recovered. Accordingly, a correction factor of 0.95 was applied to off-gas TCE measurements.

6.4.5 Mass balance experiments

Mass balance experiments allow TCE removal to be divided into air-stripped and biodegraded fractions. Parameters measured during mass balance studies include flow rate of the feed solution, TCE concentrations in both the feed stream and the reactor (including both gas and liquid phases), and mass of TCE trapped on activated carbon. Mass balance experiments were conducted from the beginning of the fill period and ended when reactor TCE concentration was no longer detectable (< 1 μg/l). Gas phase TCE samples were withdrawn from a mininert valve mounted on the reactor using a gas-tight syringe and injected into the GC for TCE measurement. The gas phase sample volume varied from 0.1 mL to 0.5 mL depending upon the TCE concentration. For aqueous phase TCE sampling, 2 mL of liquid sample was withdrawn from the reactor and preserved by injection and sealing in a 20 mL vial containing 30 μl H_3PO_4 (85%). These samples were then analyzed by GC/ECD.

6.5 Results and discussion

6.5.1 Mass balance experiment

Mass balance experiments provided a means of assessing TCE removal by different mechanisms. The major removal mechanisms were air stripping and biodegradation. Partitioning of TCE to biomass was examined theoretically and experimentally. For a suspended solids concentration of 0.1%, about 0.0084% of the TCE was expected to partition to cells, as calculated from equation 6-4a, assuming $\log K_{ow}$ for TCE = 2.29 (Weast 1992). Experimental results confirmed that TCE partitioning to cells was insignificant. Comparing the aqueous TCE concentrations of autoclaved samples to the aqueous TCE concentrations of uninocculated samples (Figure 6-3), no significant difference was observed. However, TCE adsorption by biomass might be significant at higher solids concentrations, as predicted by equation 6-5.

TCE removal by air stripping was evaluated by comparing TCE removal in an abiotic SBR to the TCE removal in the biotic reactor. Both reactors were operated under identical except that the abiotic reactor was not inoculated with microorganisms. Figure 6-4 illustrates observed TCE removal in both reactors. The presence of organisms enhanced TCE removal significantly. In the abiotic reactor, higher TCE concentrations were observed, and a longer react time was required to achieve the same TCE removal achieved in the biotic reactor.

The fate of influent TCE was determined by monitoring TCE concentrations in the reactor and in the off-gas. The portion of influent TCE removed by biodegradation was calculated from mass balance equations. In most measurements, biodegradation accounted for 80 to 95 % of TCE removal and air stripping for 5 to 10% TCE removal (Figure 6-5). Less than 5% of influent TCE was not accounted for and may have leaked from the reactor or adsorbed onto tubing or fittings. Results from the mass balance

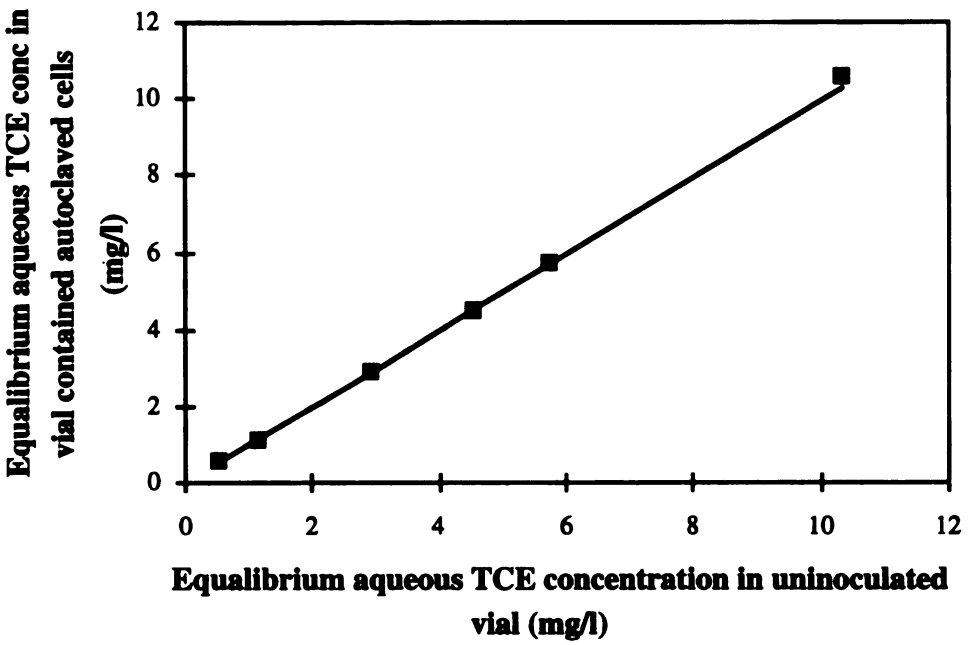

Figure 6-3 Comparison of the observed aqueous TCE concentration in uninoculated samples and samples that contained 840 mg/L of autoclaved cells. TCE concentration was measured after the sample was incubated for 2 hr at 120 rpm on a rotatory shaker . Error bars denote the standard derivation of triplicate samples.

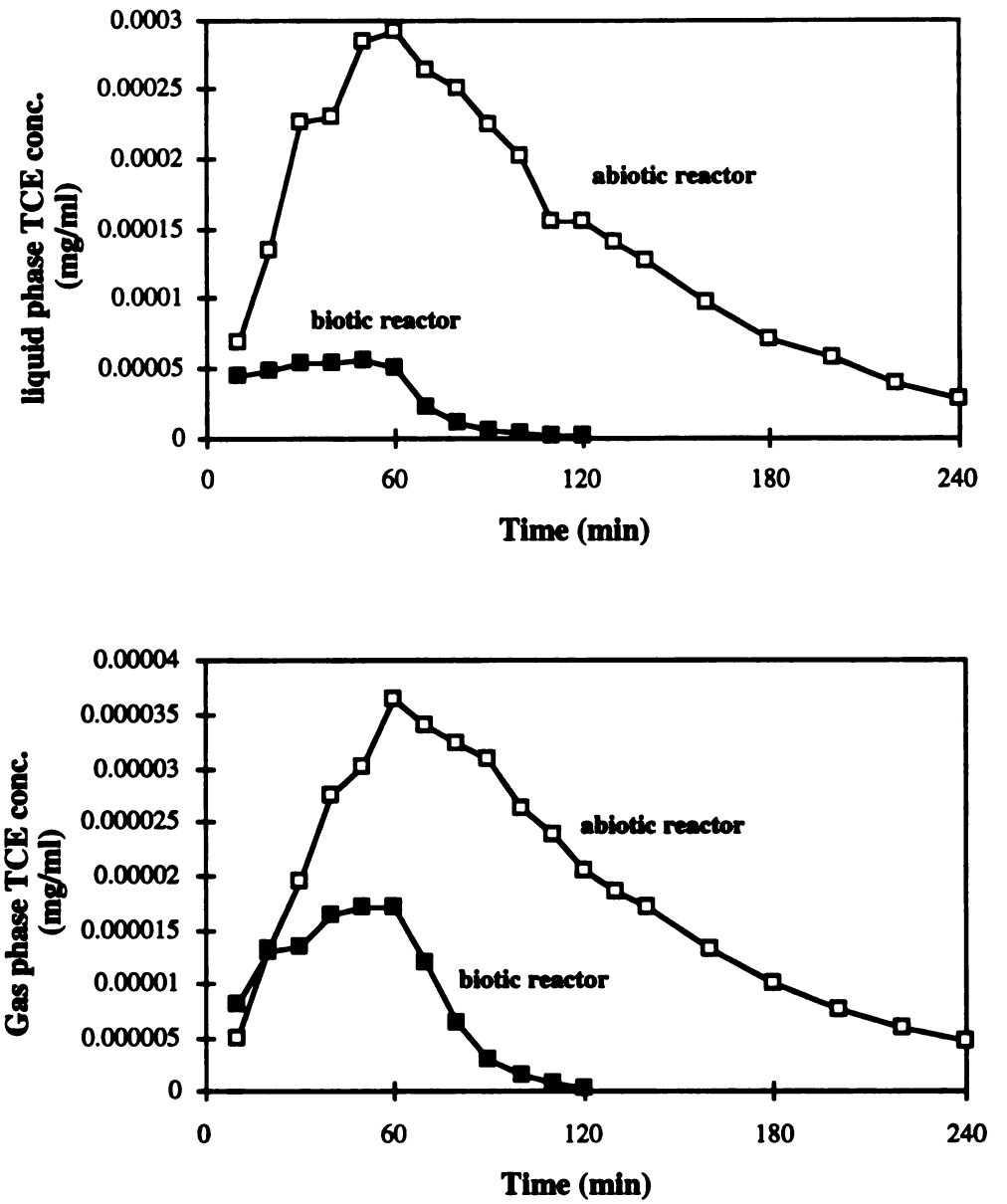

Figure 6-4 Observed TCE concentrations during fill and react period in an SBR with influent containing 0.5 mg/L TCE in (a) liquid phase and (b) gas phase.

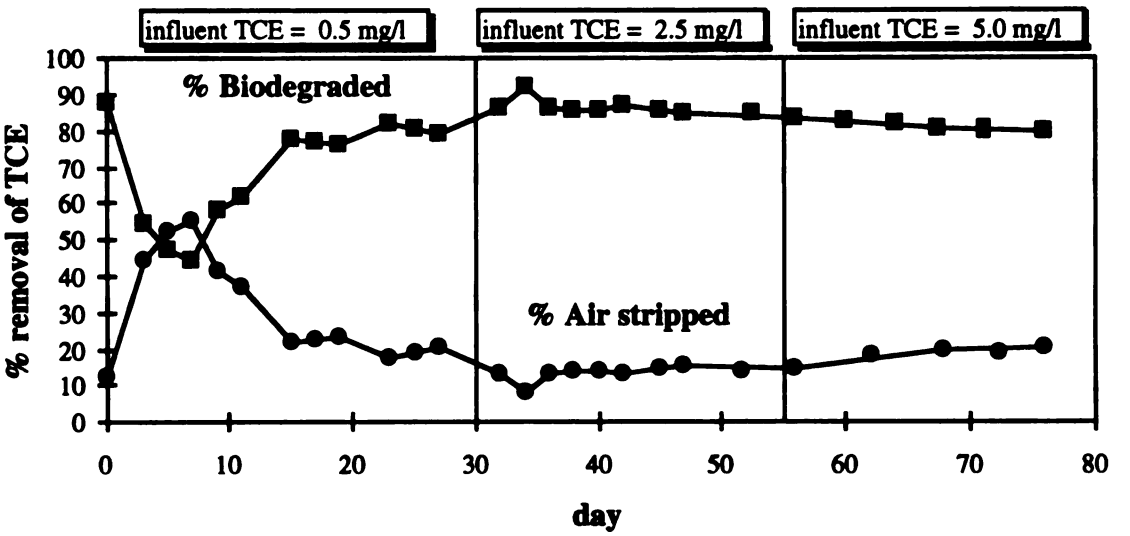

Figure 6-5 Percentages of TCE removed by biodegradation and air stripping as determined in mass balance experiments.

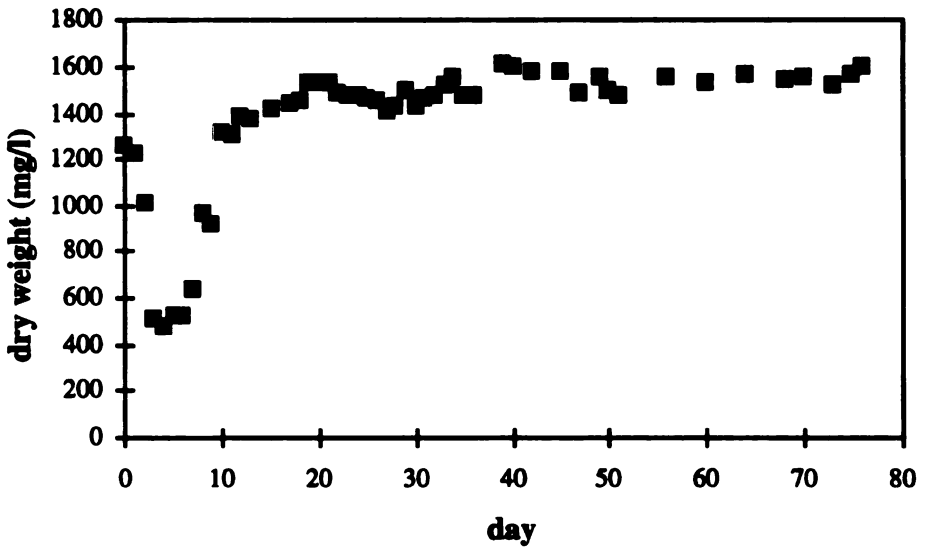

Figure 6-6 Biomass variation observed in a bench-scale SBR conducting TCE transformation.

experiments are summarized in Figure 6-5. Initially, the dominant TCE removal mechanism was biodegradation (up to 86% removal by biodegradation). When TCE feed was initiated, biomass concentration decreased (Figure 6-6) and the portion of TCE removed by air stripping increased. At the point of greatest biomass loss, up to 55% of the influent TCE was removed by stripping. As organisms acclimated to TCE, the observed cell concentration gradually returned to the initial level, and biodegradation again became the major removal mechanism of TCE.

The period of decreased TCE degradation prior to TCE acclimation might be explained by loss of total biomass or changes in community structure caused by the toxicity of TCE or its transformation products. Changes in specific rates of TCE transformation suggest initial changes in overall biomass followed by changes in community structure. Since specific rates are normalized by biomass, changes in these values are suggestive of change of community structure. As shown in Figure 6-7, loss of TCE degradation activity before day 5 was likely due to loss of biomass since specific rates of TCE transformation decreased only slightly. After day 10, however, biomass levels had recovered to pre-TCE exposure levels, but specific TCE transformation rates remained low. This suggests that loss of TCE transformation capacity was likely due to changes of community structure. After day 15, specific TCE degradation rates gradually recovered to the levels found in the inoculum, and TCE degraded without loss of transformation activity and biomass. TCE exposure apparently caused loss of biomass and TCE transformation activity for cells that had never been exposed to TCE, but 40 cycles of repeated exposure (20 days), resulted in the emergence of a new community that was stable with respect to TCE degradation.

6.5.2 Batch TCE degradation experiment

Cells harvested in the recharge stage after phenol had totally degraded were used in batch TCE degradation studies. Batch data were fitted to the integrated forms of

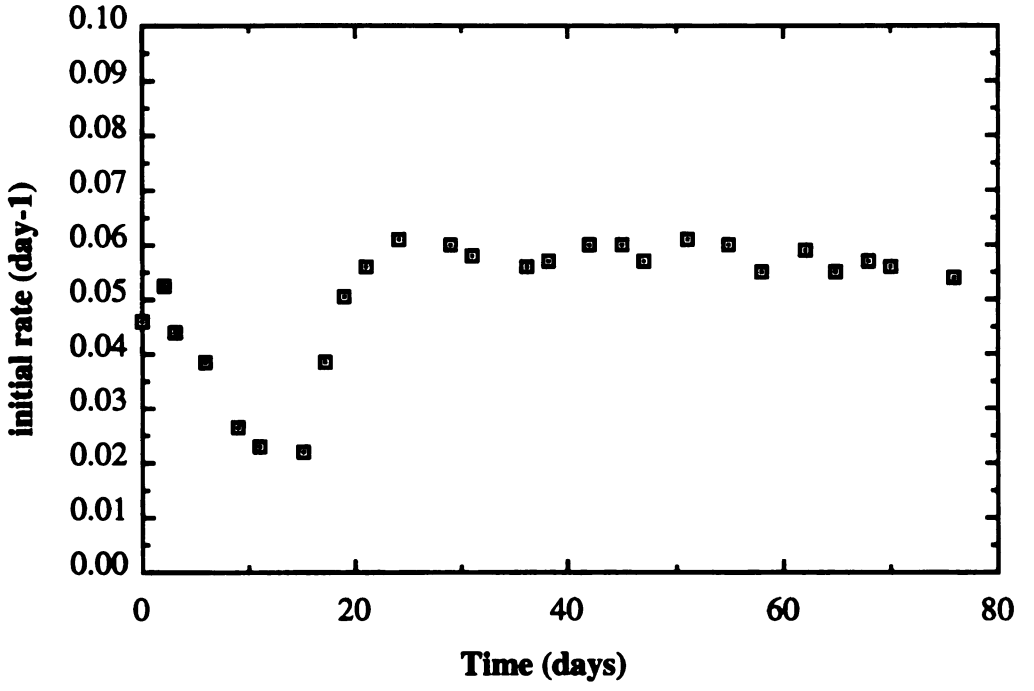

Figure 6-7 Variations in specific rate of TCE degradation during reactor operation. The initial aqueous phase TCE concentration was 1 mg/L.

equations 6-1 and 6-2, assuming negligible change in biomass concentration during the assay period (~ 30 to 60 min.). The integrated expressions were:

$$t = \frac{K_c}{k_c X_o} ln(\frac{C_o}{C}) + \frac{1}{k_c X_o}(C_o - C) \qquad (6\text{-}23)$$

$$t = \frac{1}{k_c' X_o} ln(\frac{C_o}{C}) \qquad (6\text{-}24)$$

where, C_o = initial aqueous phase TCE concentration (mg/L) and X_o = initial biomass concentration.

Initial specific rates of TCE degradation were also calculated. Data from these studies confirmed biotransformation of TCE in the bench-scale SBR and provided an independent measure of kinetic coefficients used in system modeling. Observed kinetics coefficients are summarized in Figure 6-8. Saturation kinetics adequately described TCE degradation. The maximum TCE transformation rate (k_c) was between 0.03 to 0.1 mg TCE/mg dry weight-day and the half saturation coefficient (K_c) was 0.3 ~1.0 mg/L. A typical second order rate coefficient (k_c/K_c) was ~ 0.1 l/mg-day, indicating a TCE half life on the order of 7 days for a cell concentration of 1 mg/L. There was considerable variability in the kinetic data, possibly due to changes in community structure or enzyme activity. In general, though, the observed TCE degradation rates were comparable to or greater than reported values for methanotrophic and toluene-oxidizing enrichments (Fogel et al., 1986; Strand et al., 1991; Wackett and Gibson 1988), but slower than some pure cultures like *Pseudomonas cepacia* G4 (Folsom et al., 1990), *Methylosinus trichosporium* OB3b (Brusseau et al., 1990; Fox et al., 1990; Oldenhuis et al., 1991) and certain methanotrophic mixed cultures (Alvarez-Cohen and McCarty 1991; Henry and Grbic-Galic 1991). Typical changes in the initial rates of TCE degradation in an SBR operating cycle are provided in Figure 6-9. Decline of TCE transformation rates was observed during the fill, react, settle and decant periods and recovery was observed during the recharge period.

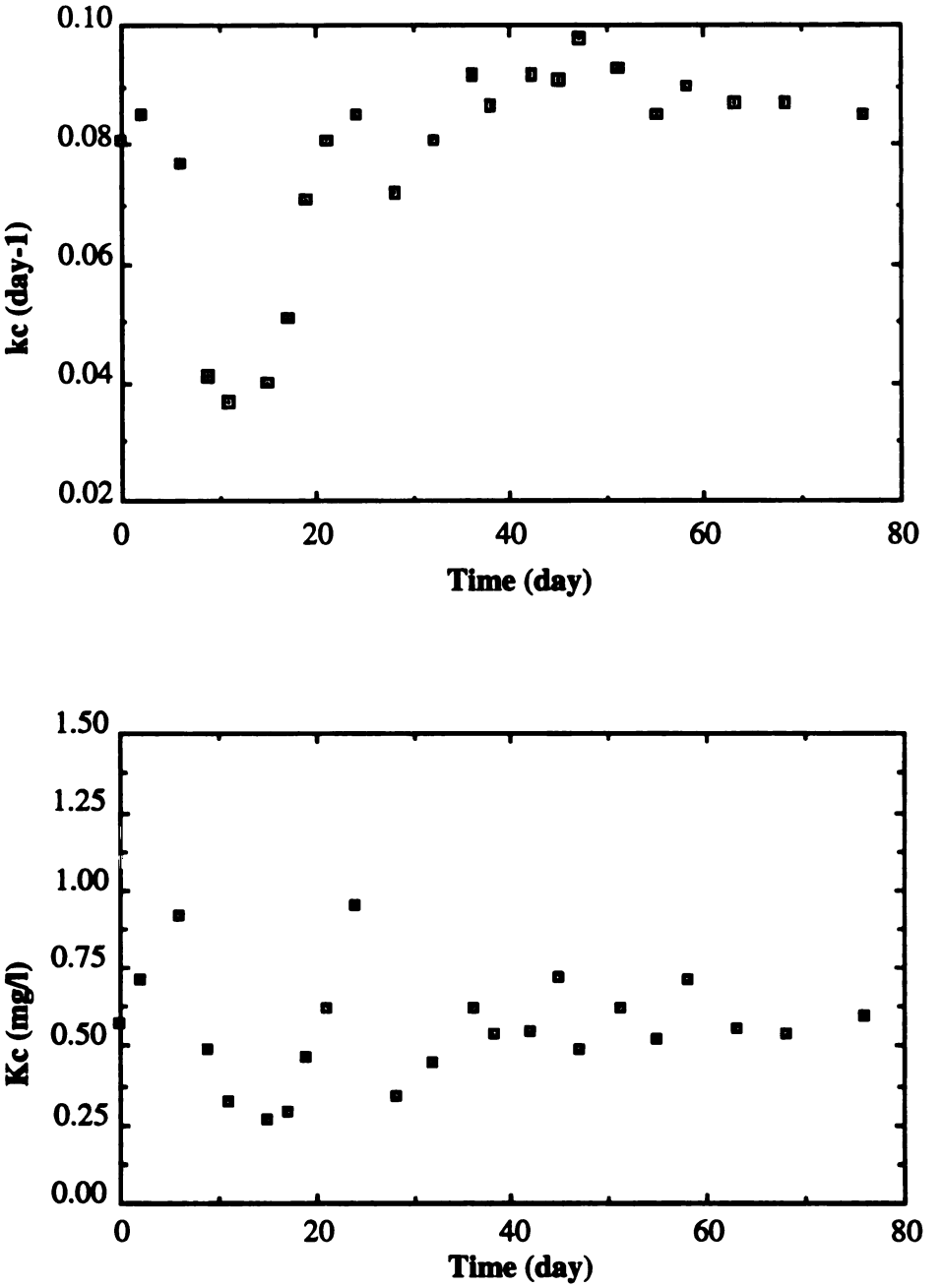

Figure 6-8 Variations in the saturation kinetic coefficients K_c and k_c for TCE degradation during reactor operation .

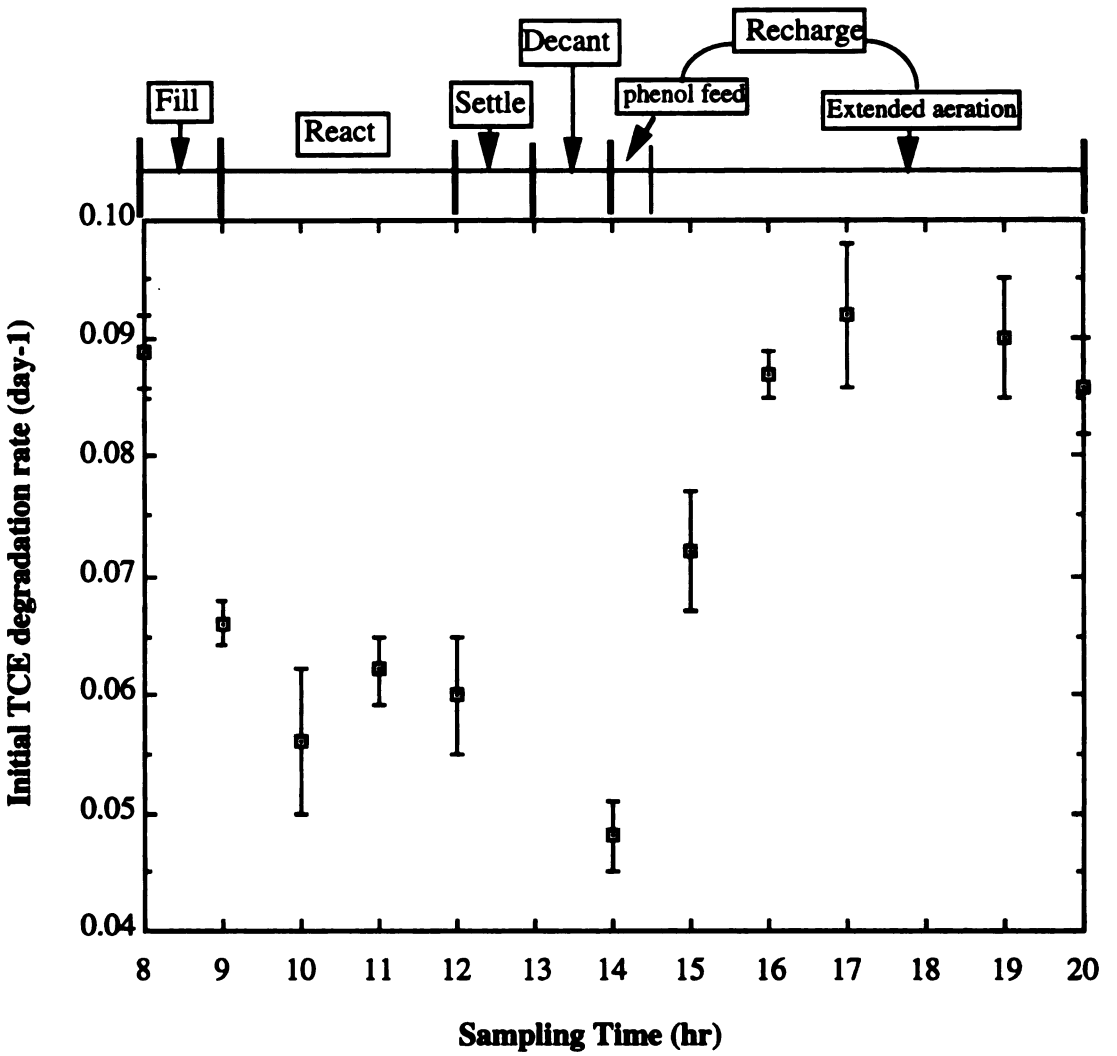

Figure 6-9 Changes of TCE degradation activity during different stages. of SBR operation. TCE degradation activity was measured as initial rates for an initial TCE concentration of 2.0 mg/L. Error bars represent the range of standard deviations.

6.6 Bench-scale SBR modeling

6.6.1 Growth substrate concentration

The major mechanism of phenol removal was biodegradation. Estimated phenol partitioning to cells is only about 0.0025% of the total phenol addition, as predicted by equation 6-4a assuming $\log K_{ow}$ for phenol = 1.50 (Weast 1992). Air stripping of phenol from the reactor was also insignificant, as indicated by a constant phenol concentration during the react period in the abiotic reactor. Biodegradation of phenol degradation was zero-order with respect to phenol concentration and first-order with respect to biomass, as shown in Figure 6-10. Typical zero-order kinetic coefficient (k^o) were between 0.5 to 1 day^{-1}. Observed phenol degradation patterns and kinetic coefficients were similar to those reported for phenol-acclaimed activated sludge (Auteinrieth et al., 1991; Rizzuti and Augueliaro 1982; Tischler and Eckenfelder 1969). Maximum phenol concentration (100 ~ 120 mg/L.) was present at the end of phenol addition. Phenol degraded to nondetect levels in 2~5 hr depending upon the influent TCE concentration. The higher the concentration of TCE in the influent, the longer the time required to consume the phenol. The recharge time required for phenol removal (2~5 hr) was shorter than the time allotted for recharge in each cycle (6 hr). This allowed for an idle period of 1 to 4 hours.

A decrease in phenol utilization rate was observed as TCE influent concentration increased. A possible reason for the decrease in phenol utilization rate was product toxicity. Others have reported that TCE breakdown products can covalently bind to cell material and can inactivate oxygenase activity (Fox et al., 1990; Wackett and Householder 1989). Inactivation of the oxygenase during TCE transformation may explain reduced phenol utilization rates. Inactivation of the oxygenase may be a reversible process (Rasche et al., 1991) or it may cause the death of cells (Heald and Jenkins 1994; Henry and Grbic-Galic 1991). The extent of cell damage caused by TCE

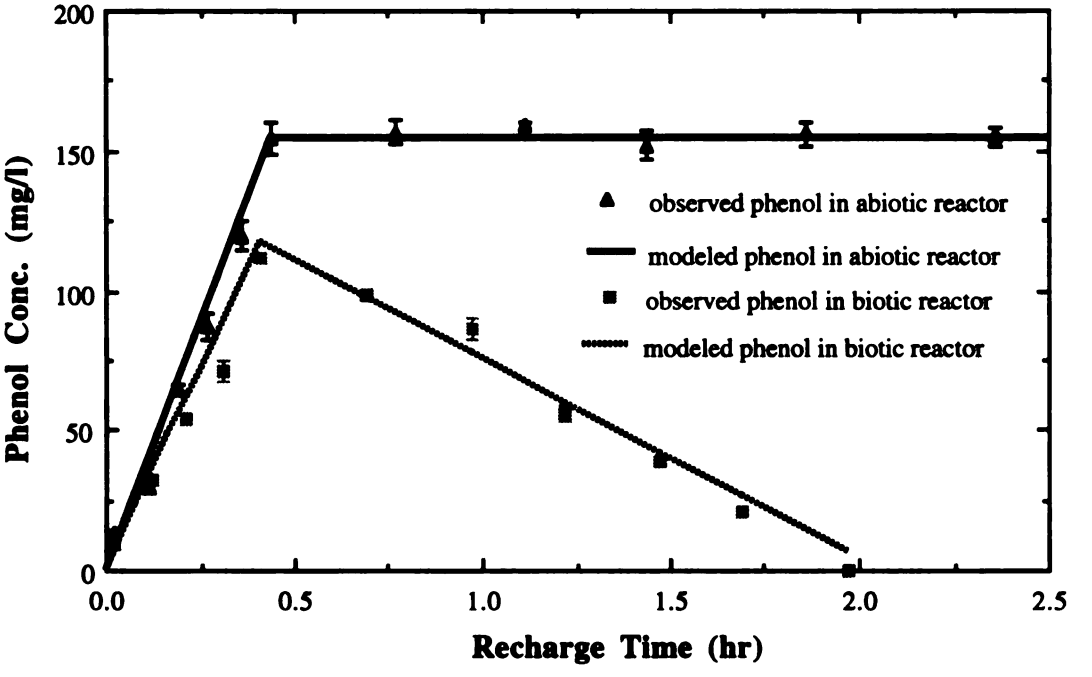

Figure 6-10 Typical observed and modeled phenol concentrations in the SBR (data was taken on day 25).

degradation is a fundamental issue related to how much growth substrate is needed for activation and how long it takes to regenerate a given level of transformation activity.

6.6.2 Nongrowth substrate concentration

Modeling TCE concentration in the SBR is more complex due to the volatility of TCE. To solve TCE mass balance equations, the overall TCE mass transfer coefficient ($K_L a_{,TCE}$) and the TCE degradation kinetic coefficients must be evaluated first. Observed TCE concentrations in the abiotic reactor were used to estimate $K_L a_{,TCE}$. A mass balance for the react period in the abiotic reactor can be derived from equation 6-17 and 6-18 by eliminating the biodegradation terms:

$$\frac{dC_L}{dt} = -K_{La,TCE}(C_L - \frac{C_g}{H_C}) \qquad (6\text{-}23)$$

$$\frac{dC_g}{dt} = K_{La,TCE}(\frac{V_L}{V_g})(C_L - \frac{C_g}{H_C}) - \frac{Q_g}{V_g}C_g \qquad (6\text{-}24)$$

For an assumed $K_L a_{,TCE}$, equations 6-23 and 6-24 can be solved simultaneously. $K_L a_{,TCE}$ was estimated by minimizing the difference between observed and modeled TCE concentrations (C_g and C_L). A $K_L a_{,TCE}$ value of 0.0175 min.$^{-1}$ was obtained for the react period. As shown in Figure 6-11, using the $K_L a_{,TCE}$ value obtained from the react period to model the fill period resulted in the C_g and C_L values for fill period that were consistent with measured values. This suggests that changes in $K_L a_{,TCE}$ during the fill period were not significant for this experimental system.

Batch TCE degradation assays were used to determine k_c and K_c, and these results cross checked well with reactor measurements. After $K_L a_{,TCE}$, K_c and k_c were obtained, equations 6-13, 6-14 and 6-16 were solved simultaneously using the software package Mathematica 2.0. As shown in Figure 6-12 and 6-13, the observed TCE concentrations in the reactor matched modeling predictions. TCE concentration increased in the fill period

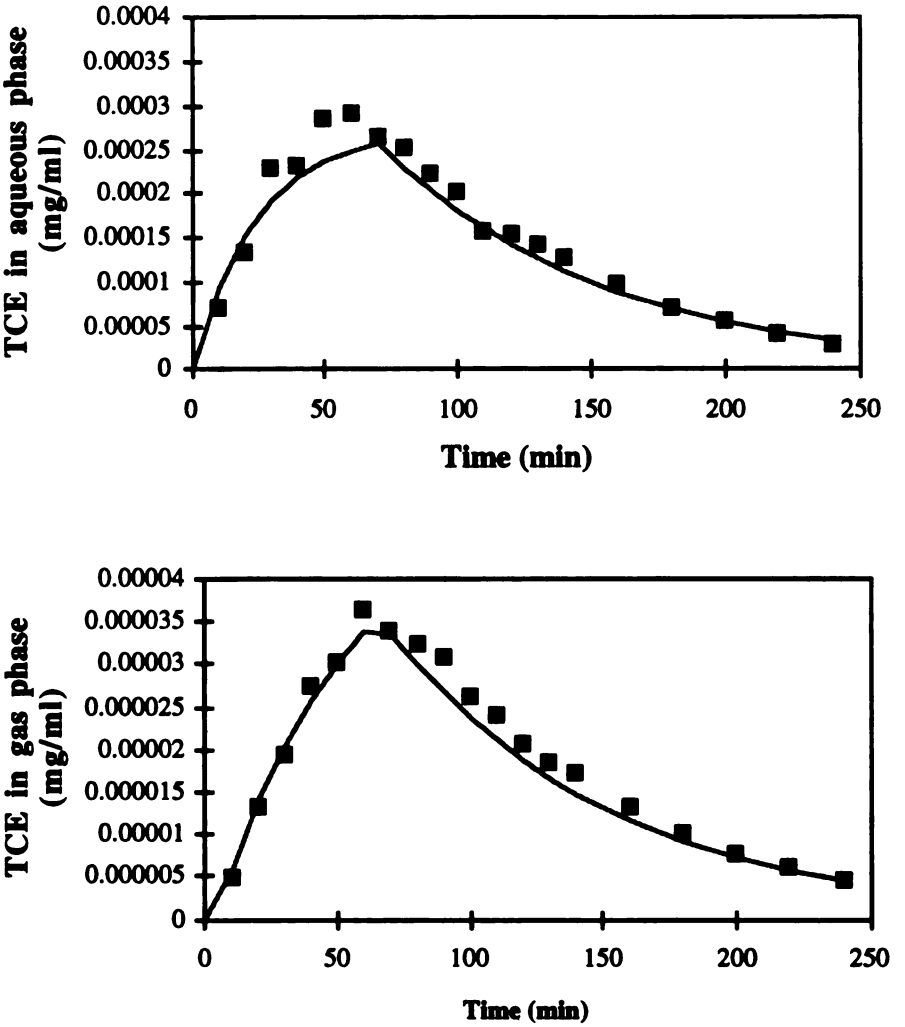

Figure 6-11. Observed and predicted TCE concentration during the fill and react stage in the abiotic reactor. Fill period was for the period t = 0 - 60 min, and the react period began at t = 60 min and continued until the end of the experiment. Predicted TCE concentrations were obtained by assuming a constant $K_L a = 0.0175\ min^{-1}$ for both the fill and react stages.

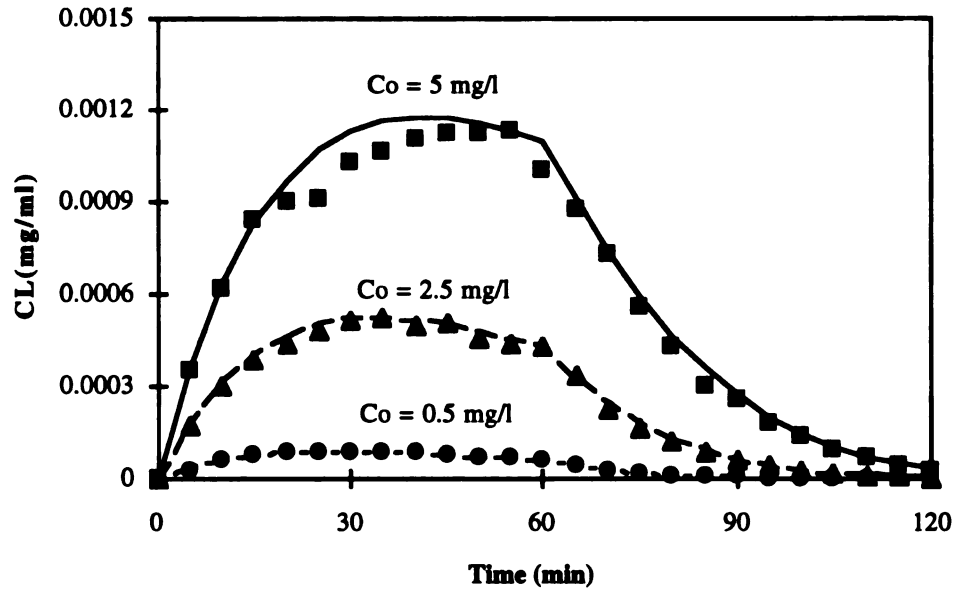

Figure 6-12 Liquid phase TCE concentrations observed and modeled in a bench-scale SBR.

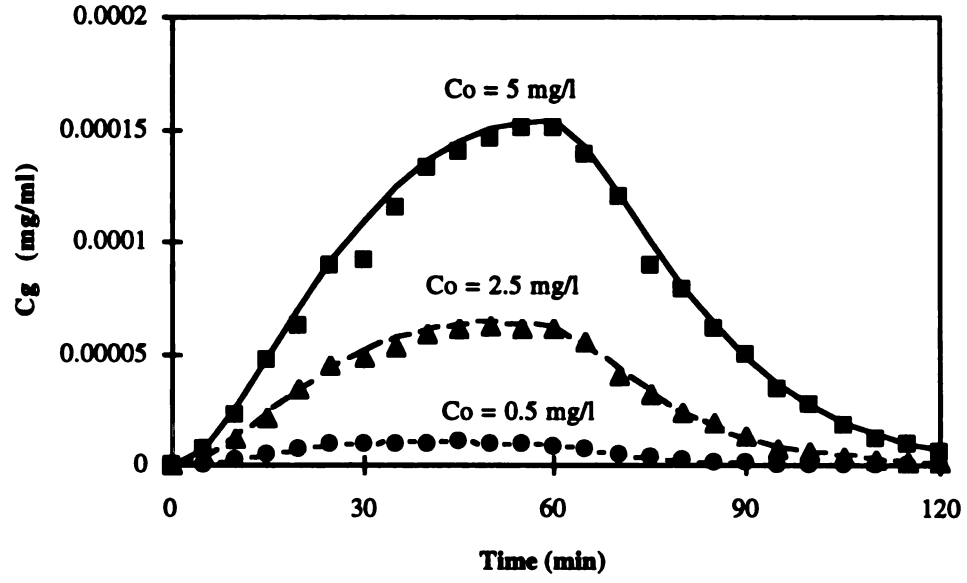

Figure 6-13 Gas phase TCE concentration observed and predicted in a bench-scale SBR.

and rapidly decreased during the react period. The typical react time for total disappearance of TCE from reactor was 40 to 90 minutes depending on the influent TCE concentration. Figures 6-12 and 6-13 also show that, in general, the model adequately predicted reactor performance. The model slightly overpredicted TCE concentration in liquid and gas phase. This might be due to losses of influent TCE by adsorption to or leakage from tubing and fittings (representing up to 5~10% of influent TCE losses, as indicated by mass balance experiments) or losses of TCE due to biodegradation in the inlet tubing (some unavoidable biofilm developed in the submerged part of influent tube). In spite of these limitations, the results indicate that the approach used provided a fair approximation of reactor performance.

The effects of $K_L a_{,TCE}$, K_c and k_c on reactor performance were evaluated and compared in Figures 6-14, 6-15 and 6-16. Increases in k_c or decreases in K_c and $K_L a_{,TCE}$ enhanced TCE removal by biodegradation and reduced the importance of air stripping.

6.7 System optimization and design consideration

The bench-scale cometabolic SBR system was not optimized for its performance although it consistently removed TCE. Several optimization procedures are possible. Aeration rates may be decreased to levels that just satisfy the oxygen requirements for TCE transformation and cell respiration . This would reduce TCE losses by air stripping. The required time for each stage might be reduced to accommodate more wastewater. The mass of phenol addition during recharge period might be reduced. The optimal t_r may range from 1.5 to 2.5 hr depending upon influent TCE concentration. One hour of settling time was adequate as the effluent suspended solids ranged from 10~30 mg/L and no bulking was observed. The required recharge time was found to be dependent upon the influent TCE concentration and might range from 2.5 to 5 hr. From batch studies, the phenol required for cell regeneration was about 15~20 mg of phenol per mg of treated TCE. Phenol addition was designed to accommodate 8~10 mg/L influent TCE and

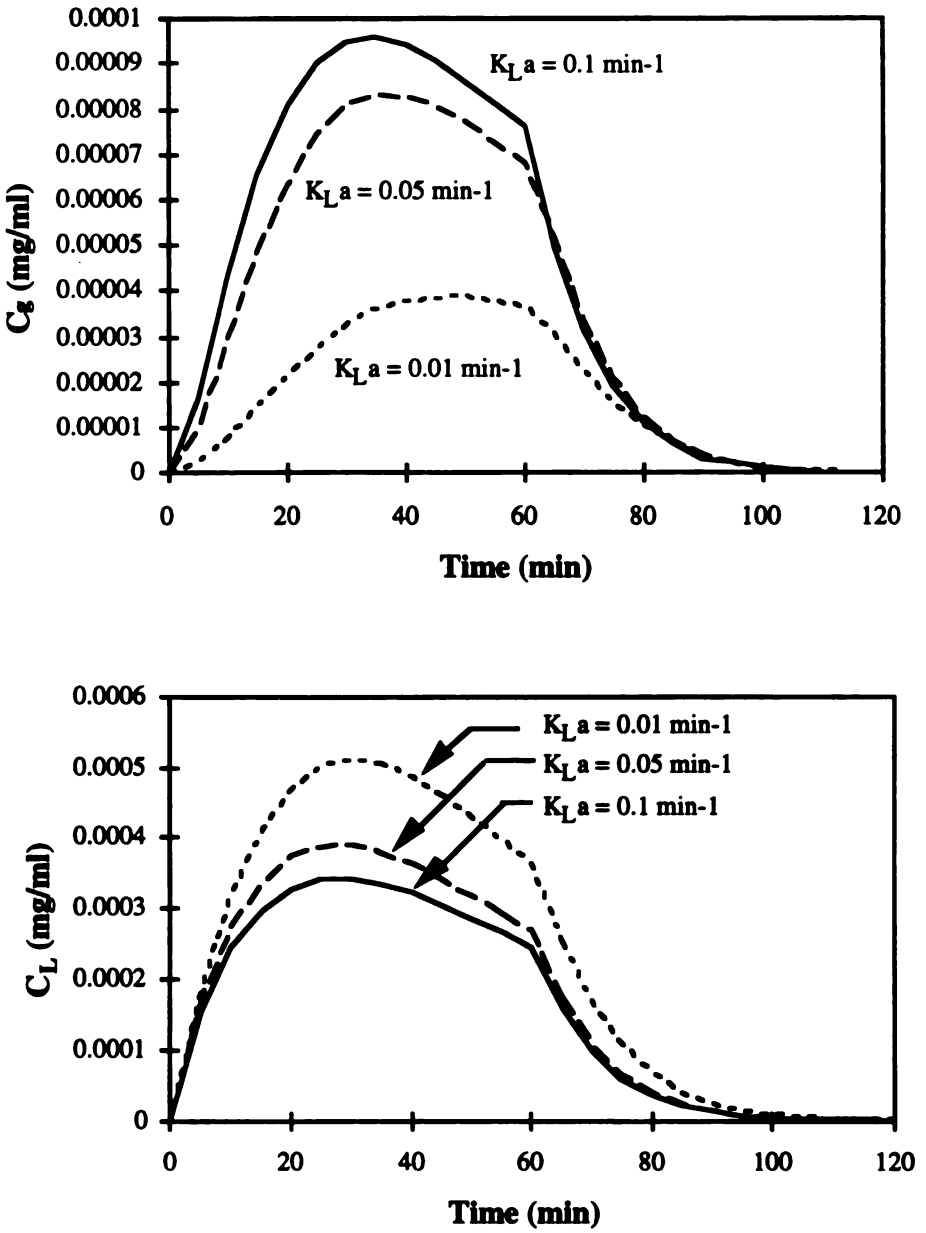

Figure 6-14 Effects of K_La on simulated liquid and gas phases TCE concentrations in an SBR. Parameters used in the simulation: k_c = 0.1 d^{-1}, K_c = 0.5 mg/L, C_o = 2.5 mg/L, X_o =1500 mg/L and k_h = 0.05 d^{-1}.

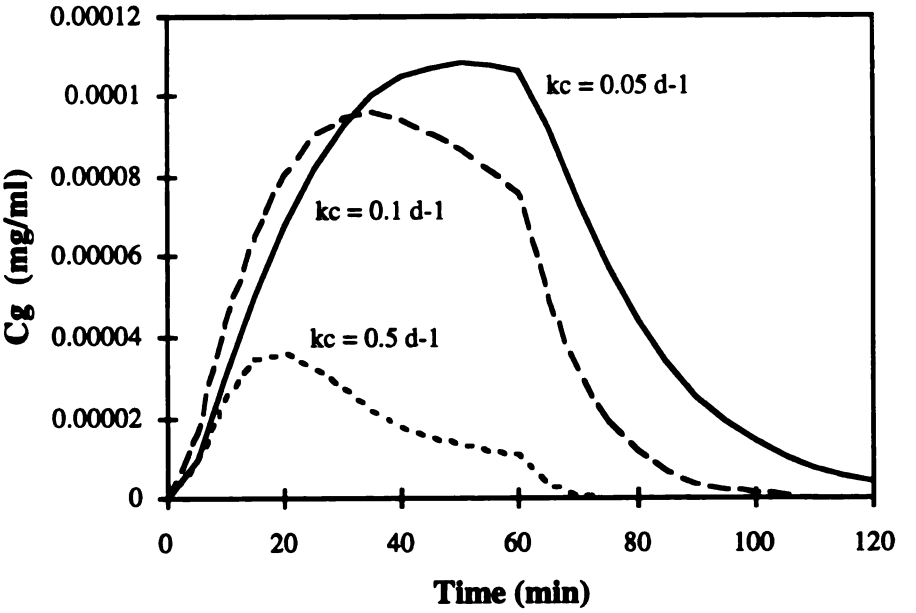

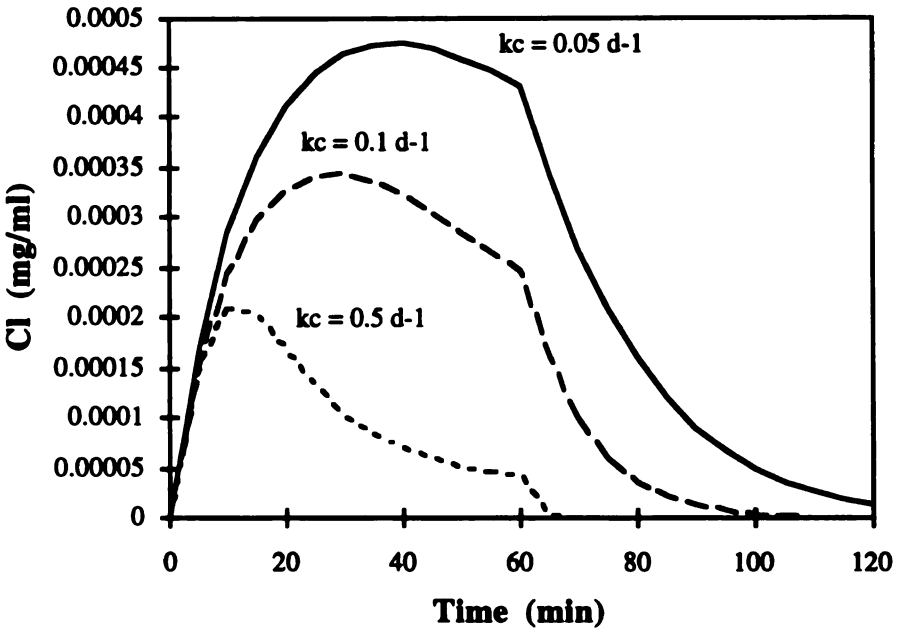

Figure 6-15 Effect of k_c on simulated liquid and gas phases TCE concentrations present in an SBR. Parameters used in simulation: K_c = 0.5 mg/L, K_La, $_{TCE}$ = 0.05 min-1, C_o = 2.5 mg/L, X_o =1500 mg/L and k_h = 0.05 d

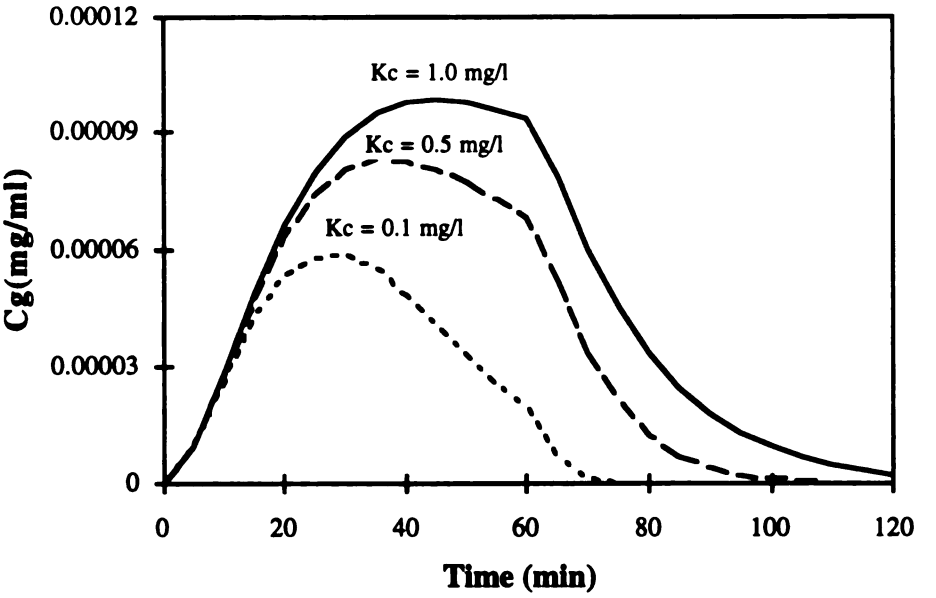

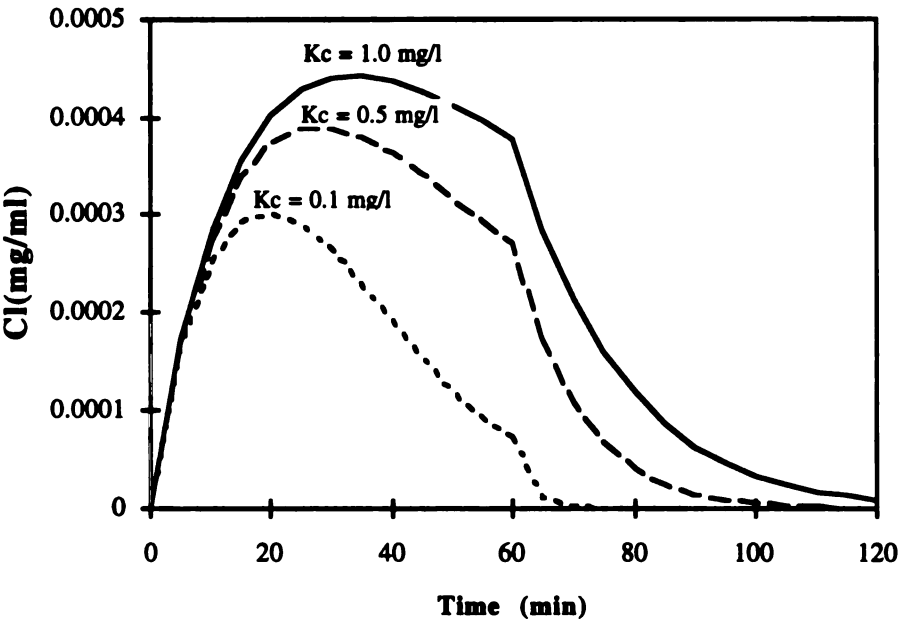

Figure 6-16 Effects of K_c on simulated liquid and gas phases TCE concentrations in an SBR. Parameters used in simulation: $k_c = 0.1\ d^{-1}$, $K_La_{,TCE} = 0.05$ min-1, $C_o = 2.5$ mg/L, $X_o = 1500$ mg/L and $k_h = 0.05\ d^{-1}$.

actually enabled degradation of 5 mg/L influent TCE without serious toxicity effects. Thus, the SBR received more phenol than needed. Batch recharge studies also indicated that phenol addition could be reduced.

6.8 Conclusions

In light of the above observations and modeling, the following conclusion may be drawn:

1. An SBR microbial community incorporating a phenol recharge stage can cometabolize TCE for extended periods without loss of transformation activity .

2. The major mechanisms involved in TCE removal from the SBR were biodegradation and air stripping, accounting for up to 95% of the TCE reduction. Slower TCE transformation kinetics and higher aeration rates increase the magnitude of air stripping losses. Faster TCE kinetics and lower aeration rates enhance biodegradation efficiency. For the bench scale SBR tested, 80 to 90% TCE was biodegraded and 5 to 10% was air stripped.

3. A shift in community structure occurred when microorganisms were first exposed to TCE. Prior to acclimation, declines in biomass and specific rates of TCE degradation were observed prior to eventual recovery.

4. Performance of the bench-scale SBR was adequately simulated by the proposed modeling procedure. The modeling process is able to predict TCE concentration and may be helpful in system design and simulation.

5. Increasing influent TCE concentration necessitates longer recharge periods because of reduced rates of phenol utilization. It is not clear whether the reduced phenol utilization rates were attributable to death of cells or inactivation of enzyme. Further research into the effects of nongrowth substrates on community structure and enzyme

inactivation will facilitate improvements in the design and operation of SBRs capable of cometabolic transformations.

Literatures cited

Alvarez-Cohen, L. and P. L. McCarty. "TCE transformation by a mixed methanotrophic culture - effects of toxicity, aeration and reductant supply." Appl. Environ.l Microbiol. 57 (1 1991): 228-235.

APHA. Standard methods for the examination of water and wastewater. 17th ed., Washington, D. C.: 1989.

Auteinrieth, R. L., J. S. Bonner, A. Akgerman, and M. Okagun. "Biodegradation of phenolic wastes." Journal of Hazardous Materials 28 (1991): 29-53.

Brusseau, G. A. , H. C. Tsien, R. S. Hanson, and L. P. Wackett. "Optimization of trichloroethylene oxidation by methanotrophs and the use of a colorimetric assay to detect soluble methane monooxygenase activity." Biodegradation 1 (1990): 19-29.

Clowater, L. M. "Variables effecting trichloroethylene transformation by methanotrophs." Master, Michigan State university, 1992.

D'Adamo, P. D. , A. F. Rozich, and A. F. Jr. Gaudy. "Analysis of growth data with inhibitory substrate." Biotechnology and Bioengineering 26 (1984): 397.

Dobbs, R. A., Leping Wang, and R. Govind. "sorption of toxic organic compounds on wastewater solids: correlation with fundamental properties." Environ. Sci. Technol. 23 (9 1989): 1092-1097.

Fogel, M. M. , A. R. Taddeo, and S. Fogel. "Biodegradation of chlorinated ethenes by a methane-utilizing mixed culture." Appl. Environ. Microbiol. 51 (1986): 720-724.

Folsom, B. R., P. J. Chapman, and P. H. Pritchard. "Phenol and trichloroethylene degradation by *Pseudomonas cepacia* G4: kinetics and interactions between substrates." Appl. Environ. Microbiol. 56 (1990): 1279-1285.

Fox, B. G., J. G. Borneman, L. P. Wackett, and J. D. Lipscomb. "Haloalkane oxidation by the soluble methane monooxygenase from *Methylosinus trichosporium* OB3b: mechanism and environmental implication." Biochemistry 29 (27 1990): 6419-6427.

Gossett, J. M. "Measurement of Henry's law constants for C1 and C2 chlorinated hydrocarbons,." Environ. Sci. Techol. 21 (1987): 202-208.

Henry, S. M. and D. Grbic-Galic. "Influence of endogenous and exogenous electron donors and trichloroethylene oxidation toxicity on trichloroethylene oxidation by methanotrophic cultures from a groundwater aquifer." Appl. Environ. Microbiol. 57 (1 1991): 236-244.

Mackay, D. and W.-Y. Shiu. "A critical review of Henry's Law constants for chemicals of environmental interest." J. Phys. Chem. Ref. Data 10 (4 1981): 1175-1197.

Martin, R. W. "Rapid colormetric estimation of phenol." Analytic Chemistry 21 (11 1949): 1419-1420.

Matter-Muller, C., W. Gujer, W. Giger, and W. Stumm. "Non-biological elimination mechanisms in a biological sewage treatment plant." Water Science and Technology 12 (1980): 299-314.

Oldenhuis, R., J. Y. Oedzes, and D. B. Janssen. "Kinetics of chlorinated hydrocarbon by *Methylosinus trichosporium* OB3b and toxicity of trichloroethylene." Appl. Environ. Microbiol. 57 (1 1991): 7-14.

Rasche, M. E., M. R. Hyman, and D. J. Arp. "Factors limiting aliphatic chlorocarbon degradation by *Nitrosomonas europaea*: cometabolic inactivation of ammonia monooxygenase and substrate specificity." Appl. Environ. Microbiol. 57 (10 1991): 2986-2994.

Strand, S. E., J. V. Wodrivh, and H. D. Stensel. " Biodegradation of chlorinated solvents in a sparged, methanotrophic biofilm reactor." Research Journal WPCF 63 (6 1991): 859-867.

Tischler, L. F. and W. W. Jr. Eckenfelder. "Linear substrate removal in the activated sludge process." In Advances in Water Pollution Research, 361-374. 2. Oxford, England: Pergamon, 1969.

Wackett, L. P. and D. T. Gibson. "Degradation of trichloroethylene by toluene dioxygenase in whole cell studies with *Pseudomonas putida* F1." Appl. Environ. Microbiol. 54 (1988): 1703-1708.

Wackett, L. P. and S. R. Householder. "Toxicity of trichloroethylene to *Pseudomonas putida* F1 is mediated by toluene dioxygenase." Appl. Environ. Microbiol. 55 (10 1989): 2723-2725.

Weast, R. C., ed. CRC handbook for chemistry and physics. 73 ed., Boca Raton, Florida: CRC Press, Inc., 1992.

CHAPTER 7

SUMMARY AND ENGINEERING IMPLICATIONS

7.1 Summary

The major objective of this work was to determine under what conditions cometabolism can be accomplished in a sequencing batch reactor and to elucidate design principles governing application of cometabolism. Theoretical considerations and modeling efforts were undertaken to develop a simulation-based design approach. Experiments were conducted to clarify the role of substrate feeding pattern on the selection of TCE degrading organisms and on the long-term stability of the resulting microbial community. Toxicity was also explored in cell viability experiments with different organisms. Experience acquired in the course of these efforts was used to operate and numerically simulate a bench-scale sequencing batch reactor with provisions for cometabolism of TCE.

7.1.1 Use of a numerical design approach for sequencing batch reactors

The design approach proposed in this work is based on the derivation and numerical solution of mass balance expressions for each phase of SBR operation. This contrasts with traditional SBR design approach in which empirical loading rates are chosen to determine reactor volume, with empirical guidelines used to establish wasting strategies and time periods for each operating stage. A simulation program enables simulation of various design options and strategies. It also enables simulation of SBR

performance, and it is adaptable for the addition of special features, such as a recharge stage for cometabolism.

Because of its dynamic mode of operation, a steady state condition does not exist for an SBR, but a repeating pattern of operation is expected for long-term operation if a repeating or constant hydraulic and substrate loading pattern can be defined. In this work, SBR design is based on the long-term repeating pattern of performance. Solids residence time (SRT), a traditional design and control parameter for activated sludge systems, was applied to SBR design, to arrive at a solids management schedule. However, SRT failed to account for dynamic changes in mean cell age during SBR operation. A more realistic estimation of average cell age (dynamic cell age) was proposed. By tracking changes in mass of each designated organism type, changes in the average population age can be predicted throughout the SBR operating cycle. Mean cell age decreases during periods of substrate feed and increases as substrate levels are depleted and endogenous decay becomes significant. SBRs must be designed so that the specified average solids residence time exceeds the minimum cell age for the slowest growing microbial population needed for proper performance of the reactor (i.e., SRT > $1/\mu_m$).

Solids control in an SBR is accomplished using a flexible solids wasting strategy. The frequency of wasting events and the quantity of solids wasted per event control the accumulation of solids. Solids concentrations in an SBR continue to increase until a wasting event. The chosen solids wasting strategy affects the extent of solids accumulation, the required time for the fill and react periods, and the volume of the reactor. SBRs with frequent solids wasting have lower suspended solids concentrations, shorter cell age, require more reactor volume and require more time for the react period. Increasing the quantity of solids wasted per wasting event has similar effects.

The number of reactor used in an SBR system affects the required total reactor volume, cell age, and the required cycle time. When more reactors are used, less total

reactor volume is needed, and shorter cycle times are possible. The incremental decrease in total volume reduction is less when the number of reactors exceeds four. Reduced cell age is also observed in SBR systems as the number of reactors is increased.

7.1.2 Effect of growth substrate feeding pattern on community structure and TCE cometabolism

Community structure and TCE cometabolism activity can be manipulated by changing growth substrate feeding pattern. For phenol, pulse feeding selected for organisms with faster phenol and TCE degradation rates. Pulse feeding also selected for a diverse bacterial community with a high concentration of TCE-degrading species and floc-forming organisms. Fluctuations of biomass concentration were more extreme and more frequent in reactors that were fed phenol continuously or semi-continuously, apparently because of the greater prevalence of predators in these reactors. The continuous and semi-continuously fed reactor communities were less diverse and dominated by fungi that degraded TCE poorly or not at all. Of the total bacterial isolates obtained, most were unable to degrade phenol or cometabolize TCE.

The experiments with growth substrate feeding pattern established that the feeding pattern was critical to SBR operation - for phenol, a pulsed feeding pattern was clearly the preferred method of feeding, both for cometabolism and for development of an enrichment with favorable settling properties.

7.1.3 Effects of TCE on cell viability

That TCE cometabolism causes loss of cell reculturability rather than temporary inhibit their growth was clearly demonstrated for *P. putida* F1 and *P. cepacia* G4. Toxicity effects were species dependent. TCE exhibited more toxic with strain F1 than with strain G4.. Loss of cell viability was not observed in a strain that grew on phenol, but did not degrade TCE. For strain G4, the extent of inactivation of cells

was independent of the TCE concentration over the TCE concentration range from 1 to 10 mg/l. Loss of cell viability caused by TCE cometabolism was linearly related to the quantity of TCE transformed. The concept of TCE transformation capacity proposed by Alvarez-Cohen and McCarty adequate described the effects of TCE toxicity on cell viability.

7.1.4 Bench-scale SBR for TCE cometabolism

A bench-scale SBR modified to include a recharge stage successfully cometabolized TCE. Up to 90% of the influent TCE was removed by cometabolism and about 10 % was air stripped. Evidence for TCE product toxicity was only noted upon initiation of TCE addition, as biomass concentrations and TCE transformation activity declined. However, after approximately 20 days of twice-daily exposure to TCE, biomass and TCE transformation activity recovered to levels observed prior to TCE exposure. No further toxic effects were observed. A mathematical model was used to simulate the major TCE removal mechanisms (biodegradation and air stripping) after stable operating conditions were achieved.

7.2 Engineering implications

The numerical, simulation-based SBR design approach described in this work offers several advantages for the design and operation of conventional SBR systems and for the extension of SBR technology to new applications, such as cometabolism. Many design and operating strategies can be evaluated. It also reduces reliance on questionable rule-of-thumb criteria and safety factors, and it provides insight into reactor performance. The ability to numerically track mean cell age is of interest because certain reactor functions are cell age dependent. A possible example is growth and nongrowth substrate additions. To eliminate competitive inhibition, nongrowth substrate should be provided when growth substrate levels are low and cells are young.

To apply SBR techniques for TCE cometabolism, a recharge stage is needed to regenerate the TCE transformation activity of organism lost during TCE degradation. Such a step enables stable operation and continuous long-term biodegradation of TCE. Manipulating the substrate delivery mode appears to be an effective way of selecting cells with the desired function. Addition of phenol in pulses worked well for phenol degradation, TCE cometabolism and cell settleability. However, the interactions of community members in the phenol enrichment is very complex and should receive additional attention in reactor design. Traditional engineering frequently ignores the role of community members, with simple steady state or empirical approaches to reactor design. This tendency may lead to an impractical design because of changes in the microbial community, especially during treatment of hazardous wastes. Dynamic and unsteady state reactor systems, like the SBR, should focus on microbial community structure, especially as it affects the stability of the reactor performance.

Transformation of TCE results in cell death. Therefore, regrowth of surviving cells to desired population levels may require long time period, especially where large quantities of TCE have been transformed. The surviving cells can be regrown during the recharge stage. Thus, the recharge time is fixed by the concentration of surviving cells and their growth kinetics. Prediction of the concentration of viable cells after TCE exposure is a crucial step in establishing the required time for recharge. Previously proposed cell viability models using the concept of transformation capacity may be applied to estimate the number of cells that survive TCE exposure.

7.3 Proposed research

To better understanding the function and limitations of SBR systems for cometabolism, the following additional studies are proposed:

1. Expansion of SBR design and simulation protocol to include a range of desired community functions, including cometabolism, denitrification, and phosphate removal. The effects of variable flows and substrate concentrations should also be explored in simulation. Commercialized design and simulation tools can be developed to assist engineers and operators in the rational design and operation of SBRs.

2. Selection and enhancement of the cometabolism activity might be achieved by better understanding of the fundamental reasons why microorganisms engage in cometabolic transformations in the first place.

3. The role of each community member should be clarified. What is the role of community members that do not degrade the growth substrate or the nongrowth substrate? Does their existence benefit cometabolizing organisms or do they interfere with the desired function of the community?

4. Studies on TCE transformation toxicity and cell viability should be extended to different types of TCE degrading organisms. This might enable selection of resistant organisms for treatment applications. Further studies should also focus on TCE toxicity in mixed cultures. Does addition of TCE to a mixed culture select for non TCE degrading organisms? To what extent are the toxic the products of TCE cometabolism available to other members of the community?

5. Operating parameters of SBRs for cometabolism should be optimized. This work demonstrated the feasibility of SBR systems for cometabolism. To optimize reactor treatment efficiency, the aeration rate may be altered, and the time allotted for each stage may be varied. Further studies should be conducted to test the impact of such changes, and a range of operating conditions should be examined.

6. As TCE degradation capacity and TCE toxicity resistance varies from organism to organism, it may be possible to enhance treatment efficiency by the addition of foreign

species. Addition of TCE-degrading isolates that are resistant to toxicity such as *P. cepacia* G4 or genetic engineered organisms, may increase treatment efficiency and improve the stability of the process. Success of such an approach would depend upon the survival of the added organism, or at least, the persistence of the added catabolic genes within the community. These issues certainly merit additional attention.

APPENDICES

APPENDIX A

DERIVATION OF CSTR STEADY-STATE SOLUTIONS USED AS THE INITIAL CONDITION FOR SOLVING SBR MODELING EQUATIONS

Consider a typical CSTR activated sludge system as indicated in Figure A-1.

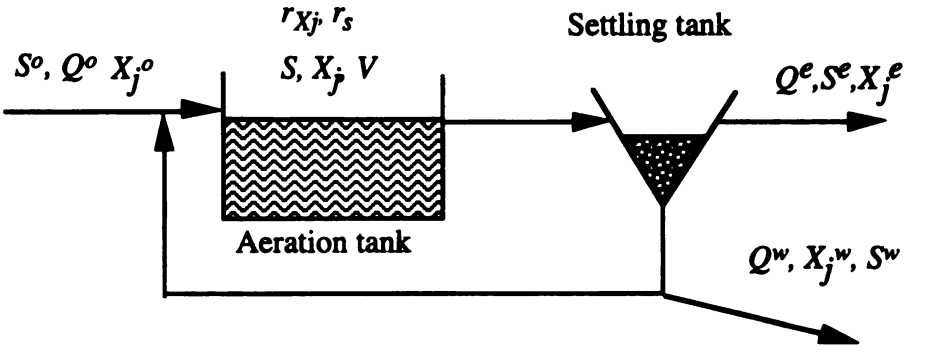

Figure A-1 Schematic of a typical CSTR activated sludge system

Mass balance equation when the system in steady-state is

in - out + source-sink = 0

Consider general suspended solids Xj,

$$Q^o X_j^o \Delta t - [Q^w X_j^w + Q^e X_j^e]\Delta t + (\textit{mass production rate})\Delta t - (\textit{mass reduction rate})\Delta t = 0$$

$$Q^o X_j^o + (\textit{mass production rate}) - (\textit{mass reduction rate}) = Q^w X_j^w + Q^e X_j^e \quad \text{(A-1)}$$

where mass production rate - mass reduction = Vr_{xj}

Subtitute $\theta_c = \dfrac{VX_j}{Q^w X_j^w + Q^e X_j^e}$ and Vr_{xj} to equation A-1 gives

$$Q^o X_j^o + Vr_{xj} = \frac{VX_j}{\theta_c} \qquad \text{(A-2)}$$

Equation A-2 divided by V and substitute V/Q^o with hydraulic residence time (θ) gives:

$$X_j = \frac{\theta_c}{\theta} X_j^o + \theta_c r_{xj} \qquad \text{(A-3)}$$

which is the form present in equation 3-13.

For example 1 in chapter 3, consider each of the different types of suspended solids in the reactor at steady state:

X_a

$$Y(S^o - S^e)Q^o - bX_aV = \frac{X_aV}{\theta_c}$$

$$X_a = \frac{\theta_c}{\theta}\left[\frac{Y(S^o - S^e)}{1 + b\theta_c}\right]$$

X_d

$$Q^oX_d^o + f_d bX_aV - k_hX_dV = \frac{VX_d}{\theta_c}$$

$$X_d = \frac{\theta_c}{\theta}\left[\frac{X_d^\circ}{(1 + k_h\theta_c)} + \frac{f_d b\theta_c Y(S^o - S)}{(1 + k_h\theta_c)(1 + b\theta_c)}\right]$$

X_i

$$(1 - f_d)bX_aV = \frac{VX_i}{\theta_c}$$

$$X_i = \frac{\theta_c}{\theta}\left[\frac{Y(S^o - S)(1 - f_d)b\theta_c}{1 + b\theta_c}\right]$$

X_r

$$Q^oX_r^o = \frac{VX_r}{\theta_c}$$

$$X_r = \frac{\theta_c}{\theta} X_r^\circ$$

X_{in}

$$Q^o X_{in}^o = \frac{V X_{in}}{\theta_c}$$

$$X_{in} = \frac{\theta_c}{\theta} X_{in}^\circ$$

S

On X_a mass balance:

$$\frac{Yk S^e X_a V}{K_s + S^e} - bX_a V = \frac{X_a V}{\theta_c}$$

$$S^e = \frac{K_s(1 + b\theta_c)}{\theta_c(Yk - b) - 1}$$

APPENDIX B

CURVE FITTING FOR TCE DEGRADATION KINETICS

Three kinetic models were examined (Table B-1). The integrated forms were obtainted by assuming the changes of cell concentration during the experimental period is negelectable. A statistic package SYSTAT 5.2.1 was used to estimate the kinetic parameters.

Table B-1. Kinetic models examined for TCE degradation

Kinetic model	General form	Integrated form	Fitted parameters
Monod	$r_c = -\frac{k_c C X}{K_c + C}$	$t = \frac{K_c}{k_c X_o} ln(\frac{C_o}{C}) + \frac{1}{k_c X_o}(C_o - C)$	k_c, K_c
First-order	$r_c = -k_c^{'} C X$	$t = \frac{1}{k_c^{'} X_o} ln(\frac{C_o}{C})$	$k_c^{'}$
Zero-order	$r_c = -k_c^{o} X$	$t = \frac{C_o - C}{k_c^{o} X_o}$	k_c^{o}

Typical TCE degradation data after 300 days of operatiion were fit to different kinetic models for each reactor. Results are summarized in Figures B1-B4. Estimated parameters and correlation coefficients are provided in Table B-2.

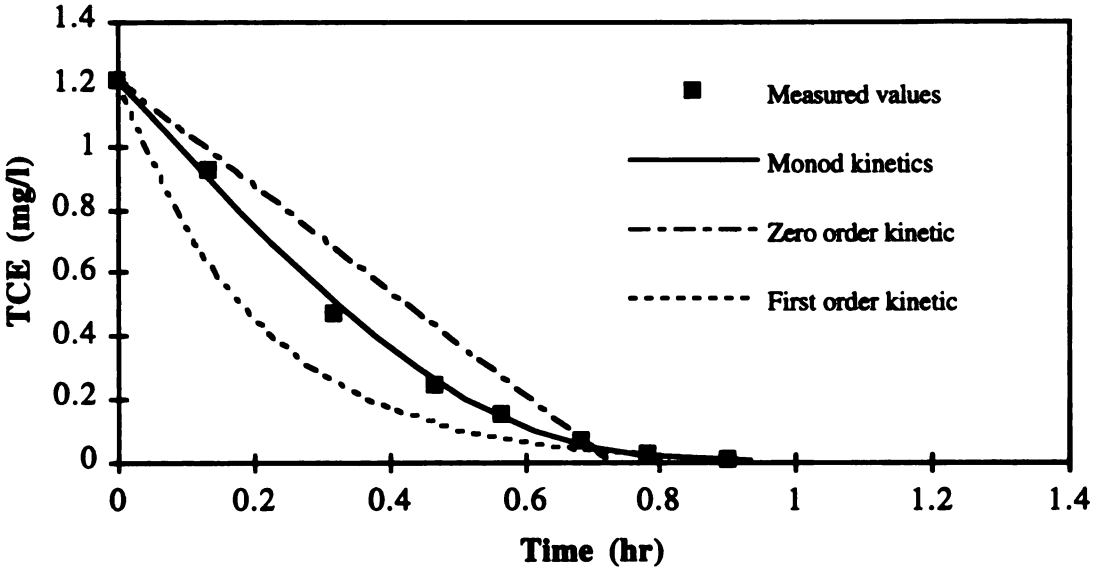

Figure B-1 Typical curve fitting results for TCE degradation observed in batch experiments using cells from reactor P.

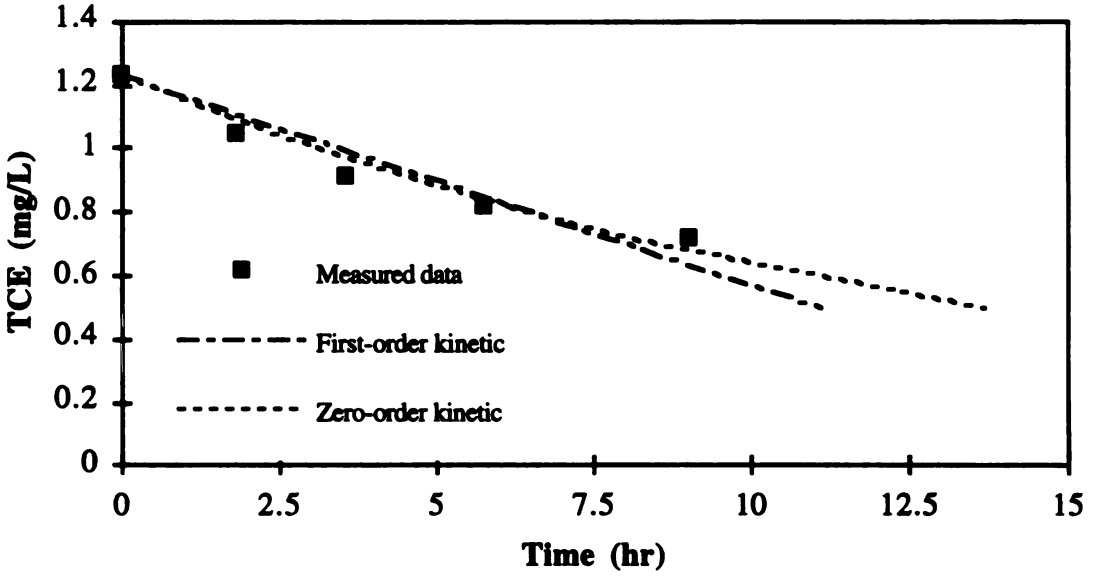

Figure B-2 Typical curve fitting results for TCE degradation observed in batch experiments using cells from reactor C.

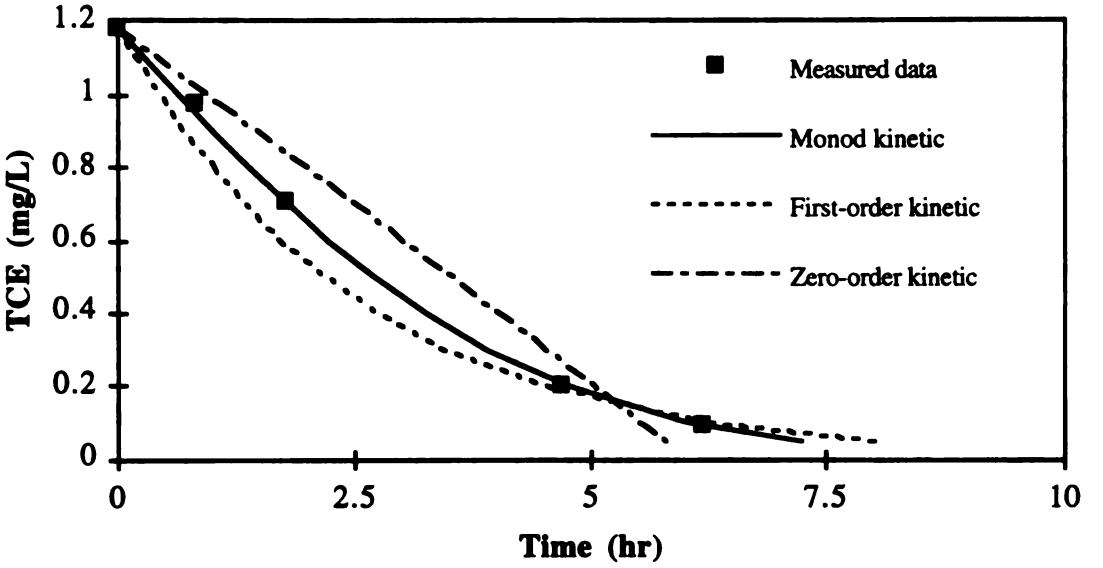

Figure B-3 Typical curve fitting results for TCE degradation observed in batch experiments using cells from reactor SC2.

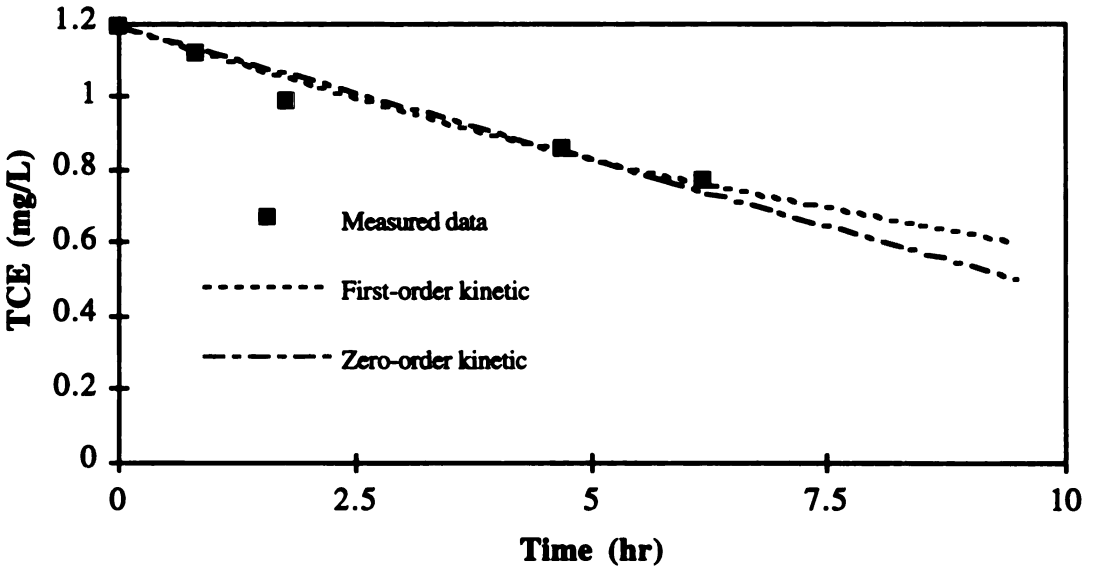

Figure B-4 Typical curve fitting results for TCE degradation observed in batch experiments using cells from reactor SC5.

Table B-2. Estimated kinetic parameters for TCE degradation

Kinetic model	Reactor P	Reactor C	Reactor SC2	Reactor SC5
Monod	k_C = 0.077 +/- 0.001 d^{-1} K_C = 0.29 +/- 0.01 mg/L r^2 = 0.9977	Fail[a]	k_C = 0.011 d^{-1} [b] K_C =0.80 mg/L r^2 = 0.9994	Fail[a]
First-order	k_C' = 0.13 +/- 0.02 L/mg-d r^2 = 0.8571	k_C' = 0.0024 +/- 0.0087 L/mg-d r^2 = 0.9543	k_C' = 0.0089 +/- 0.0050 L/mg-d r^2 = 0.9856	k_C' = 0.0018 +/- 0.0071 L/mg-d r^2 = 0.9741
Zero-order	k_C^o = 0.043 +/- 0.001 d^{-1} r^2 = 0.8950	k_C^o = 0.0024 +/- 0.0144 d^{-1} r^2 = 0.9131	k_C^o = 0.0044 +/- 0.0084 d^{-1} r^2 = 0.9631	k_C^o = 0.0018+/- 0.0095 d^{-1} r^2 = 0.9542

a. Estimated parameters out of reasonable range. Parameters (k_C and K_C) are highly correlated (>0.99).

b. Singular Hessian, standard errors are not countable.

c. +/- 95 % confidence interval.